

Studies on processing and decay of tRNA in *Trypanosoma brucei*

Dissertation

Presented in Partial Fulfillment of the Requirements for the Degree Doctor of
Philosophy in the Graduate School of The Ohio State University

By

Gabriel Silveira d'Almeida

Graduate Program in Microbiology

The Ohio State University

2023

Dissertation Committee:

Dr. Juan D. Alfonzo, Adviser

Dr. Anita Hopper

Dr. Chad Rappleye

Dr. Kurt Fredrick

Copyright by
Gabriel Silveira d'Almeida
2023

Abstract

In all domains of life, transfer (t) RNAs can be interrupted by intervening sequences (introns), which must be removed by splicing to generate mature molecules required for protein biosynthesis. In eukaryotes, the first step of tRNA splicing, intron cleavage, is catalyzed by a heterotetrameric enzyme denominated tRNA splicing endonuclease (TSEN), which in vertebrates, localizes to the nucleus, where it deals with multiple species of pre-tRNAs. The genome of the protozoan blood-borne pathogen *Trypanosoma brucei* encodes a single intron-containing tRNA: tRNA^{Tyr}_{GUA}. Previous investigations revealed the genome of *T. brucei* encodes one homolog for a TSEN subunit, the endonuclease TbSEN22, which localizes to the cytoplasm, where it partakes in tRNA splicing, raising the question on whether homologs for the other three subunits are present. Furthermore, *T. brucei* tRNA^{Tyr} presents some unique features when compared to other eukaryotic pre-tRNAs. First, the pre-tRNA^{Tyr} contains a small (11-nt) intron that receives noncanonical editing in three positions, with at least two editing events required for substrate recognition and tRNA splicing. Moreover, the mature tRNA^{Tyr} receives the unusual modification queuosine (Q) at the anticodon “wobble” position 34. This generates two subpopulations of tRNA^{Tyr} in the cell, with unmodified molecules decoding the G-ending codons for tyrosine, whilst the Q-modified ones being necessary for the efficient translation of the U-ending codons. Furthermore, the amounts of modified and unmodified tRNA dynamically change according to nutrient availability. Finally, tRNA splicing localizes to the cytoplasm of *T. brucei*, while the enzyme responsible for the Q modification localizes to the

nucleus. As such, the spliced tRNA^{Tyr} undergoes retrograde transport into the nucleus to receive Q.

In the first part of this dissertation, we utilize a combination of cellular and molecular approaches to further examine the uniqueness of *T. brucei* tRNA^{Tyr}. We show that, in this organism, tRNA^{Tyr} exists in two distinct isoforms, observable by differential electrophoresis migration: one corresponding to the expected size of the mature molecule (75 nt), and a higher molecular mass band (approx. 120-nt), corresponding to what we call alternate (alt) tRNA^{Tyr}. Additionally, we show that both isoforms exhibit unusually short half-lives when compared to other tRNAs within the same system and in other eukaryotes. Furthermore, we provide evidence implicating the stand-alone exoribonuclease RRP44 in the degradation of tRNA.

In the latter half of this dissertation, we utilize a series of biochemistry techniques and *in silico* investigations to further explore TSEN in *T. brucei*. Utilizing protein purification, we uncover two additional TSEN subunit homologs, named TbSEN12 and TbSEN17. We show that TbSEN22 and TbSEN17 contain conserved tRNA endonuclease domains, and are homologs of TSEN components TSEN2 and TSEN34, respectively, with TbSEN17 being essential for viability. Finally, we present evidence that all three subunits co-localize to the cytoplasm, corroborating tRNA splicing as a cytoplasmic event in *T. brucei*.

Acknowledgements

There are many people who have had a positive impact on my professional development during graduate school. First off, I would like to thank Dr. Juan Alfonzo and Dr. Mary Anne Rubio for the advices, life lessons, and discussions we have had over the years. None of this work would have been possible without their guidance.

I would also like to thank my lab mates who have helped me since I first joined the lab: Dr. Alan Kessler, Dr. Ian Fleming, and Dr. Katherine McKenney. They were pivotal for the success of this project and my development as a scientist, guiding me through my new lab environment, providing their expertise, and helping me with my experiments. Over the years, I have also had the pleasure to work with other students, both graduate and undergraduate. Sometimes members of the lab, sometimes visiting scholars from abroad, all of these people contributed to my development as a person and as a scientist. This group includes Ajith Jaiganesh, Dr. Amelia Staats, Dr. Ana Moro Bulnes, Caitlin Moore, David Salas, Katie Winner, Priya Srivastava, and Simran Chandawarkar. Moreover, I also receive guidance from post-docs in our lab, including Dr. Jeremy Henderson and Dr. Sameer Dixit, to whom I wish only the best for the next steps in their careers.

For my current lab mates, Ananth Casius, Aubree Zimmer, Henry Arthur, Lankani Gunaratne, and Shruti Daya, I wish only success as they develop their careers as scientists, and pursue their bachelors and doctorates.

Vita

- 2003 Sévigné High School
- 2012 B.Sc. Molecular & Cell Biology and Clinical
Analysis, Federal University of Rio Grande do
Sul
- 2014 M.Sc. Molecular and Cell Biology, Federal
University of Rio Grande do Sul
- 2017 Fellow, Center for RNA Biology, The Ohio State
University
- 2014 to present..... Graduate Teaching/Research Associate,
Department of Microbiology, The Ohio State
University

Publications

Silveira d'Almeida G, Casius A, Henderson JC, Knuesel S, Aphasizhev R, Aphasizheva I, Manning AC, Lowe T, Alfonzo JD: tRNA Tyr has an unusually short half-life in *Trypanosoma brucei*. RNA 2023, doi:10.1261/rna.079674.123.

Dixit S, Kessler AC, Henderson J, Pan X, Zhao R, D'Almeida GS, Kulkarni S, Rubio MAT, Hegedúsová E, Ross RL, et al. Dynamic queuosine changes in tRNA couple nutrient levels to codon choice in *Trypanosoma brucei*. Nucleic Acids Res [Internet] 2021; 49:12986–99.

Kessler AC, d'Almeida GS, Alfonzo JD. The role of intracellular compartmentalization on tRNA processing and modification. *RNA Biol* [Internet]. 2017;0(0):00–00

Kang B-I, Miyauchi K, Matuszewski M, D'Almeida GS, Rubio MAT, Alfonzo JD, et al. Identification of 2-methylthio cyclic N6threonylcarbamoyladenine (ms2ct6A) as a novel RNA modification at position 37 of tRNAs. *Nucleic Acids Res* [Internet]. 2016 Feb 28;45(4):2124–36

d'Almeida G, Breton M, Camargo S, Frazzon J, Pasquali G. Phylogenetic comparative and expression analysis of genes encoding dof transcription factors from *Eucalyptus grandis*. *BMC Proc* [Internet]. 2011 [cited 2011 Dec 22];5(Suppl 7):P159

Degrandi TH, de Oliveira IM, D'Almeida GS, Garcia CRL, Villela IV, Guecheva TN, et al. Evaluation of the cytotoxicity, genotoxicity and mutagenicity of diphenyl ditelluride in several biological models. *Mutagenesis* [Internet]. 2010 May [cited 2011 Oct 15];25(3):257–69

Fields of study

Major Field: Microbiology

Table of contents

Abstract	ii
Acknowledgements	iv
Vita	v
Publications	v
Fields of study	vi
Table of contents	vii
List of Tables	xii
List of Figures	xiii
Chapter 1: Introduction	1
1.1 An introduction to <i>T. brucei</i>	1
1.2 An introduction to human African trypanosomiasis.....	4
1.3 <i>T. brucei</i> as a model organism	5
1.4 RNA Splicing in <i>T. brucei</i>	8
1.5 tRNA splicing.....	12
1.5.1 Eukaryotic tRNA Splicing Pathways.....	16
1.6 Recent Findings in the Eukaryotic tRNA Splicing Endonuclease	19
1.6.1 Composition of TSEN and the Role of CLP1 in Humans	22
1.6.2 Insights into the Structure and Catalysis Mechanism of TSEN	24
1.6.3 Substrate Specificity of TSEN	25
1.6.4 TSEN and Human Disorders.....	29

1.6.5 Final Considerations	31
1.7 Overview of RNA Degradation Pathways.....	31
1.7.1 tRNA Degradation Pathways	35
1.7.2 RNA Degradation Components in <i>T. brucei</i>	35
Chapter 2: tRNA ^{Tyr} has an unusually short half-life in <i>Trypanosoma brucei</i>	37
2.1 Introduction	38
2.2 Results	41
2.2.1 tRNA ^{Tyr} has a relatively short half-life in <i>T. brucei</i>	41
2.2.2 XRNE moderately impacts alt-tRNA ^{Tyr} stability	52
2.2.3 RRP44 downregulation stabilizes alt-tRNA ^{Tyr} , alt-tRNA ^{Asp} /mature tRNA ^{Asp} but has little effect on mature tRNA ^{Tyr}	56
2.3 Discussion.....	64
2.4 Materials and Methods	71
2.4.1 Cell culturing and RNAi knockdowns	71
2.4.2 Northern blot analysis	71
2.4.3 Transcription Arrest Assays	72
2.4.4 Circular RNA analysis	73
2.4.5 RNA sequencing.....	73
2.4.6 Data Processing.....	75

2.5 Acknowledgements	75
Chapter 3: The tRNA splicing endonuclease of <i>Trypanosoma brucei</i>	76
3.1 Introduction	76
3.1.1 The search for <i>T. brucei</i> homologs of TSEN	76
3.2 Results	79
3.2.1 The <i>T. brucei</i> homologs of TSEN2 and TSEN15	79
3.2.2 TbSEN may be a heterotrimer	82
3.2.3 TbSen22 and TbSen17 contain tRNA endonuclease domains	86
3.2.4 TbSEN localizes to the cytoplasm.....	93
3.2.5 TbSEN17 is essential for viability	97
3.2.6 TbSEN activity reconstitution attempts in <i>E. coli</i>	99
3.3 Discussion.....	102
3.4 Materials and methods	109
3.4.1 EETbSEN22 TAP-Tag Purification.....	109
3.4.2 Size-exclusion chromatography	109
3.4.3 Anion-exchanging	110
3.4.4 Immunofluorescence microscopy.....	110
3.4.5 Cell culturing and RNAi knockdowns	111
3.4.6 Northern blot analysis	111

Chapter 4: Concluding remarks and future directions.....	113
4.1 Summary.....	113
4.2 Further exploring TbtRNA ^{Tyr}	116
4.3 Further exploring TbSEN and tRNA splicing.....	119
References.....	125
Appendix A: Protocols.....	144
A1: Total RNA Preparation from <i>Trypanosoma brucei</i>	144
A2: Polyacrylamide Gel Electrophoresis for RNA Separation.....	147
A3: Northern Blot Analysis.....	148
A4: Preparing And Labeling Stocks of Northern blot Probes.....	154
A5: Preparation of Plasmid DNA (Alkaline Lysis).....	156
A6: Reverse Transcription-PCR.....	160
A7: SDS Polyacrylamide gel electrophoresis for protein analysis.....	162
A8: Silver Staining of Protein Gels.....	164
A9: Western blot with Primary/Secondary Antibodies.....	167
A11: Endonuclease (TbSen) Cleavage Assay.....	172
A12: Procyclic <i>Trypanosoma brucei</i> Immunofluorescence.....	174
Appendix B: Recipes.....	173
B1: SDM-79 Medium Recipe.....	173
Appendix C: TSEN Homolog Sequences.....	176

C1: TSEN2 Homolog Sequences	176
C2: TSEN15 Homolog Sequences	196
C3: TSEN34 Homolog Sequences	203
Appendix D: Actinomycin D Uncropped Northern blot Membranes	214

List of Tables

Table A.1: Solution D Components	144
Table A.2: End-label Reaction	155
Table A.3: Plasmid DNA Preparation Solutions.....	156
Table A.4: Detailed Solution 1	158
Table A.5: Detailed Solution 2	159
Table A.6: Detailed Solution 3	159
Table A.7: Silver Staining Solutions.....	164
Table A.8: 50 µl C-labeled <i>in vitro</i> Transcription Reaction.....	169
Table A.9: 10x Cleavage Buffer.....	172
Table A.10: <i>In Vitro</i> Cleavage Reaction.....	173
Table A.11: Nikon Microscope Settings.....	184
Table B.1: SDM-79 Medium for PCF Trypanosomes (Recipe).....	173
Table B.2: Culture Media for <i>Trypanosoma brucei</i> (Personal Stock).....	175
Table B.3: Available <i>T. brucei</i> Selection Drugs in the Alfonzo Lab	175

List of Figures

Figure 1.1 The life cycle of <i>T. brucei</i>	3
Figure 1.2 <i>Trypanosoma brucei brucei</i>	7
Figure 1.3 RNA Splicing	10
Figure 1.4 tRNA ^{Tyr} _{GUA}	13
Figure 1.5 tRNA Introns.....	15
Figure 1.6 tRNA Splicing Pathway.....	18
Figure 1.7 TSEN.....	21
Figure 1.8 mRNA Decay.....	34
Figure 2.1 <i>T. brucei</i> tRNA ^{Tyr} is present in two conformers	43
Figure 2.2 Alt-tRNA ^{Tyr} does not contain an intron and neither alternative conformer contains 5' or 3' extensions corresponding to the genomic flanking regions.....	44
Figure 2.3 tRNA mapping read coverage of tRNA-Tyr-GUA-1 and tRNA-Asp-GUC-1	47
Figure 2.4 <i>T. brucei</i> tRNA ^{Tyr} is unusually unstable	50
Figure 2.5 <i>T. brucei</i> tRNA ^{Tyr} has an unusually short half-life, which is not shared by other tRNAs in the system	51
Figure 2.6 RNAi Knockdown of XRN enzymes.....	54
Figure 2.7 RT-PCR confirmations for XRN RNAi depletions	55

Figure 2.8 RNAi knockdown of Dis3L2 and RRP6.....	58
Figure 2.9 RNAi knockdown of RRP44.....	59
Figure 2.10 RNAi Knockdown of RRP44 stabilizes both tRNA ^{Tyr} conformers.....	61
Figure 2.11 Triplicate growth curve of <i>T. brucei</i> cells subjected to both RNAi knockdown and actinomycin D treatments	62
Figure 2.12 RNAi Knockdown of XRNE does not stabilize tRNA ^{Tyr} conformers.	63
Figure 2.13 The tRNA ^{Tyr} alternate conformer is not circular	70
Figure 3.1 TbSEN22.....	78
Figure 3.2 TAP-Tag Purification of TbSEN	80
Figure 3.3 Purification of EETbSEN22	84
Figure 3.4 Endonuclease Domains of TbSEN	87
Figure 3.5 Phylogeny of TbSEN	91
Figure 3.6 Immunofluorescence Microscopy of TbSEN.....	95
Figure 3.7 Knockdown of TbSEN12 and 17	98
Figure 3.8 Purification of Recombinant TbSEN	100
Figure 3.9 Proposed Model for TbSEN.....	108
Figure 4.1 Knockdown of TUT3 and 4	118
Figure 4.2 N-terminal tagging of TbSen22 with 3xHA-TurboID	123
Figure 4.3 Biotinylation assay with 3xHA-TurboID-TbSen22.....	124

Figure D.1 Uncropped Actinomycin D northern blot membranes..... 214

Chapter 1: Introduction

My research focused on two main topics: for the first, I aimed at identifying and characterizing the *Trypanosoma brucei* homologs of the components of the tRNA splicing endonuclease (TSEN), a specialized enzyme responsible for catalyzing tRNA splicing in eukaryotes. For the second, a closely-related subject, I aimed at characterizing various aspects of the decay of tRNA^{Tyr} in *T. brucei*, the single intron-containing tRNA present in the genome, and a TSEN substrate.

1.1 An introduction to *T. brucei*

T. brucei is a bloodborne protozoan parasite endemic to sub-Saharan Africa, where it can be found in over 36 countries [1][2]. The parasite is transmitted by an insect vector, the hematophagous tsetse fly (*Glossina spp.*), during a bloodmeal, and is capable of infecting both humans and animals, leading to two afflictions known as human African trypanosomiasis (HAT, also called sleeping sickness), in the first case, and “nagana” in the second case [2][3][4]. The fly needs to feed on an infected mammalian host in order to become infected, with no newly hatched flies ever been found containing the parasite [4]. Once inside the insect vector, *T. brucei* undergoes several differentiation steps, moving from the digestive tract, where it matures from procyclic trypomastigote into epimastigote, to the salivary glands, where it will become infectious in preparation for the next blood meal (metacyclic trypomastigote) (**Figure 1.1**) [4]. Once injected into a mammalian host, the parasite once again undergoes differentiation, changing into bloodstream

trypomastigote (**Figure 1.1**), which then proceeds to multiply, onsetting the disease [4].

Three subspecies are responsible for the majority of reported infections: *T. brucei gambiense*, present mainly in central and western Africa; *T. brucei rhodesiense*, present mainly in eastern and southern Africa; and *T. brucei brucei*, present mainly in central Africa [3][4][5]. Both *T. brucei gambiense* and *T. brucei rhodesiense* are capable of infecting humans, whilst using animals as reservoir, while *T. brucei brucei* is incapable of infecting humans, but presents a threat to livestock and game in the region [2][3][4][6]. Most reported instances of trypanosomiasis come from remote rural communities, with the majority (>90%) of HAT cases caused by *T. brucei gambiense* [4]. There are no vaccines for either HAT or nagana, and infection control in endemic countries relies mainly on managing tsetse fly populations, and prevention of insect bites by both usage of insect repellents and avoidance of high insect population areas [4]. After infection, disease treatment is challenging, with only a handful of drugs available capable of targeting *T. brucei*, including pentamidine, nifurtimox, eflornithine, suramin, and melarsoprol; all present major drawbacks, including low efficacy, high toxicity, and the requirement of intravenous administration for several days [4].

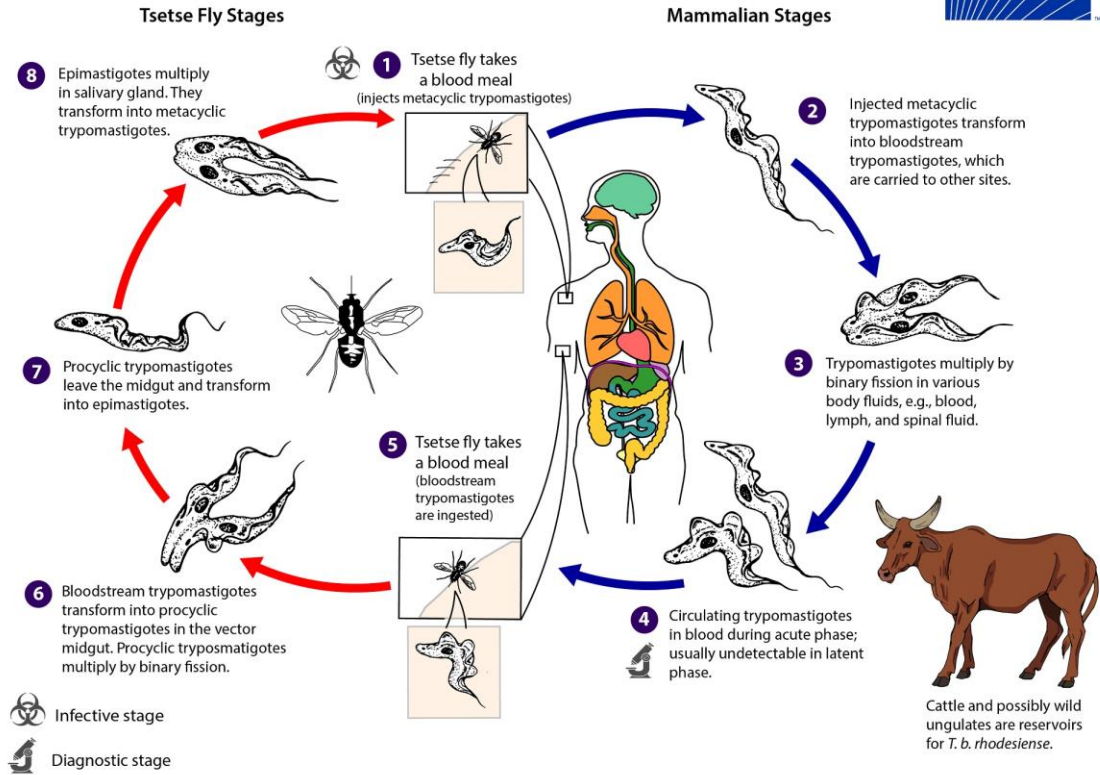


Figure 1.1 The life cycle of *T. brucei*.

The parasite begins its life cycle inside the tsetse fly salivary glands, from where it is transmitted to a mammalian host during a blood meal. Inside the host, it proceeds to change forms and multiply, leading to the onset of disease. Once the host is bitten by another fly, the parasites present in the bloodstream may infect the insect, changing forms, moving to the salivary glands, and restarting the cycle.

Adapted from centers for disease control and prevention (CDC) website.

Available at <https://www.cdc.gov/dpdx/trypanosomiasisafrican/index.html>

1.2 An introduction to human African trypanosomiasis

HAT progression can be classified into two distinct stages: haemolympathic and meningoencephalitic [4]. During the haemolympathic stage, after a short moment in the skin, the parasite is present in the bloodstream, following the tsetse fly bloodmeal, and symptoms include fever, headaches, formation of canchre in the bite location, and, more rarely, hepatosplenomegaly [4]. The parasite reproduces through binary fission, and evades human lytic factors due to being completely enveloped by a variant surface glycoprotein (VSG), which is highly immunogenic [7][8]. This glycoprotein is recognized by the host immune system, which proceeds to produce antibodies against it, curbing the parasite infection. During growth, however, about 0.1% of new *T. brucei* cells resulting from cell division express not the original parental VSG, but a different one, allowing that subpopulation to escape the action of the recently produced host antibodies [7][8][9]. This subpopulation then, proceeds to grow, leading to the recognition of the new VSG by the host immune system, the production of new antibodies, and the curbing of the parasite growth, only to allow a new 0.1% subpopulation, expressing a different VSG, to escape once again. This cycle repeats, preventing the immune system from eliminating all parasites [4][7][8]. *T. brucei* encodes several hundred genes for VSGs, and only one is expressed at a time, making the complete elimination of the parasite by the host immune system extremely difficult [7][8][9]. The second stage, called meningoencephalitic, is characterized by the invasion of the host central nervous system, and symptoms include sleep

disorders, tremors, paralysis of limbs, and, in some cases, psychiatric disorders such as irritability and aggressive behavior [4]. The disturbance of the sleep/wake cycle during this step is the origin of the name sleeping sickness [4].

1.3 *T. brucei* as a model organism

The majority of studies using *T. brucei* are performed on either the insect procyclic form or the bloodstream trypomastigote forms, which are easily cultured *in vitro* and *in vivo*, and have many tools available for genetic manipulation, including the full genome available online [1][10]. In both cases, the parasite cell has an elongated, “corkscrew” shape of about 15 – 30 μm , is capable of motility with the assistance of a single flagellum, and presents the expected compartmentalized cell organization of eukaryotes (**Figure 1.2**) [4]. One notable difference from other eukaryotes, however, is the presence of a single, tube-shaped mitochondrion that runs through the entire cell (**Figure 1.2**) [4][11]. Inside this single mitochondrion, the mitochondrial DNA can be found densely packed in a series of concatenated circles, generating a structure called kinetoplast, the defining characteristic of the class *Kinetoplastida*, in which trypanosomes are included (**Figure 1.2**) [11]. The presence of a single mitochondrion also means that trypanosomes have three very distinguishable compartments: nucleus, cytoplasm, and mitochondrion, making them an excellent model for studies of compartmentalization and subcellular localization [11]. Furthermore, trypanosomes present numerous unique biochemical pathways that distinguish

them from other eukaryotic systems, including, but not limited to, genome organization, subcellular localization of proteins, mechanisms to express both nuclear and mitochondrial genome, RNA editing, and mRNA and tRNA splicing (discussed below) [10][11][12].

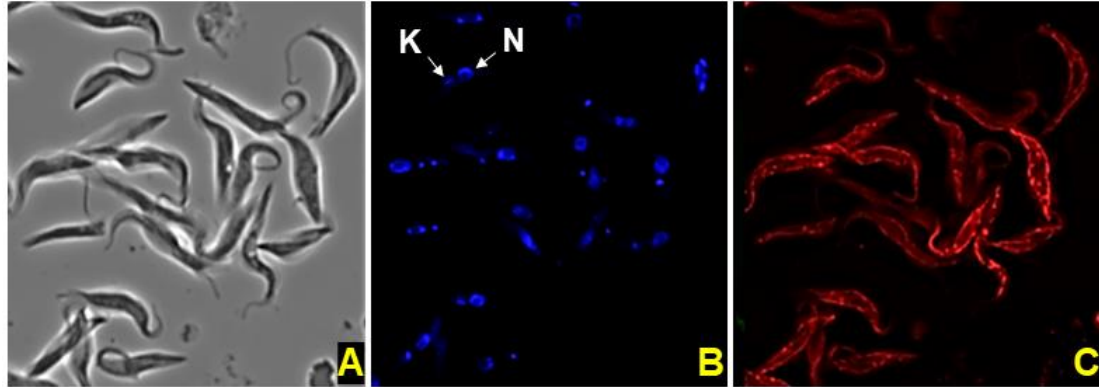


Figure 1.2 *Trypanosoma brucei brucei*

Insect procyclic trypomastigote form of *T. brucei brucei* parasites as observed under fluorescence microscopy. **A.** Bright-field microscopy denoting the elongated shape of the cells, and the presence of a single posterior flagella. **B.** 1,4',6-diamidino-2-phenylindole (DAPI) staining revealing the nucleus (N) and kinetoplast (K) in the cells. **C.** Mitotracker staining revealing the single tubular mitochondrion.

1.4 RNA Splicing in *T. brucei*

In eukaryotes, genes are typically interrupted by intervening sequences (introns), which must be removed from their respective primary transcripts in order to generate functional RNAs. These may be found intercalated with the exons of protein-coding messenger (m)RNAs, ribosomal (r)RNAs, and transfer (t)RNAs, in numbers that vary widely across different species. The removal of introns and ligation of the exons of mRNAs into a mature transcript is called splicing, which in eukaryotes, is catalyzed by the action of the spliceosome, a specialized ribonucleoprotein complex. The spliceosome is composed of five small nuclear (sn)RNAs called U1, U2, U4, U5, and U6, each complexed with at least seven proteins, forming small nuclear ribonuclear proteins (snRNP), which come together to form the core of the complex. Once the spliceosome binds an intron-containing RNA, splicing is achieved by two transesterification steps: first, the 2' hydroxyl group of an internal adenosine (present close to the 3' end of the intron) carries out a nucleophilic attack on the phosphate group of the nucleotide at the 3' end of the 5' exon, generating a 2'-5' phosphodiester bond, which gives rise to a characteristic lariat intermediate (**Figure 1.3 A**). Second, the now free 3'OH of the 5' exon attacks the phosphate group between the intron and the 3' exon, splicing the two exons together and releases the intron lariat (**Figure 1.3 A**). While these reactions are usually catalyzed at traditional exon-intron junctions, generating canonical transcripts, alternative splicing may also take place. This phenomenon, which is typical of mRNAs, involves the differential removal and/or maintenance of

introns, generating a mature transcript that differs in sequence, and consequently length, structure, stability, and translational efficiency, when compared to the canonical transcript. It is widely considered that alternative splicing ultimately contributes to genetic variability, as multiple messages can be generated from a single open reading frame (ORF) [13]. An extreme example of this is the human genome, on which upwards of 95% of multi-exon genes undergo alternative splicing [14].

The genome of *T. brucei* encodes only two mRNA introns and one tRNA intron (tRNA^{Tyr}_{GUA}, discussed below) [10]. Nevertheless, due their unique genome organization, mRNA splicing, in the form of trans-splicing, is widespread in *T. brucei*. In trypanosomes the majority of protein-coding genes are arranged in long polycistronic transcription units containing dozens of genes each, which are processed via trans-splicing in order to generate functional mRNAs [15][16]. Curiously, unlike bacterial operons, there is no functional link between genes housed inside a single transcriptional unit, and distribution appears to be random [10][17]. Transcription takes place without the action of general transcription factors, generating long polycistronic units, which are then processed by the spliceosome, including the cleavage of the individual mRNAs, and the addition of a 5'-capped spliced leader (SL) to each transcript [15][16]. The SL is a 39 nucleotide-long sequence that is transcribed and 5' capped independently, and added to all mRNAs in *T. brucei* via trans-splicing (**Fig. 1.3B**), thanks to the binding of the trans-splicing specific sRNA SLA1. [15][16].

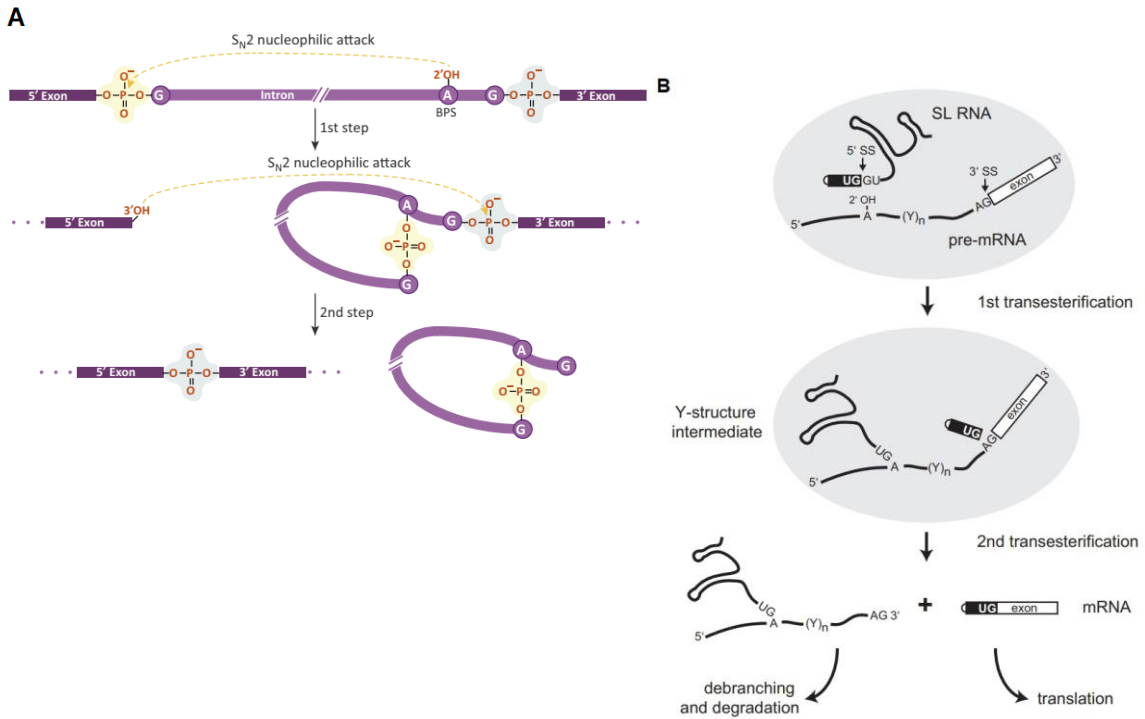


Figure 1.3 RNA Splicing

Overview of mRNA splicing mechanisms. **A.** General mechanism of cis-splicing. From top to bottom: in the first step, the 2' hydroxyl group of the intron adenosine carries out a nucleophilic attack on the phosphate group of the nucleotide at the 3' end of the 5' exon. In the second step, the now free 3'OH of the 5' exon attacks the phosphate group between the intron and the 3' exon, splicing the two exons together and releases the intron lariat. Adapted from Papasaikas & Valcárcel - The Spliceosome: The Ultimate RNA Chaperone and Sculptor [18]. **B.** General mechanism of trans-splicing. From top to bottom: in the first step, the 2' hydroxyl group of the protein-coding mRNA adenosine carries out a nucleophilic attack on the phosphate group of the nucleotide at the 3' end of the spliced leader (SL) junction site. This generates an intermediate in form of a Y-

structure. In the second step, the free 3'OH of the 5' SL attacks the 3' splice site of the protein-coding exon. The result is a protein-coding mRNA that contains the capped 39 nt SL; the remaining SL sequence ligated to the 5' UTR of the protein-coding mRNA is released in the form of a Y-structure, which undergoes debranching and degradation. Adapted from Preußner et al. - mRNA splicing in trypanosomes [19].

1.5 tRNA splicing

tRNAs are a class of short, non-coding RNAs, that traditionally function as adapter molecules, facilitating the transfer of information from mRNAs into proteins. This is achieved by delivering specific amino acids, with which the tRNAs are charged with, to the ribosome during translation. The delivery is dependent on the decoding of the mRNA message, which is read in nucleotide triplets known as codons. Each tRNA has in its structure an anticodon sequence that base-pairs with the mRNA codon, once inside the ribosome, leading to the formation of a peptide bond between the nascent polypeptide chain and the new peptide brought by the tRNA. There are a total of 64 codons that encode for 22 amino acids and three stop codons (UAG, UAA, UGA, known as “amber”, “ochre”, and “opal”), composing what is known as the genetic code. Since there are more codon possibilities than amino acids and stop codons, multiple codons can redundantly encode the same amino acid, in a phenomenon called degeneracy.

tRNAs are usually 75-100 nucleotides in length, and fold in characteristic secondary (clover leaf) and tertiary (L-shape) structures (**Figure 1.4**). The molecules are also heavily post-transcriptionally modified, undergoing editing and modification events that contribute to stability and function.

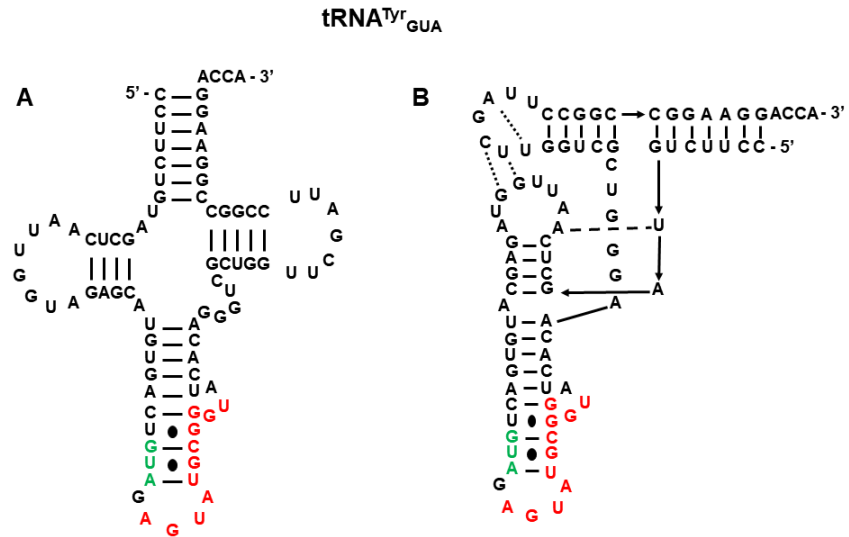


Figure 1.4 tRNA^{Tyr}_{GUA}

Structure of tRNA^{Tyr}_{GUA} of *T. brucei*. Exons are represented in black, the single intron is represented in red, and the anticodon “GUA” is represented in green. **A.** Secondary (cloverleaf) structure. **B.** Tertiary (L-shape) structure depicting tertiary contacts between the tRNA arms.

Moreover, as it is the case with mRNAs (described above), tRNAs may also be interrupted by introns that must be removed in order to generate a mature transcript (**Figures 1.4 and 1.5**). These introns are usually found in what is called the canonical position, interrupting the exons between positions 37 and 38 of the tRNA, but may also be present elsewhere (**Figure 1.5**). Indeed, introns can be found interrupting tRNAs in all domains of life: Bacteria, Archaea, and Eukarya, with considerable differences with how they are handled. In Bacteria, where tRNA introns are uncommon, the intervening sequences are removed by self-splicing mechanisms that are independent of protein components [20]. In Archaea and Eukarya, where tRNA introns are more prevalent, the intervening sequences are dealt with by specialized enzymes that recognize conserved structural elements in the tRNA and catalyze the endonucleolytic cleavage of the intron, followed by ligation of the exons [21]. In the case of Archaea, the main conserved tRNA splicing element is a bulge-helix-bulge motif (BHB) (**Figure 1.5**) [22]; In the case of Eukarya, the main conserved element seems to be a nucleotide pairing between the anticodon and the intron sequence (A-I pair, more below) (**Figure 1.5**) [23].

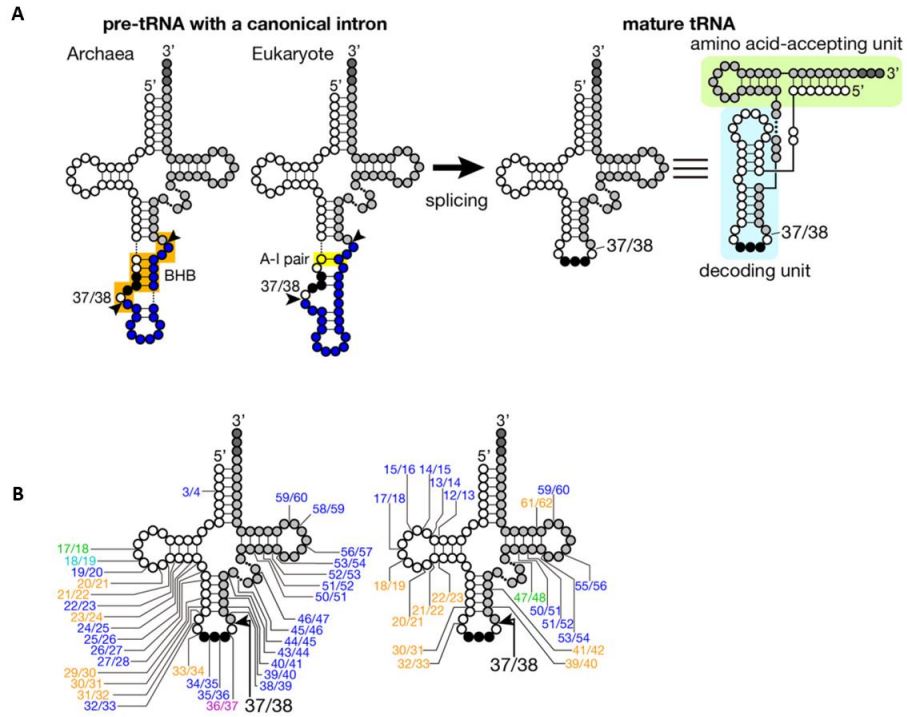


Figure 1.5 tRNA Introns

Locations of the tRNA introns in Archaea and Eukarya. **A**. The canonical 37/38 location is depicted, with intron cleavage sites denoted by black arrows. The BHB and A-I motifs are also denoted. **B**. Non-canonical locations of introns that have been described in Archaea (left) and Eukarya (right). Adapted from Yoshihisa 2014 - Handling tRNA introns, archaeal way and eukaryotic way [24]

1.5.1 Eukaryotic tRNA Splicing Pathways

In eukaryotes, the first step of tRNA splicing, intron cleavage, is catalyzed by a conserved heterotetrameric enzyme called tRNA splicing endonuclease (TSEN, further discussed below in section 1.6, and in chapter 3) (**Figure 1.6**) [25]. This is followed by a ligation step, catalyzed by either Trl1 (in most eukaryotes, in what is called 5' → 3' ligation pathway) (**Figure 1.6**), or a complex containing Archease and RtcB (in vertebrates, in what is called 3' → 5' ligation pathway) [26][27]. Interestingly, when TSEN catalyzes the cleavage of tRNAs, it generates two unusual ends in both the exons and the intron: the 3' ends contain a 2',3'-cyclic phosphate group; whilst the 5' ends contain a 5'-hydroxyl, which must be resolved prior to exons ligation and intron degradation (**Figure 1.6**) [28][26]. Finally, in the 5' → 3' pathway (Trl1), a leftover “dangling” 2'-phosphate must be removed from the splice junction of the tRNA by a third, specialized enzyme called Tpt1 (**Figure 1.6**) [26][29].

The second enzyme in the 5' → 3' pathway, Trl1, was originally described in *Saccharomyces cerevisiae*, as a multi-functional enzyme containing three domains: a C-terminal cyclic phosphodiesterase domain; a polynucleotide kinase domain; and a N-terminal adenylyl transferase domain that is similar to the one found in the T4 bacteriophage ligase [12][26]. In order, these domains are responsible for: first, the hydrolysis of the 2',3'-cyclic phosphate group; second, the phosphorylation of the 5' hydroxyl group, and third, the ligation of the two tRNAs halves [26][30].

The third and final enzyme in the 5' → 3' pathway, Tpt1, was also originally described in *S. cerevisiae* [29]. This phosphotransferase catalyzes the unusual reaction in which the splice junction leftover 2'-phosphate is transferred to NAD, generating the NAD derivative ADP-ribose 1',2'-cyclic phosphate [29].

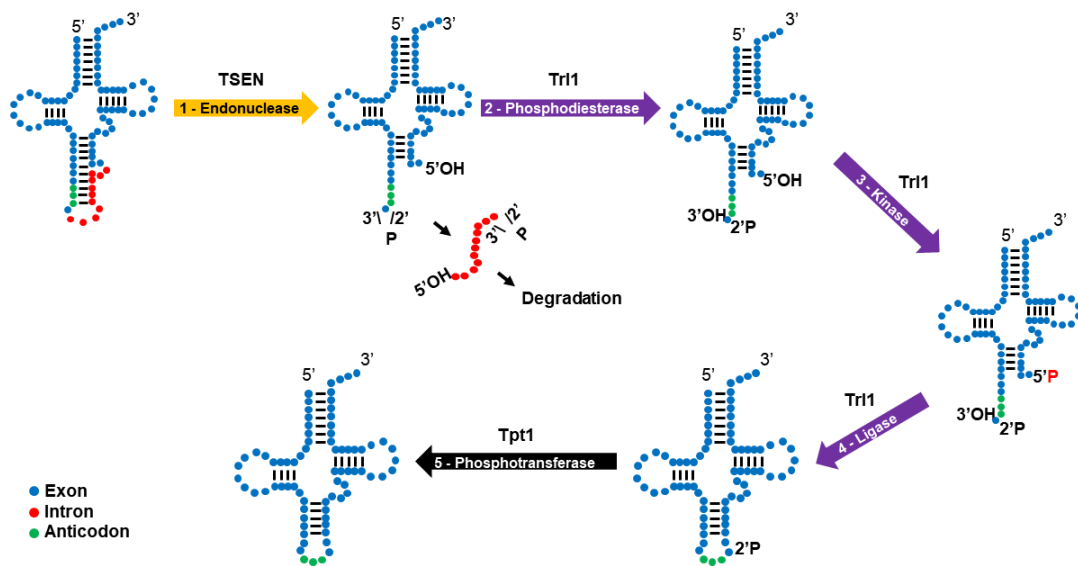


Figure 1.6 tRNA Splicing Pathway

Overview of the 5' → 3' tRNA splicing pathway, denoting five steps. From left to right: the pre-tRNA containing a canonical intron (position 37/38) undergoes endonucleolytic cleavage catalyzed by TSEN (yellow arrow). Following that, the removed intron is quickly degraded and the tRNA exon ends are subjected to cyclic phosphodiesterase (3' end) and kinase (5' end) activities prior to ligation, all catalyzed by Trl1 (purple arrows). Finally, the remaining 2' phosphate is removed by Tpt1 activity (black arrow).

1.6 Recent Findings in the Eukaryotic tRNA Splicing Endonuclease

In all domains of life, tRNAs may be transcribed containing intervening sequences (introns). How many transcripts from the tRNA gene pool contain introns varies widely from species to species, but in all cases, when present, introns must be excised in order to generate a mature tRNA that can be used for translation. Splicing of tRNAs, is therefore, essential [24]. In eukaryotes, this event is catalyzed by a conserved, specialized enzyme called tRNA Splicing Endonuclease (TSEN), composed of four subunits called TSEN2, 15, 34, and 54 (**Fig. 1.7**) [24][25]. Subunits TSEN2 and 34 each contain an RNA endonuclease active site at the C-terminus, with conserved tyrosine, histidine and lysine, residues that are believed to cleave RNA through an acid-base catalysis mechanism (**Fig. 1.7**) [24][25]. Subunits TSEN15 and 54 contain no enzymatic active sites, but are required for tRNA splicing nevertheless, possibly through other mechanisms, including substrate recognition and correct assembly of the enzyme complex (**Fig. 1.7**) [24][25]. In our project, we have investigated the blood-born pathogen *Trypanosoma brucei* TSEN homolog (TbSEN), attempting to determine the core enzyme composition, reconstitute enzymatic activity, and assay substrate specificity, all to various degrees of success. Bioinformatic analysis and biochemistry approaches including tandem affinity purification assays (TAP), and size-exclusion chromatography (SEC), revealed three *T. brucei* homologs to subunits TSEN2, 15, and 34, named TbSEN17, 12 and 22 after their approximate molecular weights, all smaller than their counterparts in other organisms, and co-

purifying with an approximate weight of 66 kDa. Our studies did not produce a homolog for the largest subunit TSEN54, however, the 66 kDa enzyme purified from *T. brucei* cultures was capable of tRNA cleavage in assays using *in vitro* transcribed *T. brucei* pre-tRNA, indicating that the subunit is either not required for activity, or that TbSEN has an alternative composition, possibly an heterotrimer, on which TSEN54 is missing. In this summary, I will review the main findings published in three recent articles that have pushed the boundaries of our previous understating of this enzyme, comparing them to previously published information. I will also relate the findings, when appropriate, to our own studies in *T. brucei*.

1.6.1 Composition of TSEN and the Role of CLP1 in Humans

As mentioned above, the eukaryotic enzyme is a heterotetramer composed of four core subunits: TSEN2, 15, 34, and 54 [25]. In humans, however, TSEN co-purifies with the additional polyribonucleotide kinase CLP1, a conserved member of the eukaryotic mRNA 3' polyadenylation machinery that has been implicated in the phosphorylation of the 3' ends of both tRNA exons and introns, although its actual role in tRNA splicing pathway remains somewhat unclear [31]. Mutations in CLP1 that lead to loss of kinase activity impact tRNA splicing, which in turn, lead to the implication of CLP1 in the splicing pathway, including maintenance of TSEN complex integrity, promotion of intron degradation, and even participation in a possible alternative tRNA ligation pathway [32].

Recently, the Stanley group was able to reconstitute human TSEN activity by using, first, a recombinant system based in *Escherichia coli*, and second, a mammalian expression system based on HEK293 cells [33]. For the prokaryotic system, all four subunits were expressed from a single vector in *E. coli* BL21, and purified using both a hexa-histidine C-terminally-tagged TSEN15, followed by SEC, with confirmation of the heterotetramer complex by multi-angle light scattering (MAL) analysis [33]. Activity assays performed with *in vitro* transcribed human pre-tRNA showed this enzyme to be active, indicating that the core enzyme, without CLP1, is capable of tRNA cleavage [33]. Indeed, attempts to generate a TSEN-CLP1 complex in *E. coli* were unsuccessful, indicating that, *in vivo*, the proteins must undergo additional post-translational modifications in order

to associate [33]. For the eukaryotic system, again all four subunits were expressed from a single vector, and purified with both FLAG and Strep tags, this time present in all subunits [33]. As before, activity assays performed with *in vitro* transcribed tRNAs showed the enzyme to be active, as long as all four subunits are co-expressed [33]. Co-expression of TSEN and CLP1 using this system led to the purification of a TSEN-CLP1 complex, but had no impact on the activity of the enzyme when tested *in vitro*, indicating that CLP1 is not required for tRNA cleavage [33]. Indeed, further investigations utilizing human and insect cells showed that depletion of CLP1 leads to an increase in tRNA splicing efficiency, detected by the accumulation of tRNA intronic circular RNAs (tricRNAs), the circularized excised tRNA introns that are known to be byproducts of metazoan tRNA splicing pathways [33]. These results indicate that, in spite of co-purifying with TSEN, CLP1 is not required for tRNA splicing, but rather, acts as a repressor of intron processing in animal cells, since the 3'-phosphorylated introns resulting from CLP1 activity cannot be correctly circularized down the processing pathway [33].

Interestingly, in our own studies with TbSEN, we had similar results attempting to purify the individual subunits using *E. coli* BL21. TbSen subunits are TbSEN12 (homolog of TSEN15), TbSen17 (TSEN34), and TbSEN22 (TSEN2). In our studies, when using affinity purification with hexa-histidine tags followed by SEC, only TbSEN12 was soluble when expressed alone, with TbSEN22 being partially soluble, and TbSen17 completely insoluble and unrecoverable from the

pellets. Recombinant TbSEN17 was successfully recovered with the use of a solubility-increasing maltose-binding protein (MBP) tag, but, as with the other two subunits, no tRNA cleavage activity was detected *in vitro*. Co-expression of all three subunits from a single vector in *E. coli* increased solubility for TbSEN17 and 22, but failed to reconstitute activity as well.

1.6.2 Insights into the Structure and Catalysis Mechanism of TSEN

In the year following the Stanley group study, the Trowitzsch group reconstituted the activity of human TSEN, this time utilizing a system that takes advantage of the vector series MultiBac, which allows expression of eukaryotic proteins in insect cells [34]. This reconstitution allowed the group to further investigate the structure, activity, and assembly of TSEN. First, co-expression analyses followed by SEC showed that the TSEN subunits can form stable (but inactive) heterodimers: TSEN15-34, and TSEN2-54 [34]. Furthermore, stoichiometric mixtures of the dimers can form active heterotetramers, corroborating previously published data obtained from yeast-two hybrid assays in *S. cerevisiae*, and suggesting that TSEN subunits assemble first as inactive heterodimers, and then form an active heterotetramer [34]. Following that, to further investigate the enzyme structure, the group then performed x-ray crystallography on the TSEN15-34 heterodimer [34]. Crystallization of the whole subunits proved difficult, so the group resorted to limited proteolysis assays followed by SEC in order to obtain the smallest possible heterodimer, which ended

being composed of residues 23-170 of TSEN15, and 208-310 of TSEN34 [34]. This smaller heterodimer was then successfully crystalized, and revealed two domain-swapped TSEN34 (bound by a helix in the N-terminus), each bound to TSEN15 at their C-terminus [34]. While the domain-swap is probably an artifact of the limited proteolysis assay, the 2.1 Å crystal structure obtained allowed the study of the interface between TSEN34 and 15, revealing a typical endonuclease fold harboring the catalytic triad Tyr²⁴⁷/His²⁵⁵/Lys²⁸⁶, two structural water molecules, and a conserved eukaryotic motif YY, which is implicated in structure stabilization [34]. Considering these structures are conserved across eukaryotic and archaeal endonucleases, this data strongly corroborates the idea that TSEN is evolutionary conserved, and may have originated from a common ancestor through gene duplication and differentiation [34]. Furthermore, the presence of the catalytic triad in the fold corroborates the hypothesis that these residues are, indeed, related to a general acid-base catalysis mechanism, conserved throughout archaeal and eukaryotic endonucleases [34]. Truly, in the papers reviewed in this summary, substitutions made in the catalytic triad of either histidine (the putative general acid), or all three residues for alanine were used to generate inactive enzymes [33][34][35].

1.6.3 Substrate Specificity of TSEN

As stated above, TSEN targets and cleaves the introns from pre-tRNAs, a crucial step in tRNA maturation, however, our knowledge of the enzyme substrate

recognition is somewhat limited. The archaeal TSEN homologs have been shown to recognize substrate based on a bulge-helix-bulge (BHB) motif, on which two bulges of three nucleotides are separated by a helix of four nucleotides [24]. In such case, the intron itself seems to be the main determinant for splicing, and as long as the BHB motif is present, the enzyme is able to cleave the intron from any position in the tRNA [24]. A second mechanism also described in archaea, is the presence of two anticodon-intron (A-I) base pairs, that were shown to be required for splicing of introns in the anticodon loop, and seem to be related to structural stability of the tRNA [24]. Eukaryotic pre-tRNAs contain one A-I base pair, formed by a pyrimidine located two nucleotides upstream of the anticodon and a purine located three nucleotides upstream of the 3' splice site, inside the intron sequence, but no BHB motifs [24]. Interestingly, work performed on *Xenopus* demonstrated the eukaryotic enzyme is capable of recognizing the BHB motif when using a hybrid archaeal-eukaryotic pre-tRNA for cleavage assays, indicating an ancestral mechanism for pre-tRNA recognition [36]. The mature structure of tRNA has also been suggested to play a role in substrate recognition in Eukaryotes, including interaction with conserved nucleotides present in the tRNA exons, and a TSEN54-dependent "ruler" mechanism suggested in *Saccharomyces cerevisiae*, where the enzyme accurately measures the pre-tRNA mature structure in order to position the TSEN2/34 active sites at the correct cleavage locations [24]. Finally, the *S. cerevisiae* TSEN has also been shown to cleave the mitochondrial *CBP1* mRNA through recognition of a secondary structure motif, indicating that the eukaryotic

TSEN may possess a broader substrate specificity than previously thought [37]. The three studies reviewed in this summary have reinforced this idea: first the Stanley group showed that human TSEN is capable of cleaving short, “mini” intron constructs that include only the anticodon loop, *in vitro* [33]. This activity is not detected when using a catalytically dead mutant TSEN, indicating that human TSEN does not require the full tRNA cloverleaf structure for activity [33]. This knowledge was then, further developed by the Trowitzsch group, who showed through fluorescence anisotropy assays that human TSEN binds to both mature and pre-tRNA molecules with very similar affinities, and that the A-I base pair is indeed important for cleavage activity, but that the identity of the nucleotides that form said pair is not [34]. Perhaps the most innovative work on this matter, however, was performed by the van Hoof group more recently. Based on the idea that TSEN may have a broader substrate specificity than tRNAs, the group utilized a protocol of parallel analysis of RNA ends (PARE) to identify possible mRNA splicing substrates in *S. cerevisiae* [35]. This protocol is based on the conserved mRNA decay pathways housed in eukaryotes: briefly, when RNA is cleaved by an endonuclease, a 5' monophosphate is left behind (either by the endonuclease activity, or by a subsequent phosphorylation, depending on the pathway) [35]. The 5' monophosphate becomes target for subsequent RNA degradation by the conserved 5'→ 3' Xrn1 and Rat1 exonucleases in the cytoplasm and nucleus, respectively [35]. Depletion of these enzymes leads to accumulation of cleaved 5' monophosphate RNAs in the cell [35]. Taking advantage of this, the PARE protocol

ligates a linker to the 5' end of the accumulated 5' monophosphate RNAs in an Xrn1 and/or Rat1 depletion background, allowing for their deep sequencing and identification [35]. By comparing the library of accumulated RNAs obtained from the Xrn1/Rat1 depletion background to the library of accumulated RNAs obtained from both Xrn1/Rat1 and TSEN depletions, the group was able to identify which RNAs are most likely cleaved by TSEN (meaning, the RNAs that do not appear in the library when TSEN is depleted) [35]. This comparison led to the identification of 39 RNAs, out of which the most promising candidates were all mRNAs of mitochondrial proteins: COQ5, PKP2, DLD1, ERV1, MIS1, YHRO33W, MDL1, and the already known CBP1 [35]. Remarkably, the identified mRNAs do not share secondary structure motifs with either tRNAs or CBP1, but do contain a conserved motif upstream of the cleavage site that is enriched for adenines (A) at position -1 (and to a lesser extent, positions -2 and -3), that was shown to be required for efficient cleavage by TSEN, indicating the enzyme is capable of recognizing mRNAs using different determinants than those utilized for tRNAs [35]. Put together, these findings lead the group to propose a novel mRNA decay pathway, based around the participation of TSEN, called tRNA endonuclease-initiated decay (TED) [35].

In *T. brucei*, an equally remarkable substrate recognition mechanism was described in a previous study from our group: the pre-tRNA^{Tyr} intron must be edited in at least two out of three possible positions before undergoing splicing by TbSEN [12]. In this organism, the genomic-encoded intron does not conform to the intron-

exon structure described as canonical in other eukaryotes, and the editing events, performed by yet unidentified enzymes, seem to correct that, including the generation of the required A-I base pair [12]. Whether the TbSEN substrate recognition mechanism relies on other determinants remains to be uncovered.

1.6.4 TSEN and Human Disorders

Mutations in all four TSEN subunits and CLP1 have been linked to a subset of human neurodegenerative disorders called pontocerebellar hypoplasia (PCH), which affect neurons located in the cerebellum and pons [38]. Intriguingly, the identified mutations are neither located in the catalytic site of TSEN, nor in particularly conserved regions of the proteins, meaning their role in disorder onset remained unclear [34]. Recently, the Trowitzsch group investigated the effects of a number of these mutations, utilizing recombinant versions of mutant TSEN subunits in pull down experiments in HEK293 cells, followed by Western blotting, differential scanning fluorimetry (DSF), and *in vitro* cleavage assays [34]. Interestingly, when compared to WT TSEN, the mutants presented no difference in complex assembly and pre-tRNA cleavage kinetics, but showed reduced denaturing temperatures that ranged from 6.5 to 1.2° C, depending on the mutation [34]. These results suggested that a reduced thermostability may be responsible for PCH phenotypes, but left the group wondering why there was no detectable effect in assembly or pre-tRNA cleavage [34]. Considering the low abundance of TSEN in human cells (about 100 molecules per cell), it was possible that the

deleterious effects of reduced TSEN stability may have been hidden by the high expression levels of the recombinant system, and by the *in vitro* cleavage assays, so the group proceeded the investigations by utilizing patient-derived skin fibroblasts containing the common PCH mutation TSEN54^{A307S} (present in about 90% of recognized TSEN-linked PCH) [34]. In contrast to previously tested recombinant TSENs, lysates obtained from these cell lines presented drastic reduction in pre-tRNA splicing efficiency when compared to control, as well as unbiased accumulation (up to 6-fold) of pre-tRNAs, as showed by hydro-tRNA seq [34]. Furthermore, immunoprecipitation followed by Western blot analysis utilizing α -TSEN34 antibodies showed a reduction in TSEN2 and 54 co-precipitation, indicating that, while the steady-state of each individual subunit was not altered, the association between them was compromised [34]. Taken together, these results indicate that TSEN-linked PCH mutations leads to thermal destabilization of the proteins *in vivo*, which in turn, leads to compromised complex assembly and pre-tRNA cleavage efficiency [34]. The reasons for why the PCH phenotype is present only in a subset of neurons, when the reduced tRNA cleavage activity can be detected in other cell types such as skin fibroblasts, remains undisclosed. It is possible that cerebellar and pons neurons are particularly susceptible to the accumulation of pre-tRNAs, and that other cells can tolerate it, or that the impaired TSEN activity may affect cerebellum and pons-specific tRNAs, such as isodecoders that are crucial for specific tissue development, or tRNAs that act as

signaling molecules, both cases having been previously described in mammals [34].

1.6.5 Final Considerations

It is inspiring to see the advancements made in the knowledge of eukaryotic tRNA splicing and TSEN: in under two years, we were supplied with publications describing the reconstitution of human TSEN activity in multiple systems, paving the way for studies of substrate specificity, complex assembly, structure crystallization, and eventual relationship to a group of neurodegenerative disorders. In our studies on TbSEN, we stopped short of reconstituting activity in *S. cerevisiae*, and while there are no disorders to be studied in *T. brucei*, considering the uniqueness of this TSEN homolog, I am confident that a reconstituted enzyme will allow the uncovering of unusual steps in this particular tRNA splicing pathway, as well as the investigation of potential TbSEN inhibitors, which in turn, may pave the way to novel treatments for trypanosomiasis.

1.7 Overview of RNA Degradation Pathways

As it is the case with other molecules in the cell, transcripts from all RNA polymerases undergo a continuous cycle of synthesis and decay that helps keeping their biological function (in this case gene expression) properly regulated. In the case of mRNAs, which exist largely for the purpose of protein synthesis, the number of proteins produced from a single transcript can be controlled not only by

translation efficiency, but also by the rate of transcription, stability of the transcript, and rate of decay of the molecule. Herewith, old, damaged, and no longer necessary transcripts must be dealt with before they accumulate in the cell, generating potentially toxic proteins.

There are three major classes of enzymes involved in three different activities for RNA decay: 5'→3' exonucleases; 3'→5' exonucleases; and endonucleases. Concerning mRNAs, in the first class, after polyA shortening (see below), the transcript is decapped at the 5' end by a specialized enzyme, such as DCP2 and NUDT16. This recruits specialized enzymes to the 5' end of the RNA, which is then subjected to exonucleolytic cleavage by proteins such as XRN1 and RAT1 (**Figure 1.8**). In the second class, the poly-A tail at the 3' end is shortened by deadenylases that include PARN, PAN2, PAN3, and/or polyuridylated by terminal uridylyltransferases (TUTases) such as TUT4. This recruits enzymes to the 3' end of the RNA, which is then subjected to exonucleolytic cleavage by proteins such as Dis3L2, and the exosomal components RRP44 and RRP6 (**Figure 1.8**) [39]. The majority of mRNA decay in the cell is performed through exonucleolytic cleavage, and both 5'→3' and 3'→5' cleavage may happen concomitantly for the same transcript (**Figure 1.8**). Finally, for the third class of enzymes, some mRNAs undergo an endonucleolytic cleavage performed by proteins such as PMR1 and IRE1, somewhere in the middle of the ORF. This releases a 5' and a 3' end that can be targeted by exonucleases from the previous two classes (**Figure 1.8**).

These three classes of enzymes are conserved among Bacteria, Archaea, and Eukarya, where they compose the basis of RNA degradation in different pathways. Examples of these pathways for mRNAs in eukaryotes include: first, the nonsense-mediated decay (NMD), where transcripts containing premature stop codons are degraded in the nucleus by decapping followed by 5' exonucleolytic activity [40]; second, the "no-go" decay (NGD), where mRNAs bound to stalled ribosomes are subjected to endonucleolytic cleavage, followed by 5' and 3' exonucleolytic degradation [41]; third, the non-stop decay (NSD), where transcripts lacking stop codons (and therefore stalling ribosomes at their 3' ends) are degraded by recruited exosome components in a 3'→5' polarity [42]. Moreover, the nucleases responsible for these pathways are usually not acting alone, but rather, associated in complexes that include the exosome (both nuclear and cytoplasmic), the nuclear TRAMP complex, and the cytoplasmic Ski complex (also involved in viral suppression) [43].

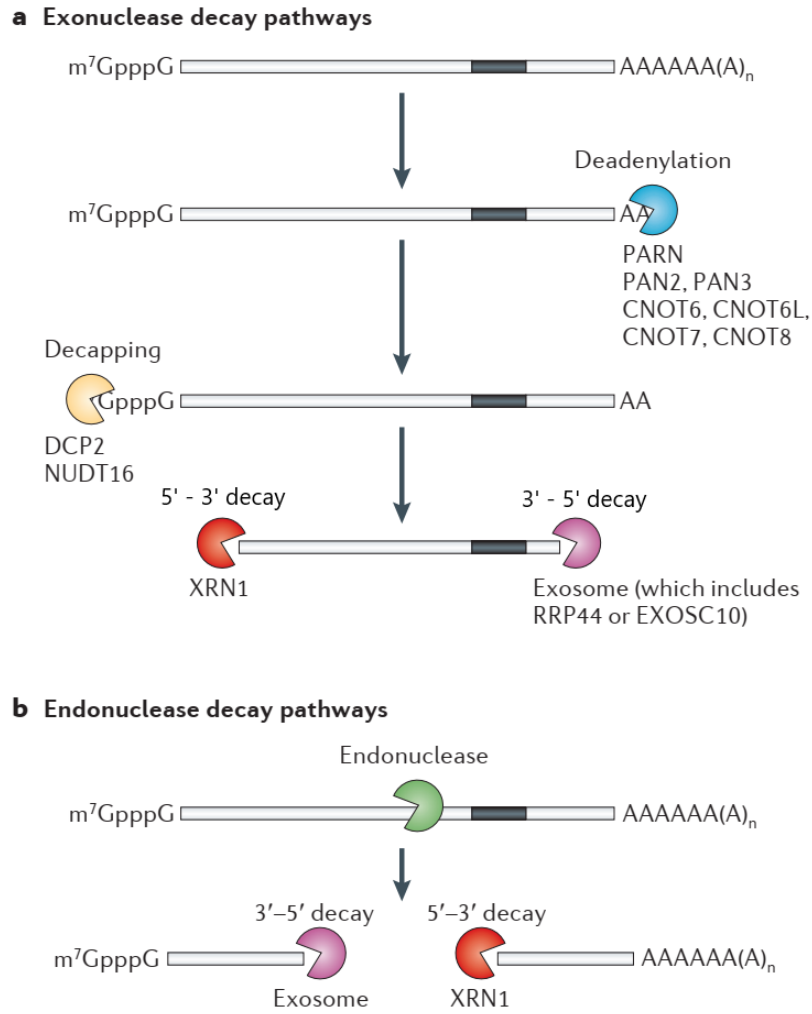


Figure 1.8 mRNA Decay

Overview of enzymatic activities involved in mRNA Decay. **A.** In the exonuclease pathways, the mRNA is decapped and/or deadenylated, followed by the activity of 5'→3' and 3'→5' polarity exonucleases. **B.** In the endonuclease pathway, an endonuclease first cleaves the mRNA inside the ORF, followed by transcript degradation by exonucleases of the corresponding polarity. Adapted from Schoenberg & Maquat 2012 - Regulation of cytoplasmic mRNA decay [44].

1.7.1 tRNA Degradation Pathways

As stated above, tRNAs are among the most stable RNAs in the cell, with long half-lives when compared to other transcripts. Nevertheless, accumulation of non-functional tRNAs may be deleterious to the cell, so they are subjected to similar surveillance and degradation pathways, involving the same enzymes denoted above. Surveillance and degradation of tRNAs has been generally classified into two major types: nuclear surveillance and rapid tRNA decay (RTD).

Nuclear surveillance is the earliest pathway in tRNA degradation. In this pathway, incorrectly transcribed, poorly processed, and hypomodified pre-tRNAs in the nucleus are recognized by Trf4, Air2 and Mtr4 from the TRAMP complex, which proceeds to oligoadenylate the tRNA at the 3' end (through Trf4 activity) [45]. This oligoadenylated tRNA is then targeted for 3'→5' endonucleolytic degradation by RRP6 from the nuclear exosome [45].

RTD is the following surveillance system for tRNAs in the cell. In this pathway, defective, undermodified and damaged mature tRNAs are recognized and degraded by the 5'→3' exonucleases RAT1 (in the nucleus), and XRN1 (in the cytoplasm), as well as the 3'→5' exonuclease RRP44 (cytoplasmic exosome) [46].

1.7.2 RNA Degradation Components in *T. brucei*

The *T. brucei* genome encodes homologs for the majority of the required components of the RNA surveillance and degradation systems described above, including the exosome components RRP44 and RRP6 [47], Dis3L2 [48], TUT3 and

4 [49], and a total of six homologs of XRN1, called XRNA-F [50]. The *T. brucei* exosome has been extensively studied, and seems to operate in similar fashion to other eukaryotes, being present both in the nucleus and the cytoplasm, and being recruited for RNA degradation during similar pathways [47]. Dis3L2 has not yet being assigned a function in *T. brucei*, but contains the conserved 3'→5' exonuclease active site previously described in yeast [48][51]. TUT3 and 4 contain the conserved TUTase active sites, but have also not being assigned functions [49]. Finally, XRNA but not B-F has been showed to be essential in *T. brucei*, and involved in mRNA degradation, in a similar fashion to XRN1 in yeast [50]. We further investigate the roles of these enzymes in tRNA degradation in chapter 2.

Chapter 2: tRNA^{Tyr} has an unusually short half-life in *Trypanosoma brucei*

Following transcription, tRNAs undergo a series of processing and modification events to become functional adaptors in protein synthesis. Eukaryotes have also evolved intracellular transport systems whereby nucleus-encoded tRNAs may travel out and into the nucleus. In trypanosomes, a complete set of tRNAs is also imported from the cytoplasm into the mitochondrion, which lacks tRNA genes. Differential subcellular localization of the cytoplasmic splicing machinery and a nuclear enzyme responsible for queuosine modification at the anticodon “wobble” position appear to be important quality control mechanisms for tRNA^{Tyr}, the only intron-containing tRNA in *T. brucei*. Since tRNA-guanine transglycosylase (TGT), the enzyme responsible for Q formation, localizes to the nucleus, and cannot act on an intron-containing tRNA, retrograde nuclear transport is an essential step in maturation. Unlike maturation/processing pathways, the general mechanisms of tRNA stabilization and degradation in *T. brucei* are poorly understood. Using a combination of cellular and molecular approaches, we show that tRNA^{Tyr} has an unusually short half-life. tRNA^{Tyr}, and in addition tRNA^{Asp}, also show the presence of slow-migrating bands during electrophoresis, we term these conformers: alt-tRNA^{Tyr} and alt-tRNA^{Asp} respectively. Although we do not know the chemical or structural nature of these conformers, alt-tRNA^{Tyr} has a short half-life resembling that of tRNA^{Tyr}; the same is not true for alt-tRNA^{Asp}. We also show that RRP44, which is usually an exosome subunit in other organisms, is involved in

tRNA degradation of the only intron-containing tRNA in *T. brucei* and partly responsible for its unusually short half-life.

2.1 Introduction

Transcription of tRNA genes in eukaryotes is catalyzed by RNA polymerase III (RNA Pol III), which generates molecules with 5' and 3' extensions. Depending on the organism, a variable number of tRNAs also contain introns, found between position 37 and 38 of the anticodon loop. Maturation of tRNA precursors by terminal definition, posttranscriptional modification, and splicing, shapes tRNA structure, function, and metabolic fate. For example, some modifications, particularly those occurring in the anticodon loop, are important for translational efficiency and/or accuracy; others may affect folding and/or the stability of the molecule. In trypanosomatids, which include members of the genus *Trypanosoma* and *Leishmania*, all tRNAs are encoded in the nucleus, while the mitochondrial genome is devoid of tRNA genes. Thus, mitochondria-destined tRNAs are exported to the cytoplasm and then imported into the mitochondrion, with initiator tRNA^{Met} being the only exception. During intracellular transport, tRNAs can be modified in any of these compartments [52].

In *T. brucei*, only tRNA^{Tyr} (Tb927.4.1219) contains an intron, which, similarly to *S. cerevisiae*, is spliced in the cytoplasm [53][54]. Apparently, trypanosomes maintain the eukaryotic tRNA splicing machinery to service a single tRNA, whose

unconventional features include one of the shortest known introns (11 nucleotides) that undergoes noncanonical base editing, a prerequisite for cleavage by the tRNA-splicing endonuclease [12]. The peculiarities extend to the mature molecule, which contains the modified nucleotide queuosine (Q) at the anticodon “wobble” position 34: the enzyme responsible for this modification is nuclear [55]. Hence, after splicing, this tRNA undergoes retrograde transport from the cytoplasm to the nucleus to receive Q, before being exported back into the cytoplasm [55]. Finally, both Q-modified and unmodified tRNA^{Tyr} co-exist in the cytoplasm and engage in translation, where the unmodified tRNA can decode the G-ending codons for tyrosine, while the Q-modified tRNA is necessary for the efficient translation of the U-ending codons [56]. Three other tRNAs (Asp, Asn and His) also contain Q, but since these do not contain introns, they are exported from the nucleus after Q formation, with presumably no need for retrograde nuclear transport [55]. Lastly, the Q-containing tRNAs are preferentially imported into the mitochondrion, but how the mitochondrial import machinery discriminates their unmodified counterparts is unclear [57].

Concomitantly to maturation, tRNAs are also subjected to quality surveillance. In *S. cerevisiae*, 5'-3' exoribonucleases XRN1 (cytoplasmic), and RAT1 (nuclear) perform the rapid tRNA decay pathway (RTD) which, eliminates hypomodified tRNAs to safeguard translation [46]. *T. brucei* encodes six orthologous XRN enzymes (A to F), but their functions in tRNA decay are unclear.

In many systems, the exosome, a multi-protein complex containing several 3'-5' exoribonucleases, orchestrates general and controlled RNA degradation, with the latter contributing to maturation of rRNA and other non-coding RNAs [58][59]. The *S. cerevisiae* exosome is formed by ten core protein components and associated ribonucleases RRP6 and RRP44 [60]. The *T. brucei* exosome contains many homologs of the exosome components from other systems, with the exception of RRP44 [47]. In *T. brucei*, RRP44 is an autonomous exoribonuclease found in the nucleus and cytoplasm [47][61]. In the former, it participates in rRNA maturation, but it may also play a role in polycistronic mRNA processing [47][61]. However, little is known about tRNA stability determinants and decay mechanisms in trypanosomes. Because a stable structure and extensive modifications protect tRNAs from degradation, in other systems, tRNAs are relatively long-lived, with half-lives exceeding 60 hours [62][63][64][65][66][67].

The unusual intracellular transport dynamics leading to persistence of tRNA^{Tyr} variants in the cytoplasm and nucleus raised the question of how tRNA^{Tyr} escapes degradation mechanisms that, in other systems, mediate the removal of improperly processed tRNAs, such as the rapid tRNA decay pathway of *S. cerevisiae* mentioned above. We assessed the relative stability of several tRNAs in *T. brucei* including tRNA^{Tyr}. Using Northern hybridization analysis, we show that tRNA^{Tyr} and tRNA^{Asp} have unusual isoforms, which we term alt-tRNA^{Tyr} and alt-tRNA^{Asp}, respectively, as opposed to “canonical” tRNA^{Tyr} and “canonical tRNA^{ASP}”, which we referred to as simply tRNA^{Tyr} and tRNA^{Asp}. We also show that tRNA^{Tyr}

has a strikingly short half-life. Thus, we explored the contribution of the 5'-3' RNA degradation pathway exemplified by XRN family members, and the 3'-5' pathway, exemplified by RRP6, Dis3L2, and RRP44, to this phenomenon. We find that RRP44 plays a role in the steady-state levels of alt-tRNA^{Tyr} and alt-tRNA^{Asp} and tRNA^{Asp}, but it has little effect on tRNA^{Tyr}. However, following actinomycin D treatment only the half-life of alt-tRNA^{Tyr} and tRNA^{Tyr} is increased, while the half-life of the equivalent tRNA^{Asp} species remained unchanged. In addition, out of the XRNs tested, only XRNE had a modest impact on the levels of alt-tRNA^{Tyr} but no effect on the other species. Taken together the decay kinetics of the different tRNA species suggest that the short half-life of tRNA^{Tyr} may be due to its unusual intracellular transport dynamics, while alt-tRNA^{Tyr} may serve as a repository for tRNA^{Tyr}.

2.2 Results

2.2.1 tRNA^{Tyr} has a relatively short half-life in *T. brucei*

Recent studies have highlighted targeting of hypomodified tRNAs by the rapid tRNA decay pathway (RTD), orchestrated in *S. cerevisiae* by different nuclear and cytoplasmic enzymes [68]. Given the elaborate intracellular transport dynamics of tRNA^{Tyr} in *T. brucei*, we analyzed total RNA samples by Northern blot hybridization with oligonucleotide probes for tRNA^{Tyr}. We observed two distinct hybridization signals: a 75-nt band corresponding to the expected size of the

mature molecule, and a slower-migrating band, resolving with a size consistent with approximately 125-nt (**Fig. 2.1 A**). Significantly, the size difference between the slower migrating band and the mature (~45 nt) is larger than what can be accounted for by 3' poly-U extensions previously described [69], and does not contain an intron [53] and **figure 2.2** in this work. We refer to it as an alternative isoform of the tRNA (alt-tRNA^{Tyr}) (**Fig. 2.1 A**). An alternative isoform was also detected in tRNA^{Asp} (Tb927.7.6824), but not in other tRNAs tested (**Fig. 2.2 and 2.4**). To investigate the behavior of alt-tRNA^{Tyr}, we grew *T. brucei* Lister 427 procyclic cells for 108 hours, allowing the parasites to reach stationary phase (**Fig. 2.1 B**). Samples were collected at 12h time intervals and analyzed by northern blot hybridization, revealing that alt-tRNA^{Tyr} relative amounts vary along with cell density, reaching a maximum of 45-55% of the total tRNA^{Tyr} at approximately 72h of growth, before stabilizing during the stationary phase, at approximately 40% of the late logarithmic phase (**Fig. 2.1 C-D**). However, the steady-state levels of the tRNA^{Tyr} remained constant (**Fig. 2.1 E**).

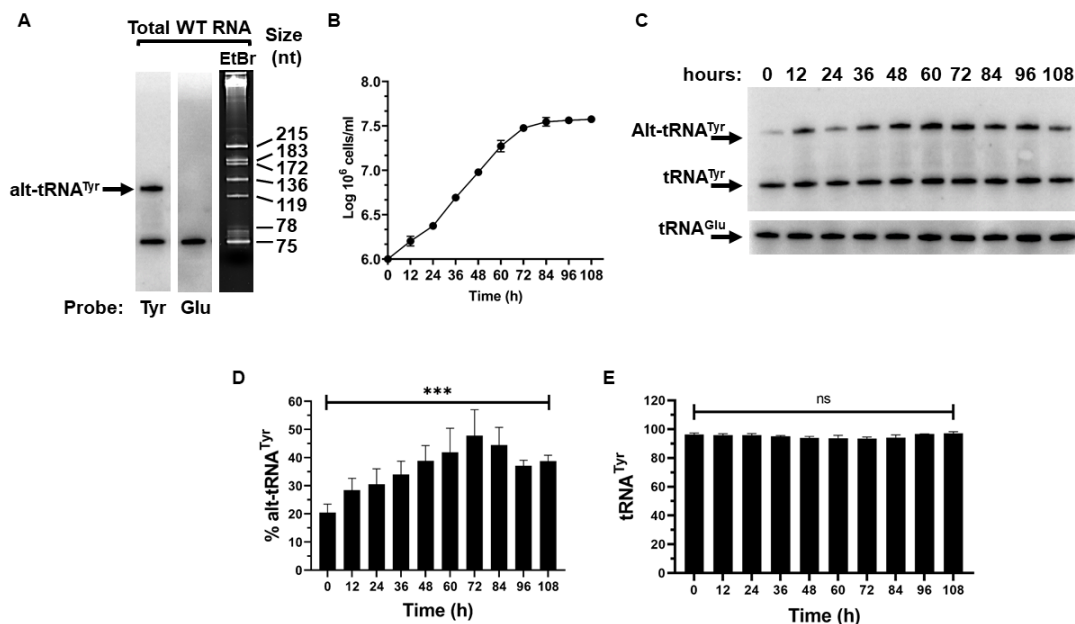


Figure 2.1 *T. brucei* tRNA^{Tyr} is present in two conformers

A. Northern blot hybridization performed on total RNA sample extracted from *T. brucei* reveals two forms of tRNA^{Tyr}, including the mature (75-nt) band and a higher (approx. 120-nt), alternate conformer. **B.** Cumulative triplicate growth curve of WT *T. brucei* cells where total RNA was collected at every time point. **C.** Northern blot hybridization performed on the extracted total RNA samples revealing the mature and alternate conformers of tRNA^{Tyr}. The tRNA^{Glu} was used as loading control. **D.** Plotted amounts of alternate conformer (alt-tRNA^{Tyr}) in relation to tRNA^{Tyr}. **E.** Plotted amounts of mature tRNA^{Tyr}. Plotted amounts of mature tRNA^{Tyr} in D and E are the result of at least 3 biological replicas. Asterisks denote significance as determined by a 1-way ANOVA yielding a P-value of 0.0003 for the data in D. “ns” stands for non-significant by the same test.

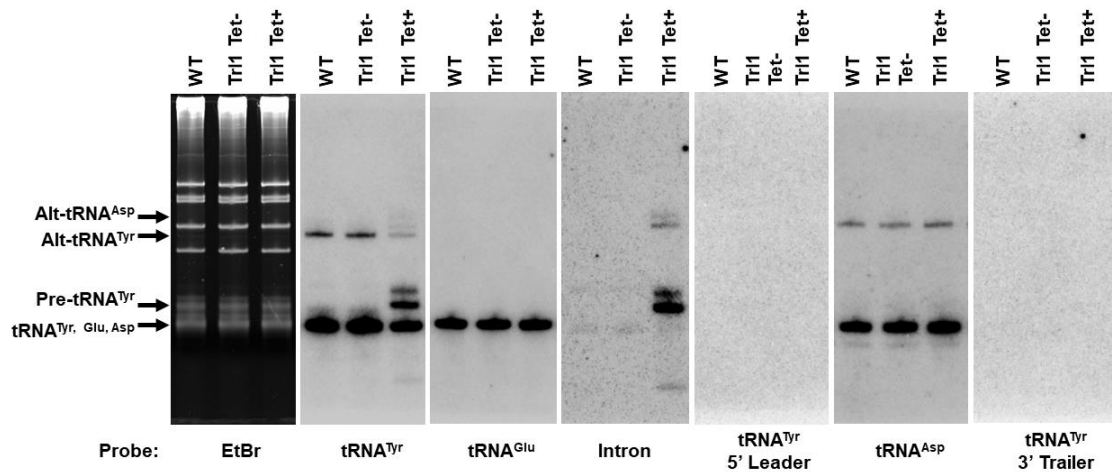


Figure 2.2 Alt-tRNA^{Tyr} does not contain an intron and neither alternative conformer contains 5' or 3' extensions corresponding to the genomic flanking regions

From left to right: Northern blot hybridization performed on total RNA sample extracted from WT and Trl1 RNAi strains of *T. brucei* utilizing probes specific for tRNA^{Tyr} (mature, intron-specific, 5' leader, and 3' trailer), tRNA^{Glu}, and tRNA^{Asp}. Probes: tRNA^{Tyr} CCTTCCGGCCGGAATCGAACCAGCGAC; tRNA^{Tyr} (Intron) GATACCTGCAAACCTCTAC; tRNA^{Tyr} (Leader) CTGACTGCCGCAGTAGTCGGG; tRNA^{Tyr} (Trailer) CGTTTGTGGGCGTGAAAAAGT; tRNA^{Asp} CGGGTCACCCGCGTGACAGG;

It is unlikely that the slower migrating alt-tRNA band is due to the presence of the intron given the existence of alt-tRNA^{Asp}, where the latter is not encoded with an intron. Nonetheless to rule this possibility, we performed Northern blots using an intron probe specific for the edited intron of tRNA^{Tyr} [12]. We also probe for the predicted 5' and 3' flanking regions. As a control, we used RNA isolated from down-regulation of TRL1, the putative splicing ligase of *T. brucei*, which we had shown to lead to accumulation of intron-containing tRNA [53]. Neither probe detect an intron signal in RNA from wild-type cells or the uninduced TRL1 control (**Fig. 2.2**). To further assess the nature of the 5' and 3' ends of tRNA^{Tyr} and tRNA^{Asp}, we also demethylated total tRNA from wild type cells with the demethylase AlkB followed by Ordered Two-Template Relay (OTTR sequencing) as described in the materials and methods. We plotted the sequences of CCA-containing mature tRNA reads from the +AlkB treated *T. brucei* OTTR-seq library. We found that all sequence reads start at the 5' most end of the tRNA transcript and end with the - CCA tail, no extra nucleotides were observed at either end, ruling out the possibility that the alt-tRNAs are the result of nucleotide additions at either end (**Fig. 2.3**). We also plotted the pre-tRNA reads from the +AlkB treated OTTR-seq library, where only extensions +/- 2 nucleotides beyond the mature tRNA transcript were deemed a pre-tRNA read. In this case some of the reads extend a few nucleotides into the leader sequence, and also contained extensions of ~5-7 Us at the 3' most end of the reads. The 3'-U extensions are consistent with what was previously described in the intron-containing tRNA [69]. In the case of tRNA^{Tyr}, one can see the presence

of the intron in further support of these species as pre-tRNA reads (**Fig. 2.3 A-C**). Notably, in both cases manual searches for longer reads still containing the core tRNA^{Tyr} and tRNA^{Asp} sequence were performed, but no anomalous long sequences were detected. Furthermore, we also inspected tRNA^{Asn}, which gets Q but does not have either an intron or an alternative form. This tRNA also does not contain any 5' or 3' extensions suggesting that the nature of the alt-tRNAs is not dependent on Q. Taken together, the finding that neither the intron-specific probe nor the flanking regions probes hybridized with either the mature or the alt-tRNA band in the wild type or TRL1 uninduced control (**Fig. 2.2**) in agreement with the sequencing data in **figure 2.3**.

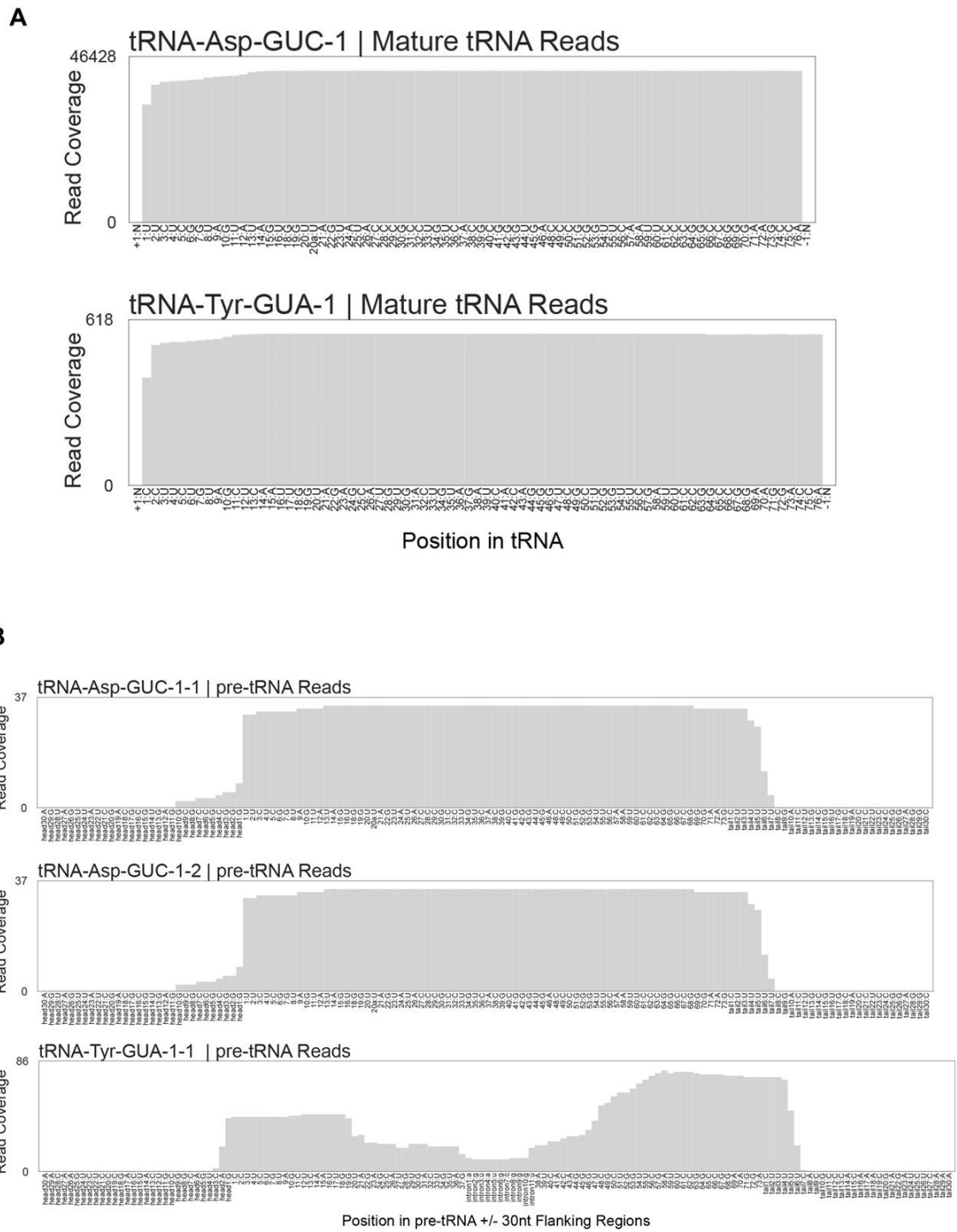


Figure 2.3 tRNA mapping read coverage of tRNA-Tyr-GUA-1 and tRNA-Asp-GUC-1

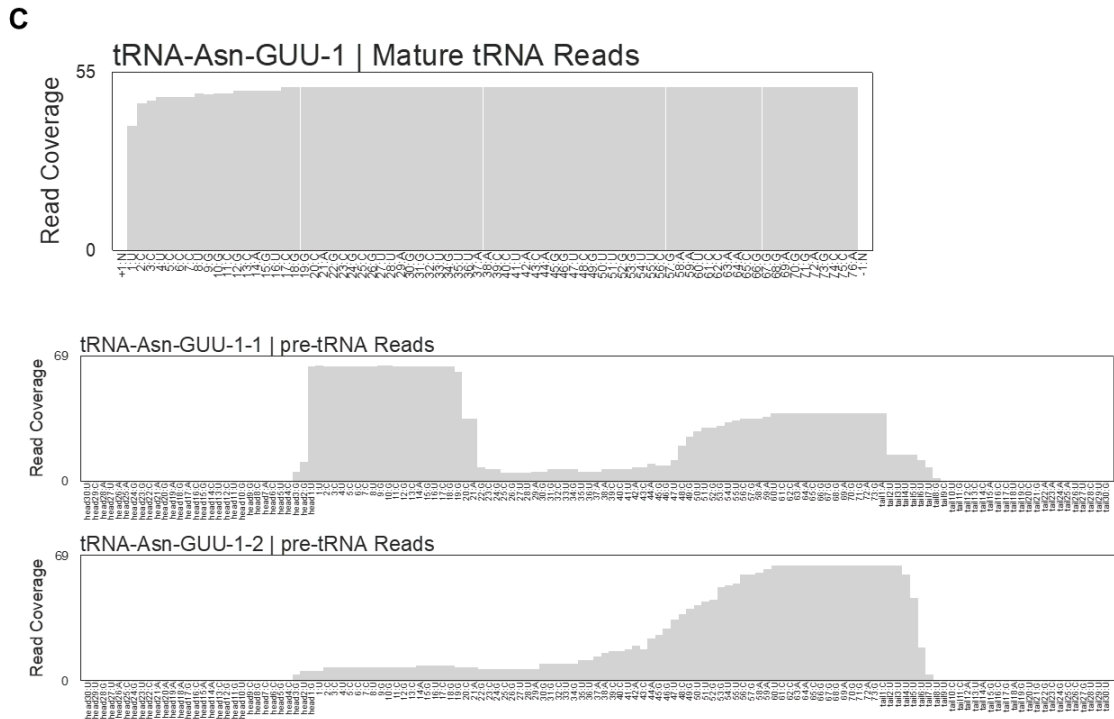


Figure 2.3 tRNA mapping read coverage of tRNA-Tyr-GUA-1 and tRNA-Asp-GUC-1

A. Read coverage of the tRNA mapping reads for tRNA-Asp-GUC -1 (top) and tRNA-Tyr-GUA-1 (bottom) from 5' (left) to 3' (right). **B.** Read coverage of the pre-tRNA mapping reads for tRNA-Asp-GUC-1-1 (top), tRNA- Asp-GUC-1-2 (middle), and tRNA-Tyr-GUA-1 (bottom) from 5' (left) to 3' (right). **C.** Read coverage of mature for tRNA-Asn-GUU-1-1 (top) and pre-tRNA mapping reads to tRNA- Asn-GUU-1-2 (middle and bottom). Sequences shown here were obtained from sequencing both the slow migrating band and the mature band present in gels.

To investigate the relationship between the alt-tRNA and the canonical species, we enquired whether the alt-tRNA^{Tyr} is an intermediate feeding into the overall pool after additional processing, or a “dead-end” product of aberrant tRNA^{Tyr} maturation. Thus, we measured its general stability, we treated *T. brucei* cultures with the transcriptional elongation inhibitor actinomycin D. Although this inhibitor has been associated with inducing nucleolar stress in other systems, it has been the inhibitor of choice for these types of studies in the trypanosome system [70][71][72]. Upon actinomycin treatment, we continued cell cultivation for 36h. Total RNA was prepared from samples collected at the indicated time points (**Fig. 2.4 and 2.5**). As shown, there is an observed increase in levels of alt-tRNA^{Tyr} in the first 3 hours of treatment. Similar behavior has been described for mRNA studies in *T. brucei*, this phenomenon was ascribed to the existence of a pool of precursors that feed into the system [72]. These experiments also revealed that tRNA^{Tyr} and alt-tRNA^{Tyr} have unusually short half-lives of 10.3 h and 6.9 h, respectively (**Fig. 2.4 and 2.5**). In contrast, the levels of other tested tRNAs remained stable for 36 hours following actinomycin D treatment (**Fig. 2.4 and 2.5 D**). We performed similar experiments for tRNA^{Asp}, which is the other tRNA displaying an alternative isoform. In contrast to tRNA^{Tyr} and alt-tRNA^{Tyr}, both tRNA^{Asp} and alt-tRNA^{Asp} remained stable for 36 hours (**Fig. 2.4**).

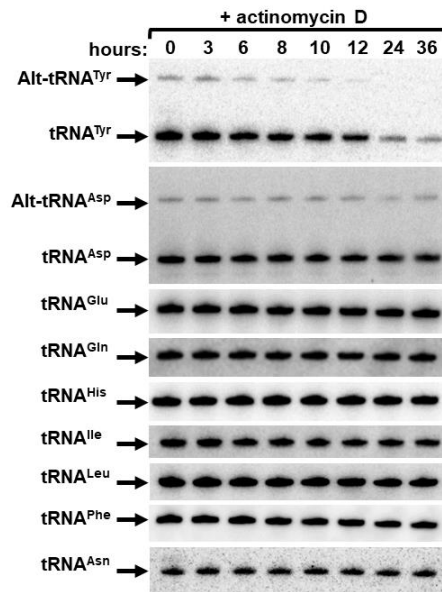


Figure 2.4 *T. brucei* tRNA^{Tyr} is unusually unstable

Northern blot hybridization performed on the extracted total RNA samples from *T. brucei* cells subjected to Actinomycin D treatment revealing the mature and alternate conformers of tRNA^{Tyr}. The same membrane was then stripped, and probed for tRNAs: Asp, Glu, Gln, His, Ile, Leu, Phe, and Asn. The tRNA^{Glu} was used as loading control. See **Appendix D** for uncropped membranes.

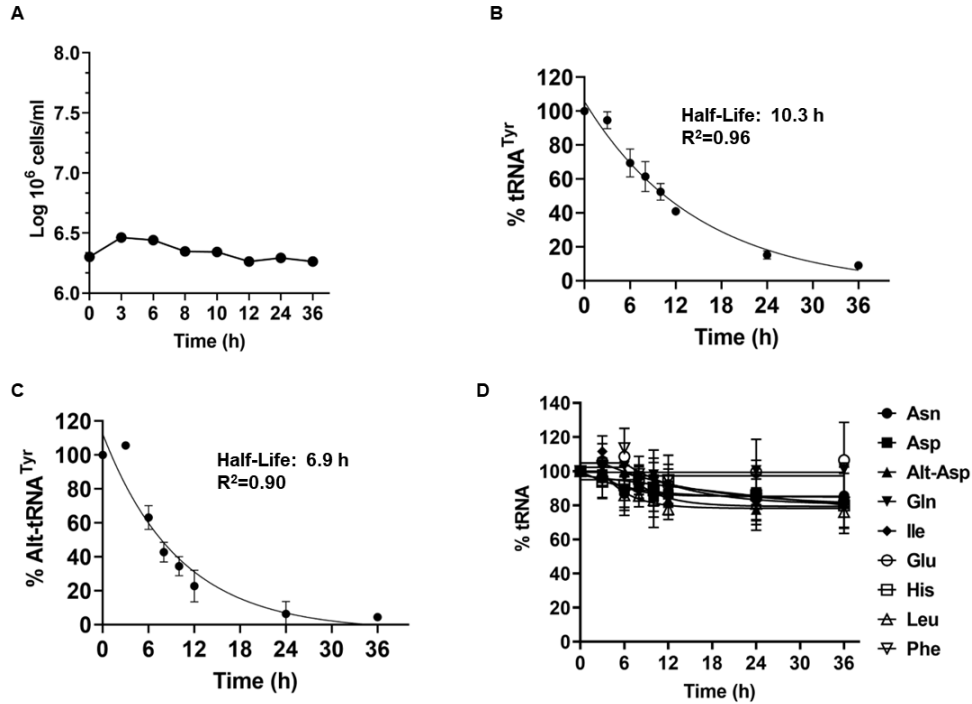


Figure 2.5 *T. brucei* tRNA^{Tyr} has an unusually short half-life, which is not shared by other tRNAs in the system

A. Triplicate growth curve of WT *T. brucei* cells subjected to Actinomycin D treatment where total RNA was collected at the time points indicated. **B** and **C.** Linear regression calculations utilizing the amounts of mature and alternate conformer tRNA^{Tyr}. **D.** Linear regression calculations utilizing the amounts of other tRNAs. Data were fit to a one-phase decay. All data plotted were the result of 3 biological replicas.

2.2.2 XRNE moderately impacts alt-tRNA^{Tyr} stability

Despite their remarkable stability, tRNAs eventually decay via pathways that have been extensively studied in eukaryotes [68][73][43][46]. Rapid tRNA Decay (RTD) targets hypomodified tRNAs in *S. cerevisiae*, and involves 5'-3' cytoplasmic XRN1 and the nuclear RAT1 exoribonucleases [43][73][46]. The *T. brucei* genome encodes six XRN homologs: XRNA (Tb927.7.4900), XRNB (Tb927.5.2450), XRNC (Tb927.8.2810), XRND (Tb927.10.6220), XRNE (Tb927.5.3850), and XRNF (Tb927.11.1550) [72]. XRNA has been localized to the nucleus and the cytoplasm, and it is functionally linked to degradation of unstable (half-lives < 30 min) developmentally-regulated mRNAs [72][71]. XRNB and C localize to the cytoplasm, and apparently play negligible roles in RNA degradation [72]. The function of nuclear XRND remains unclear, as it is the case for XRNF [72]. XRNE has been localized to the nucleolus and has been implicated in rRNA processing and assembly [74]. To investigate whether the XRN homologs participate in tRNA^{Tyr} decay, we systematically knocked down their expression by inducible RNAi. Induced and mock-treated transgenic RNAi cell lines were grown for 10 days [75]. Total RNA was collected after six days of RNAi induction for Northern blot hybridization (**Fig. 2.6 and 2.7**). RNAi downregulation of XRNA, B and C caused varying growth defects, while XRNE RNAi displayed none. RNAi failed to appreciably downregulate XRND and XRNF expression, and these proteins were not explored further. A minor, but statistically significant alt-tRNA^{Tyr} accumulation was observed in XRNE RNAi (**Fig. 2.6 E**), while XRNA, B and C

knockdowns did not affect the steady-state levels of either tRNA^{Tyr} or alt-tRNA^{Tyr} (**Fig. 2.6 B-D**). We conclude that XRNE has a small effect in tRNA^{Tyr}/alt-tRNA^{Tyr} turnover, while XRNA, B and C are not involved. XRND and F could not be evaluated, so their participation in tRNA turnover remains undisclosed.

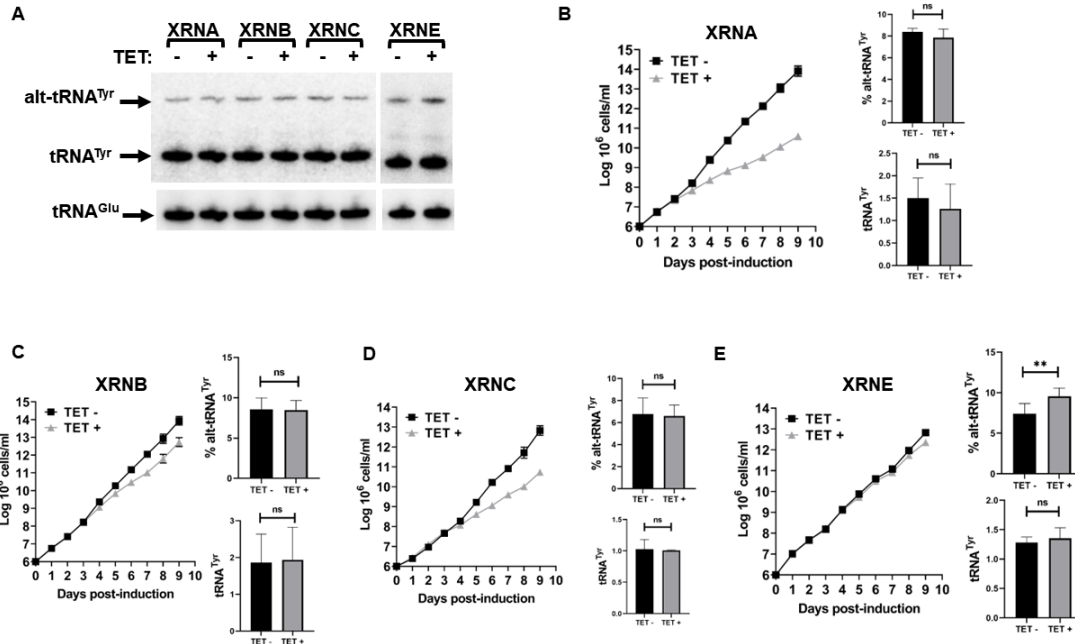


Figure 2.6 RNAi Knockdown of XRN enzymes

A. Northern blot hybridization performed on the extracted total RNA samples revealing the mature and alternate conformers of tRNA^{Tyr}. The tRNA^{Glu} was used as loading control. **B to E.** Triplicate growth curve of *T. brucei* cells subjected to tetracycline-induced protein knockdown where total RNA was collected on day 6. Cell concentrations shown on Y axis are cumulative. Relative amounts of alternate conformer tRNA^{Tyr} and mature tRNA^{Tyr}. The graphs are the result of 3 biological replicas. The asterisks in “E” denote significance based on a two-tailed paired T-test with a P-value of 0.006. “ns” stands for non-significant by the same test.

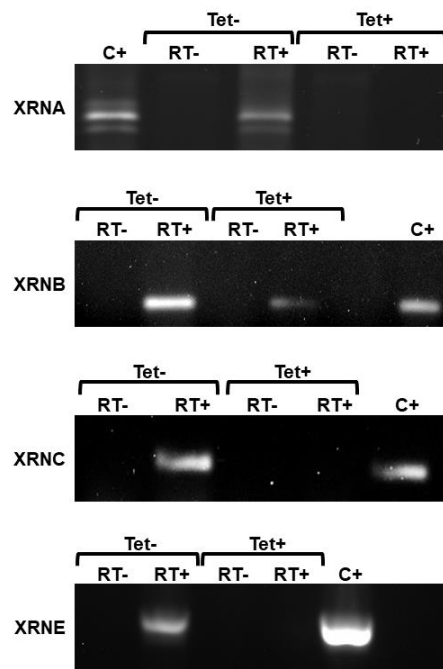


Figure 2.7 RT-PCR confirmations for XRN RNAi depletions

All PCR products were resolved in 1% agarose gels. Products corresponding to knockdown genes should be reduced under tetracycline treatment when compared to untreated controls and WT. C+ stands for positive control, which in this figure is the corresponding gene amplified from genomic DNA extracted from *T. brucei*.

2.2.3 RRP44 downregulation stabilizes alt-tRNA^{Tyr}, alt-tRNA^{Asp}/mature tRNA^{Asp} but has little effect on mature tRNA^{Tyr}.

We next tested the possible involvement of exosome subunits in tRNA^{Tyr}/alt-tRNA^{Tyr} decay. The exosome of *T. brucei* has similar properties to that of *S. cerevisiae*, with two exceptions: 1), the 3'-5' exoribonuclease RRP6 is present in stoichiometric amounts in both nuclear and cytoplasmic fractions, whilst in *S. cerevisiae*, it is nuclear only; and 2) , the 3'-5' exoribonuclease RRP44 is an autonomous enzyme and does not associate with the exosome [47]. Conversely, homologs for other subunits, do associate with the exosome [47]. The established roles for RRP44 and RRP6 in *T. brucei* are limited to rRNA processing [47]. Furthermore, we also assessed a potential role for Dis3L2 in tRNA degradation. Dis3L2 is a 3'-5' endonuclease that is structurally similar to RRP44, but lacks the PIN domain, which is necessary for interaction with the exosome [51]. Dis3L2 is a cytoplasmic enzyme present in many eukaryotes, including *T. brucei* [51][76][48]. In *S. pombe*, Dis3L2 has been implicated in an RNA degradation pathway independent from RTD and the exosome, whilst in *Drosophila*, a role in cell proliferation and tissue growth has been suggested [51][76].

Downregulation of Dis3L2 and RRP6 led to growth defects as compared to the RNAi uninduced control (TET-) but had little effect on the steady-state level of tRNA (**Fig. 2.8**). RRP44 down-regulation caused a growth defect and led to a statistically significant accumulation of alt-tRNA^{Tyr} (**Fig. 2.9 C**). Remarkably, the steady-state levels of alt-tRNA^{Asp}, and tRNA^{Asp} were also increased (**Fig. 2.9 D**).

But the levels of mature tRNA^{Tyr} remained unchanged (**Fig. 2.9 C**). We note that the levels of alt-tRNA^{Tyr} (~20%) vs the mature form were lower than in figure 1D. This can be explained by the experimental set up: time-resolved RNAi is performed by periodic dilution to keep the culture in exponential growth. In other words, cell density is kept at $\sim 3\text{-}5 \times 10^6$ cells/ml, comparable to 12-24 hours in the growth curve from **figure 2.1 B**, and the bar graph in **2.1 D**.

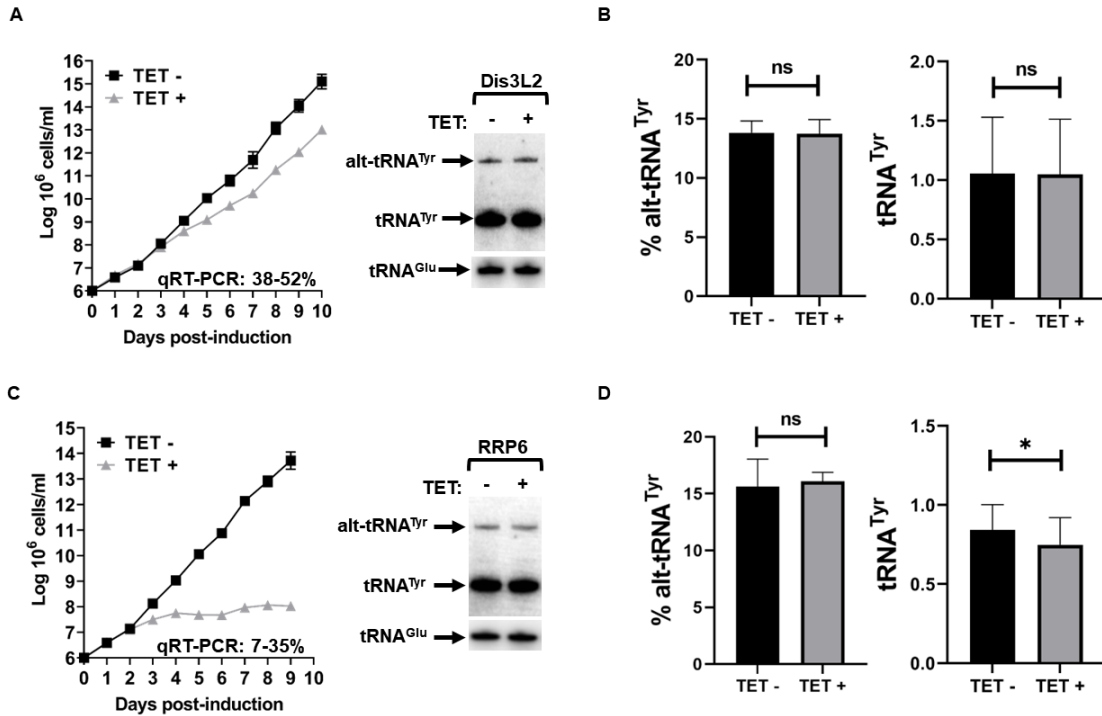


Figure 2.8 RNAi knockdown of Dis3L2 and RRP6

A and **C**. Triplicate growth curve of *T. brucei* cells subjected to tetracycline-induced protein knockdown where total RNA was collected on day 6, and Northern blot hybridization performed on the extracted total RNA samples revealing the mature and alternate conformers of tRNA^{Tyr}. Cell concentrations shown on Y axis are cumulative. **B** and **D**. Relative amounts of alternate conformer tRNA^{Tyr} and mature tRNA^{Tyr}. The graphs are the result of 3 biological replicas. The asterisk in “D” denotes significance based on a two-tailed paired T-test with a P-value of 0.03. “ns” stands for non-significant by the same test.

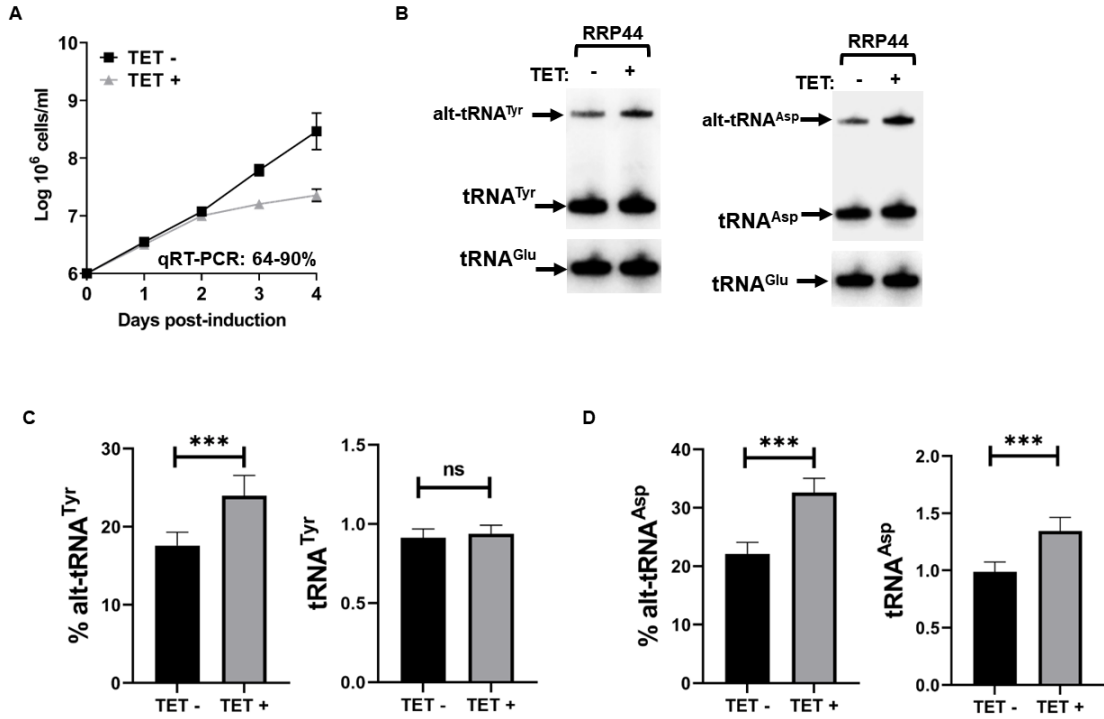


Figure 2.9 RNAi knockdown of RRP44

A. Triplicate growth curve of *T. brucei* cells subjected to tetracycline-induced protein knockdown where total RNA was collected on day 4. Cell concentrations shown on Y axis are cumulative. **B** Northern blot hybridization performed on the extracted total RNA samples revealing the mature and alternate conformers of tRNA^{Tyr} and tRNA^{Asp}. **C** and **D**. Relative amounts of alternate conformer tRNA^{Tyr} and tRNA^{Asp}, and mature tRNA^{Tyr} and tRNA^{Asp}. The graphs are the result of 3 biological replicas. The asterisks in “C” denotes significance based on a two-tailed paired T-test with a P-value of 0.0009. The asterisks in “D” denote P values of 0.0008 for both alt-tRNA^{Asp} and tRNA^{Asp}. “ns” stands for non-significant by the same test.

Considering alt-tRNA^{Tyr} stabilization by RRP44 RNAi, we inquired whether RRP44 depletion would affect the half-life of this tRNA. We performed the transcription arrest assay as in **figure 2.2**, but under RRP44 knockdown conditions, whereby actinomycin D was added on day 4 post RNAi induction. Cells were then harvested at various time points, and total RNA was analyzed by northern blot hybridization (**Fig. 2.10**). Downregulation of RRP44 led to an increase in the half-life of both tRNA^{Tyr} and alt-tRNA^{Tyr}, from 14.4 h and 8.5 h in the uninduced control (**Fig. 2.10 A, C, E**) to 24.7 h and 11.6 h respectively in RNAi-induced samples (**Fig. 2.10 B, D, F**). Taken together, these experiments lead to the conclusion, that RRP44 is partially responsible for the unusually short half-life of tRNA^{Tyr} and its alternate isoform.

Given the observed effect of XRNE down regulation on the levels of alt-tRNA^{Tyr} (**Fig. 2.6 E**), we also performed similar actinomycin D experiments as above. As in the case of XRNE, actinomycin D had little effect on cell viability beyond growth arrest when comparing the uninduced to the RNAi induced cells (**Fig. 2.11**). Furthermore, down-regulation of XRNE had negligible effect on the half-life of alt-tRNA^{Tyr} (**Fig. 2.12**) Taken together beyond redundancy in function among the nuclease tested here, only RRP44 has a significant contribution to the unusually short half-life of tRNA^{Tyr}.

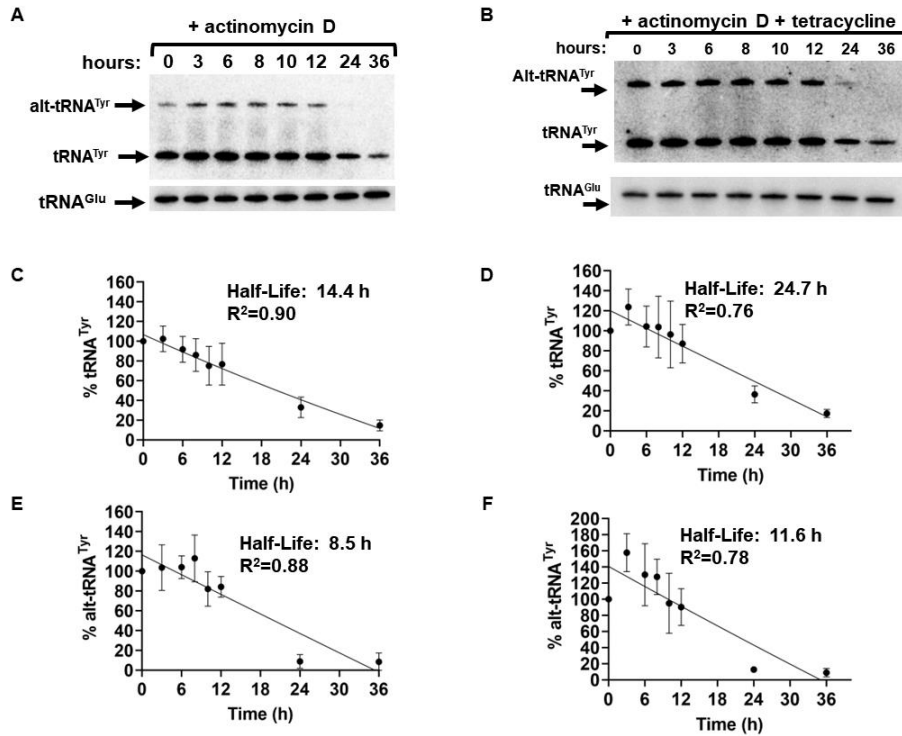


Figure 2.10 RNAi Knockdown of RRP44 stabilizes both tRNA^{Tyr} conformers

A and **B**. Northern blot hybridization performed on the extracted total RNA samples from RRP44 RNAi strain *T. brucei* cells subjected to Actinomycin D treatment with and without RRP44 depletion. The tRNA^{Glu} was used as loading control. **C** to **F**. Linear regression calculations utilizing the amounts of mature and alternate conformer tRNA^{Tyr} with and without RRP44 depletion. Data were fit to a one-phase decay with R² values as indicated. All data plotted were the result of 3 biological replicas.

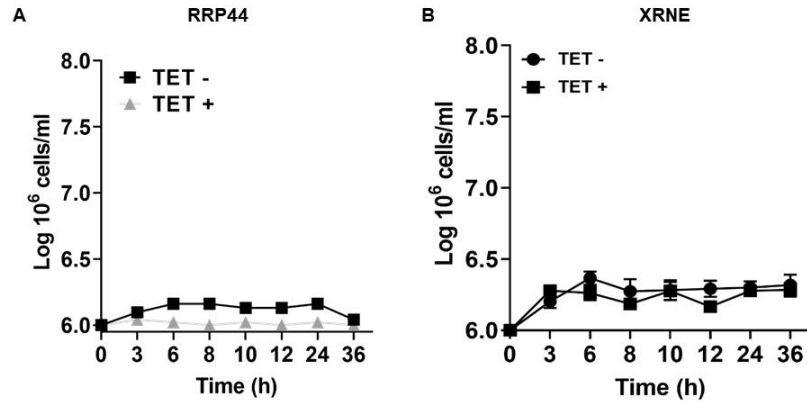


Figure 2.11 Triplicate growth curve of *T. brucei* cells subjected to both RNAi knockdown and actinomycin D treatments

Total RNA was collected at every time point. **A.** RRP44 growth curve. **B.** XRNE growth curve. Cell concentrations shown on Y axis are cumulative

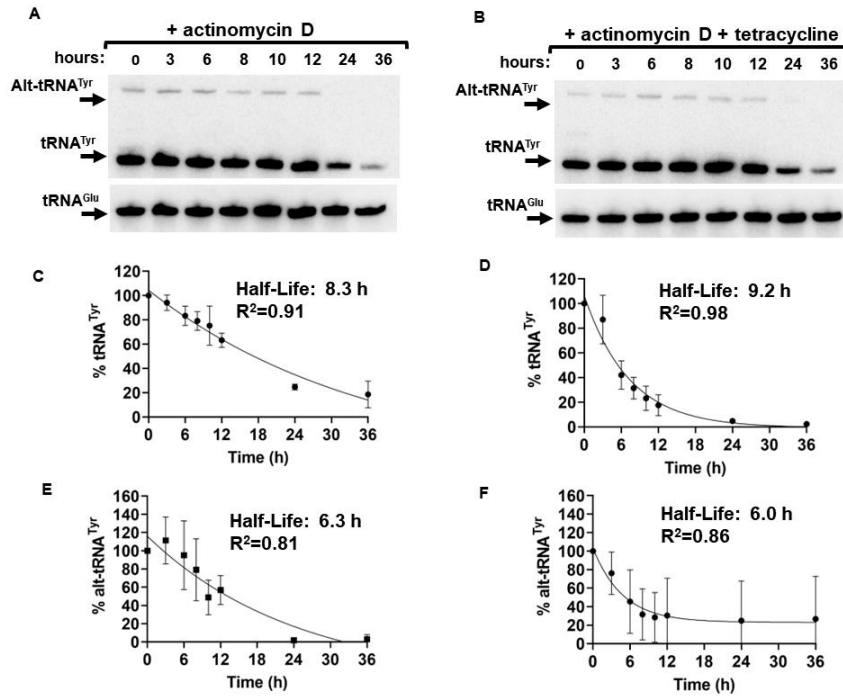


Figure 2.12 RNAi Knockdown of XRNE does not stabilize tRNA^{Tyr} conformers.

A and **B**. Northern blot hybridization performed on the extracted total RNA samples from XRNE RNAi strain *T. brucei* cells subjected to actinomycin D treatment with and without XRNE depletion. The tRNA^{Glu} was used as loading control. **C** to **F**. Linear regression calculations utilizing the amounts of mature and alternate conformer tRNA^{Tyr} with and without XRNE depletion.

2.3 Discussion

The rate of transcription, maturation and decay dictates the steady-state levels of tRNAs in cells, which are, in turn, crucial for protein synthesis. Conversely, the long half-lives of mature tRNAs are seemingly at odds with rapid responses to environmental changes that require translational reprogramming. This places emphasis on tRNA decay pathways such as the 5'-3' RTD and 3'-5' exosome pathways, which actively scrutinize tRNAs [47][45](Chernyakov et al. 2008). The frontline of tRNA scrutiny is nuclear surveillance, which eliminates incorrectly transcribed and hypomodified tRNAs by targeting aberrant molecules to the TRAMP complex, leading to A-tailing by Trf4 and 5 non-canonical poly(A) polymerases, followed by degradation by the nuclear exosome-associated 3'-5' exoribonuclease RRP6 [45]. Correctly processed tRNAs are further inspected by the nuclear and cytoplasmic RTD pathways (Chernyakov et al. 2008). In RTD, the major surveillance system for tRNA quality in eukaryotes, defective, damaged and hypomodified molecules are degraded by enzymes such as 5'-3' exoribonucleases XRN1 and RAT1 [46]. These enzymes can either recognize the molecule directly, or be recruited by other proteins, such as the CCA-adding enzyme (CAE) [77]. This enzyme, which has the canonical function of adding CCA to the 3'-end of newly synthesized tRNAs, can also recognize aberrant tRNAs and mark them for degradation by the RTD components by the addition of a CCACCA "degradation tag" [77]. These essential functions have also been described in *T. brucei*, where CAE localizes to the nucleus, cytoplasm, and mitochondrion [78]. These pathways

likely recognize uniform tRNA features, which makes the relative instability of *T. brucei* tRNA^{Tyr} intriguing.

Considering the rapid turnover, tRNA^{Tyr} may appear as a major target for the tRNA degradation pathways, including RTD and nuclear surveillance, however, our results provide no indication of their functioning in affecting tRNA steady-state levels. The XRN1 homolog, XRNE, was the only tested 5'-3' exonuclease to exert a small, but statistically significant effect on tRNA^{Tyr} stability. We cannot rule out, however that some among the six XRNs have redundant roles, and that a more severe effect on stability may have been masked by the other homologs. Along these lines, we emphasize that since neither XRND nor XRNF could be efficiently down-regulated by our RNAi approach, their involvement in tRNA stability will remain an open question. Moreover, RRP44 depletion affects both tRNA^{Tyr} conformers, which leads to a statistically significant increase in tRNA^{Tyr} stability. Unlike in other eukaryotes, *T. brucei* RRP44 does not associate with the exosome in any compartment [47]. *T. brucei* RRP44 reportedly performs canonical rRNA maturation function in the nucleus but has no assigned function in the cytoplasm [47][79]. Curiously, an effect on steady-state levels was also observed for tRNA^{Asp} and alt-tRNA^{Asp} under RRP44 knockdown conditions, but neither showed the shorter half-life observed with alt-tRNA^{Tyr}/tRNA^{Tyr}. Finally, *T. brucei* RRP44 is capable of degrading structured RNAs, such as stem-loops, *in vitro* [61]. This activity is dependent on the RRP44 exonuclease domain, and can be observed even in structured substrates that lack of 3' overhangs [61]. Thus, it

is imaginable that a biological function of RRP44 is in the turnover of tRNA^{Tyr}, and potentially tRNA^{Asp}.

In recent years there are many reports of tRNA fragments playing crucial roles in cell function. It is possible that the short half-life of tRNA^{Tyr} may be due to fragment generation, however, we did not observe any tRNA fragments in our experiments, even after gross over-exposure of the northern membranes, thus we think this possibility unlikely. *T. brucei* also encodes a homolog of the 3'-5' exoribonuclease Dis3L2, which has been described in other eukaryotes as a stand-alone enzyme that is structurally similar to RRP44, and implicated on its own RNA degradation pathway [51][76][48]. We explored the possible involvement of the *T. brucei* homolog in tRNA^{Tyr} degradation, however, our knockdown assays and northern blot analysis showed no effect on the tRNA stability, albeit we confirmed that the enzyme is essential for fitness. However, we cannot currently rule out the possibility of functional redundancy between these enzymes.

As stated above, the tRNA^{Tyr} of *T. brucei* presents several unusual features that are extended in this study. We find that tRNA^{Tyr} is present as two separate isoforms: the mature-sized 75-nt tRNA^{Tyr}, and the ~120-nt alt-tRNA^{Tyr}, both of which are remarkably unstable for a tRNA, presenting short half-lives of only 10.3 h and 6.9 h, respectively. This rapid turnover seemingly comes into conflict with the “high cost” of synthesizing a mature tRNA^{Tyr} in *T. brucei*, as that involves use of the cytoplasmic splicing machinery, editing and modification events, and multi-directional transport. It also seems to be unrelated to the modification Q, as the

other three Q-modified tRNAs in *T. brucei* did not show unusual stability by northern analysis. Furthermore, we had reported that the Q modification undergoes dynamic changes according to nutrient availability, meaning, when the concentration of certain nutrients present in the media are altered, the amount of Q-modified tRNA^{Tyr} changes in a predictable way, affecting codon choice for tRNA^{Tyr}, but seemingly not for other Q-tRNAs [56]. Taken together, these discoveries imply that, tRNA^{Tyr} may function not only as a translation-competent molecule, but also as a nutrient sensor, in a network that regulates dynamic synthesis and removal of Q modification. Mature tRNAs act as nutrient sensing molecules in eukaryotes, with uncharged tRNAs signaling nutritional stress, leading to reduction in global protein biosynthesis during starvation of specific amino acids [80][81]. Moreover, as mentioned above, tRNA fragments are also implicated in signaling pathways in bacteria and eukaryotes [82][81]. Considering the rapid changes in nutrient availability that *T. brucei* may face when changing from vector to host, and vice-versa, we propose that the rapid turnover of tRNA^{Tyr} ensures equally rapid changes in protein biosynthesis.

Currently, the identity of alt-tRNA^{Tyr} remains unclear. Circularization would explain the observed differences in electrophoretic mobility between the alt-tRNA and mature tRNA bands. Circular RNAs (circRNAs) were first described over 40 years ago in eukaryotes, initially as either the products of self-splicing introns in single-cellular organisms, or somewhat rare, aberrant and poorly processed transcripts, that had no discernible function [83][84]. Recently, however, circRNAs

have been brought to prominence, revealed as innate products of transcription that are generated through a mechanism dubbed “back splicing”, and shown to differ in stability and abundance from their linear counterparts [85]. Some circRNAs accumulate in a tissue-specific manner in metazoans, sometimes possessing regulatory functions in specific cell types [86]. Finally, tRNAs can generate their own abundant class of circular RNAs, called tRNA intronic circular RNAs (tricRNAs), which are produced during tRNA splicing [87][88][89]. Considering this information, we wondered whether alt-tRNA^{Tyr} was a circularized version of mature tRNA^{Tyr} in *T. brucei*, and performed a two-dimensional gel Northern blot hybridization assay as previously described [90]. This can assay reveal circular RNA bands based on aberrant migration patterns during the second phase of electrophoresis separation. In all our assays, however, alt-tRNA^{Tyr} migrated in a straight line during this step, consistent with the migration expected for a linear molecule (**Fig. 2.13**).

A second possibility is that the slower migration of alt-tRNAs is due to extensions at the 5' or 3' end, however the OTTR sequencing provided partially rules out this scenario, although we cannot formally refute the argument of the existence of a yet to be identified modification that prevents sequencing for the true alt-tRNA and therefore skews what can be seen in our sequence analysis. Lastly, it is possible the alt-tRNA is a repository for the mature form of the molecule. Indeed, we notice that in the northern blots performed for the transcription arrest assay under RRP44 depletion, the bands corresponding to mature tRNA^{Tyr}

remains stable until the 12h time point, when alt-tRNA^{Tyr} is still present (**Fig. 2.10 B**). After that threshold, alt-tRNA^{Tyr} is no longer detectable in the membrane, and the mature tRNA^{Tyr} finally starts to diminish (**Fig. 2.10 B**). This would indicate that alt-tRNA^{Tyr} may be converted into mature form, perhaps to help maintain appropriate levels of tRNA^{Tyr}. However, currently it is not clear if the short half-lives of both tRNA species is just coincidental as we have failed to establish a strict precursor-product relationship with the assays provided.

Taken together, our results show that tRNA^{Tyr} is indeed a unique molecule in *T. brucei*: a strikingly unstable tRNA present as two isoforms that is subjected to multiple transactions including intron editing, backbone modification and intracellular transport, and yet escaping most common RNA degradation pathways, to be regulated by RRP44 exonuclease.

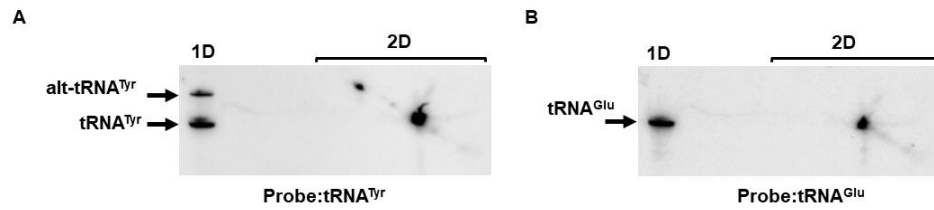


Figure 2.13 The tRNA^{Tyr} alternate conformer is not circular

A. Two-dimensional gel Northern blot hybridization performed on *T. brucei* 29-13 WT extracted total RNA samples revealing the mature and alternate conformers of tRNA^{Tyr}. **B.** Northern blot hybridization revealing tRNA^{Glu} on the same gel.

2.4 Materials and Methods

2.4.1 Cell culturing and RNAi knockdowns

T. brucei 29-13 procyclic cells [91] were cultured at 27° C in SDM-79 media supplemented with 10% FBS, and growth was assessed by counting with Neubauer chambers. Gene knockdowns were performed with p2T7-177 plasmids as previously described [75]. RNAi was induced by addition of 1 µg/ml tetracycline to the media, generating a dsRNA from two head-to-head T7 promoters [75]. Target regions for knockdowns were selected with the RNAit online tool (<https://dag.compbio.dundee.ac.uk/RNAit/>), and oligos generated were as follow:

XRNA: For TGCGATCTCATCTTCGGTTCG; Rev TAGGAAGGAGAACCGAGCGA;
XRNB: For GCGAACGCAAAAGTTGGACT Rev CCGTGCATAGCCAATCAACG
XRNC: For CCAAGTTGACAACGGTGACAG Rev GAACAACCCCCGTTTCGTTG
XRND: For ATTCGGATGGGACCCTGAGA Rev GGGAAACTTCGCAGCTACCT
XRNE: For GCCAGCGAAAGATACTTGCG Rev TGTCGGTTTCTCTCAGCACC
XRNF: For CCGACTTGGTGCTAGTTGGT Rev CGATGGATCTGAGAGCCCAC
Dis3L2: For GTGTGATAGCCGTCCTCGAG Rev CGTGGCAGGGTCGATACTAC
RRP6: For TCCCTTCAATTGAGCAGCGT Rev ATGGCACCTTCCTTCAGCTC
RRP44: For AGAGTGAGGCTGCTGTTTCC Rev GCCGATGCACAATTACGTCC.

2.4.2 Northern blot analysis

Cells at mid to late log (6×10^6 to 1×10^7 cells/ml), were harvested by centrifugation at 1400 g for 10 min and washed twice with PBS. Total RNA was

isolated from pellets using a guanidinium thiocyanate-phenol-chloroform protocol as previously described [92]. Samples containing 5 µg of total RNA were resolved in denaturing 8M urea 8% polyacrylamide gels, electroblotted into Zeta-probe nylon membranes according to manufacturer protocol (Bio-Rad), then UV-cross-linked for 1 min. Northern blot hybridization was performed according to manufacturer specifications using ³²P-labeled oligonucleotides. After hybridization, membranes were exposed overnight to a phosphorimager screen. Blots were analyzed using a Typhoon FLA 9000 scanner and the ImageQuant TL software (GE Healthcare). Probes used for Northern hybridization were as follows (5'–3' orientation):

tRNA ^{Asn}	CTCCTCCCGTTGGATTCTG;	tRNA ^{Asp}
	CGGGTCACCCGCGTGACAGG;	tRNA ^{Gln}
	CAGGATTCGAACCTGGGTTTTCTG;	
tRNA ^{Glu}	TTCCGGTACCGGGAATCGAAC;	tRNA ^{His}
	GGGAAGACCGGGAATCGAAC;	tRNA ^{Ile}
	GGGGTTCGAACCCGCGATATTCGGT;	tRNA ^{Leu}
	AACCCACGCCTCCGGAGAG;	
tRNA ^{Phe}	GCGACCCGGGATCGAACCCAGGGACC;	tRNA ^{Tyr}
	CCTTCCGGCCGGAATCGAACCCAGCGAC;	tRNA ^{Tyr}
	(Intron)	
	GATACCTGCAAACCTCTAC;	tRNA ^{Tyr} (Leader)
	CTGACTGCCGCAGTAGTCGGG;	
	tRNA ^{Tyr} (Trailer)	
	CGTTTGTGGGCGTGAAAAAGT.	

2.4.3 Transcription Arrest Assays

Cultures containing cells at early log (2 x 10⁶ cells/ml) received actinomycin D (in DMSO) to a final concentration of 10 µg/ml, and were incubated at 27° C

under transcription arrest whilst cells were harvested by centrifugation at scheduled time points, following protocol [72]. Total RNA was isolated from pellets using a guanidinium thiocyanate-phenol-chloroform protocol as previously described [92].

2.4.4 Circular RNA analysis

Cells at mid to late log were harvested, and total RNA was isolated from pellets as described above. Samples containing 5 µg of total RNA were resolved first on a 5% polyacrylamide gel for the first dimension, then moved to a 10% polyacrylamide to be resolved in the second dimension. Samples were then electroblotted into Zeta-probe nylon membranes according to manufacturer protocol (Bio-Rad), then UV-cross-linked for 1 min. Northern blot hybridization was performed according to manufacturer specifications using ³²P-labeled oligonucleotides. After hybridization, membranes were exposed overnight to a phosphoimager screen. Blots were analyzed using a Typhoon FLA 9000 scanner and the ImageQuant TL software (GE Healthcare).

2.4.5 RNA sequencing

Prior to library preparation, AlkB treatment of the RNA was carried out as previously described [93] followed by RNA 3' de-phosphorylation [94]. Briefly, samples were treated with T4 Polynucleotide Kinase (T4PNK; New England Biolabs) in a modified 5x reaction buffer (350 mM Tris-HCl, pH 6.5, 50 mM MgCl₂,

5mM dithiothreitol) under low pH conditions in the absence of ATP for 30 mins. This RNA was used for to generate OTTR-seq as previously described [95]. Briefly, total AlkB and PNK-treated RNA was 3' tailed using mutant BoMoC RT in buffer containing only ddATP for 90 minutes at 30 °C, with the addition of ddGTP for another 30 minutes at 30 °C. This was then heat-inactivated at 65 °C for 5 minutes, and unincorporated ddATP/ddGTP were hydrolyzed by incubation in 5 mM MgCl₂ and 0.5 units of shrimp alkaline phosphatase (rSAP) at 37 °C for 15 minutes. 5 mM EGTA was added and incubated at 65 °C for 5 minutes to stop this reaction. Reverse transcription was then performed at 37 °C for 30 minutes, followed by heat inactivation at 70 °C for 5 minutes. The remaining RNA and RNA/DNA hybrids were then degraded using 1 unit of RNase A at 50 °C for 10 minutes. cDNA was then cleaned up using a MinElute Reaction CleanUp Kit (Qiagen). To reduce adaptor dimers, cDNA was run on a 9% UREA page gel, and the size range of interest was cut out and eluted into gel extraction buffer (300mM NaCl, 10mM Tris; pH 8.0, 1mM EDTA, 0.25% SDS) and concentrated using EtOH precipitation. Size-selected cDNA was then PCR amplified for 12 cycles using Q5 High-fidelity polymerase (NEB #M0491S). Amplified libraries were then run on a 6% TBE gel, and the size range of interest was extracted to reduce adaptor dimers further. Gel slices were eluted into gel extraction buffer (300mM NaCl, 10mM Tris; pH 8.0, 1mM EDTA) followed by concentration using EtOH precipitation. Final libraries were pooled and sequenced on an Illumina NextSeq500 using a 150-cycle high-output kit.

2.4.6 Data Processing

Sequencing adaptors were trimmed from raw reads using cutadapt, v1.18, and read counts were generated for tRNAs using tRAX (Holmes *biorxiv*). Briefly, trimmed reads were mapped to the mature tRNAs of the *Trypanosoma brucei* *Lister 427* genome assembly obtained from GtRNAdb and the reference genome sequence using Bowtie2 in very-sensitive mode with the following parameters to allow for a maximum of 100 alignments per read: --very-sensitive --ignore-quals --np 5 -k 100. Mapped reads were filtered to retain only the “best mapping” alignments. Raw read counts of tRNAs and pre-tRNAs were computed using tRNA annotations from GtRNAdb.

2.5 Acknowledgements

We thank all members of the Alfonzo laboratory for comments and discussions. The present work was funded in part by National Institutes of Health (NIH) Grants GM132254 and GM084065-11 to J.D.A., RO1AI152408 to R.A., R01AI113157 to I.A., and by the National Human Genome Research Institute, National Institutes of Health (NHGRI, NIH) HG006753 grant to T.L.

Chapter 3: The tRNA splicing endonuclease of *Trypanosoma brucei*

3.1 Introduction

In all domains of life, tRNAs can be interrupted by introns, which must be excised in order to generate mature molecules that can be used for translation. The way introns are dealt with differs greatly between the three major domains, Bacteria, Archaea, and Eukarya. Whilst bacterial introns are removed via self-splicing mechanisms that are independent of protein components, archaeal and eukaryotic introns are always removed by specialized proteins [24]. In eukaryotes, the first step of tRNA splicing, intron cleavage, is catalyzed by an heterotetrameric enzyme called TSEN, which is composed of four subunits called TSEN2, 15, 34, and 54 [25]. While a more in-depth review of the eukaryotic TSEN, including structure, substrate recognition, and relationship to human disease, is presented in chapter 1 (sections 1.5 - 1.6), this chapter will focus on the *T. brucei* homolog of TSEN, TbSEN, which was a point of focus in my PhD project.

3.1.1 The search for *T. brucei* homologs of TSEN

The genome of *T. brucei* encodes a single intron-containing tRNA, tRNA^{Tyr}_{GUA} (Tb927.4.1219), a single-copy gene [12]. Since tRNA splicing is an essential mechanism, the Alfonzo group explored the splicing system of *T. brucei*. Bioinformatics analysis, including the utilization of the yeast and human TSEN subunit sequences as query to research the available *T. brucei* genome database, revealed a putative homolog for TSEN34, dubbed TbSEN22 (Tb927.11.9740) after

its smaller molecular weight of 22 kDa [12]. This homolog contained a predicted tRNA endonuclease domain at the C-terminus (accession cd22363), but no other identifiable elements. RNAi knockdown of this protein resulted in growth phenotype and accumulation of pre-tRNA^{Tyr}, which led the authors to uphold TbSEN22 as a *Trypanosoma* homolog of TSEN34 (**Fig. 3.1 B and C**) [12]. Furthermore, sequencing of isolated *T. brucei* pre-tRNA^{Tyr} revealed, shockingly, that the intron sequence does not correspond to the genomic one, diverging in three positions: i2, i4, and i8 (**Fig. 3.1 A**) [12]. These intronic positions are noncanonically edited by enzymes still at large, with i2 and i8 undergoing G to A editing, whilst i6 undergoes A to U editing (**Fig. 3.1 A**) [12]. Molecules with edited positions i4 and i6, dubbed “Edit2 tRNA^{Tyr}”, correspond to about 64% of the pre-tRNA^{Tyr} population, while molecules containing all three positions edited (“Edit3 tRNA^{Tyr}”) correspond to the remaining 36% [12]. Finally, *in vitro* activity assays utilizing partially-purified TbSEN22 and *in vitro* transcribed Edit2, 3, and unedited pre-tRNA^{Tyr}, showed the edited molecules are more efficiently cleaved, indicating edited tRNA to be the preferred substrate for TbSEN [12].

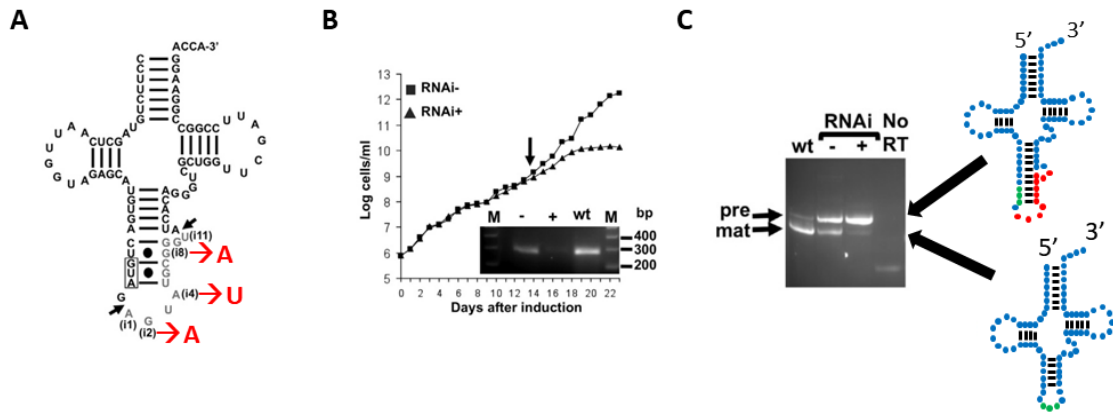


Figure 3.1 TbSEN22

TbSen22 is a homolog of TSEN34 in the *T. brucei* genome. **A.** Diagram representing how tRNA^{Tyr} intron is edited in up to three positions prior to splicing. **B.** Growth curve depicting knockdown of TbSEN22 leads to growth defects in *T. brucei*. **C.** RT-PCR denoting knockdown of TbSen22 leads to pre-tRNA^{Tyr} accumulation in *T. brucei*. Adapted from Rubio et al. - Unusual Noncanonical Intron Editing Is Important for tRNA Splicing in *Trypanosoma brucei* [12].

3.2 Results

3.2.1 The *T. brucei* homologs of TSEN2 and TSEN15

With the confirmation of TbSEN22 as an endonuclease subunit, we moved from sequence comparison to biochemistry, in an effort to identify the remaining TbSEN components. Since TSEN is an heterotetrameric enzyme, in both yeast and humans all four components can be co-purified with the use of a single tagged subunit [33][34]. Considering this, we wondered whether TbSEN could also be purified by a tagged TbSEN22 subunit. For this end, a *T. brucei* (lister 927) strain containing a tandem-affinity purification (TAP) tag positioned N-terminally to TbSEN22 in one locus was utilized (**Fig. 3.2 A**) [96]. As this strain also carries a knockout of the other locus of TbSEN22, it was dubbed “Exclusive Expressor (EE) TbSEN22”, since all copies of the protein produced by the cells are TAP-tagged (**Fig. 3.2 A**) [96]. EETbSEN22 cells were allowed to grow in a six-liter culture before being harvested by centrifugation. Cells were ruptured by sonication to generate a clear lysate by high-speed centrifugation. Clear lysates were then bound to IgG, followed by anti-protein C matrices (**Fig. 3.2 B**) as determined by protocol [96] (see materials and methods). Purified samples were resolved by SDS-PAGE for confirmation by silver staining and western blot, as well as mass spectrometry analysis by collaborators in the Trotta group, at PTC Therapeutics (**Fig. 3.2 C and D, see Appendix A7 to 9 for pertinent protocols**).

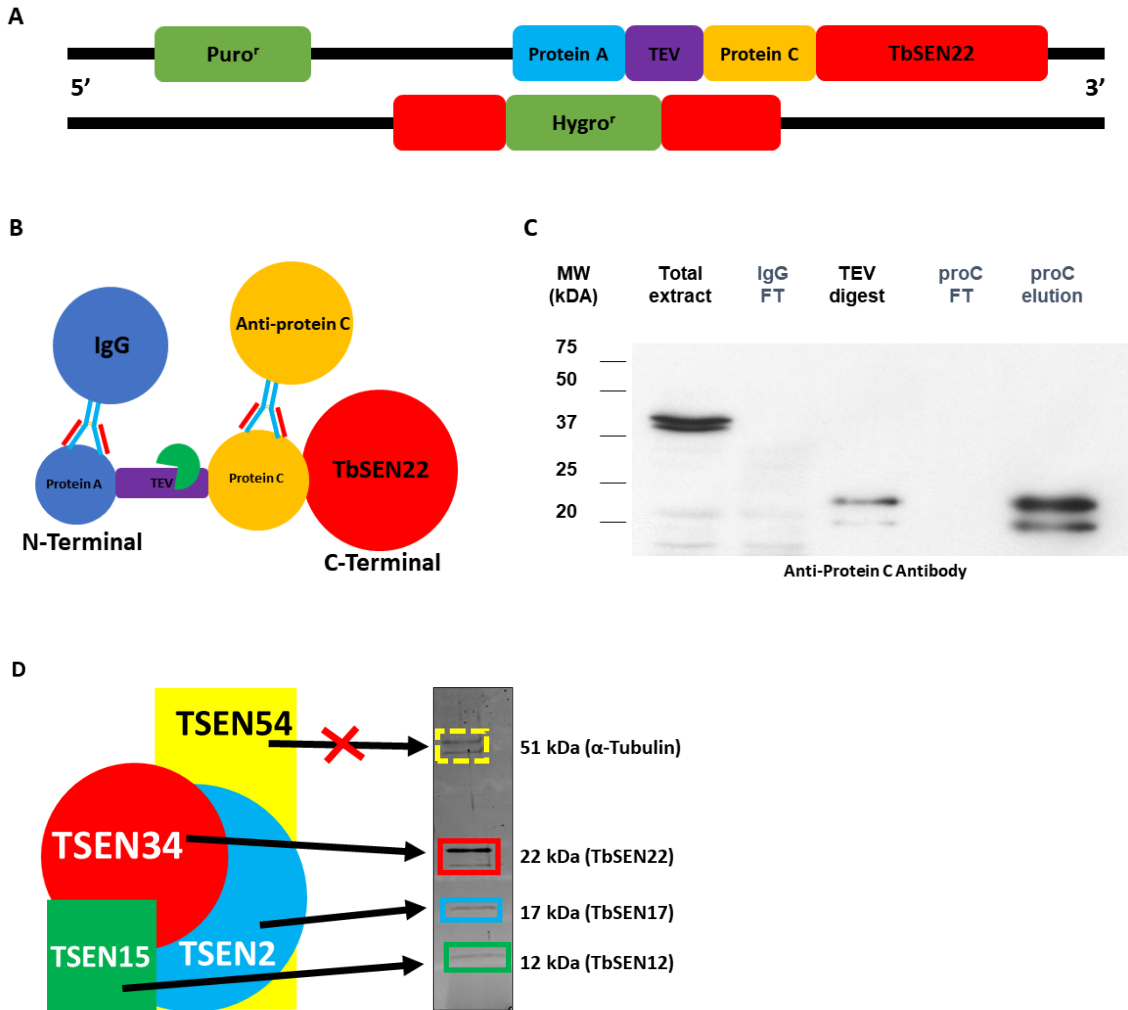


Figure 3.2 TAP-Tag Purification of TbSEN

Overview of TAP-Tag purification of TbSEN22. **A.** Genomic context of strain EETbSEN22 utilized for the protein purification. **B.** Diagram depicting the purification of TAP-TbSEN22 utilizing IgG and Anti-Protein C matrices. **C.** Western blot analysis revealing TAP-TbSEN22 with mouse anti-protein C HRP. Size difference indicates before and after TEV protease cleavage for release from IgG

matrix. **D.** Diagram of the expected TSEN subunits as compared to a silver-stained gel depicting the isolated bands.

TAP-tag purification of TbSEN22 lead to the co-purification of three other proteins: a 12 kDa putative homolog of TSEN15; a 17 kDa putative homolog of TSEN2; and the 55 kDa α -Tubulin, a common contaminant and artifact of the TAP tag used in this assay (**Fig. 3.2 D**) [96]. In similar fashion to TbSEN22, the proteins were named after their smaller molecular weight: TbSEN12 (Tb927.3.5560), and TbSEN17 (Tb927.6.4790). Similar to TbSEN22, TbSEN17 contains a predicted tRNA endonuclease domain at the C-terminus (accession cd22363), while TbSEN12 contains no identifiable domains. Finally, we notice that, even though this protocol was able to co-purify putative homologs for TSEN2 and TSEN15, no putative homolog for TSEN54 was purified, and no tRNA endonuclease enzymatic activity was detected *in vitro* from the final anti-protein C elution (**Fig. 3.3 B**).

3.2.2 TbSEN may be a heterotrimer

With the identified homologs of TSEN subunits, but no enzymatic activity detected after eluting from anti-Protein C, we wondered whether our bioinformatics and biochemistry analysis missed the remaining TSEN54 homolog in *T. brucei*. To investigate the enzyme further, we performed size-exclusion chromatography on cleared lysates obtained from EETbSEN22, followed by linear regression calculations to uncover the approximate molecular weight of TbSEN. Our results showed that TbSEN elutes with a size consistent with that of a heterotrimer that is composed of TbSEN12, 17, and TAP-22 (~38 kDa), on a range of 58 to 72 kDa, with a median at 66 kDa (**Fig. 3.3 A**). Furthermore, the eluted sample was capable

of cleaving Edit2 tRNA^{Tyr} *in vitro* (**Fig 3.3 B, see Appendix A10 for pertinent protocol**), indicating that a homolog of TSEN54 is either not required for activity, or that TbSEN has an alternative composition, possibly a heterotrimer, on which TSEN54 is missing. Further chromatography assay attempts to isolate TbSEN included anion exchanging (Q-Sepharose), cation exchanging (Mono-S), and affinity matrices (Heparin). Of these, only Q-Sepharose, where the protein elutes at ~ 350 mM salt concentration, led to the co-elution of TAP-TbSEN22 while maintaining endonuclease activity (**Fig. 3.3 C-D**). Multiple chromatographic methods used in tandem, such as anion exchanging followed by size-exclusion, resulted in activity loss, and by the end of this analysis, we could not obtain a purified TbSEN that would reveal only three bands on a silver-stained protein gel whilst still maintaining endonuclease activity.

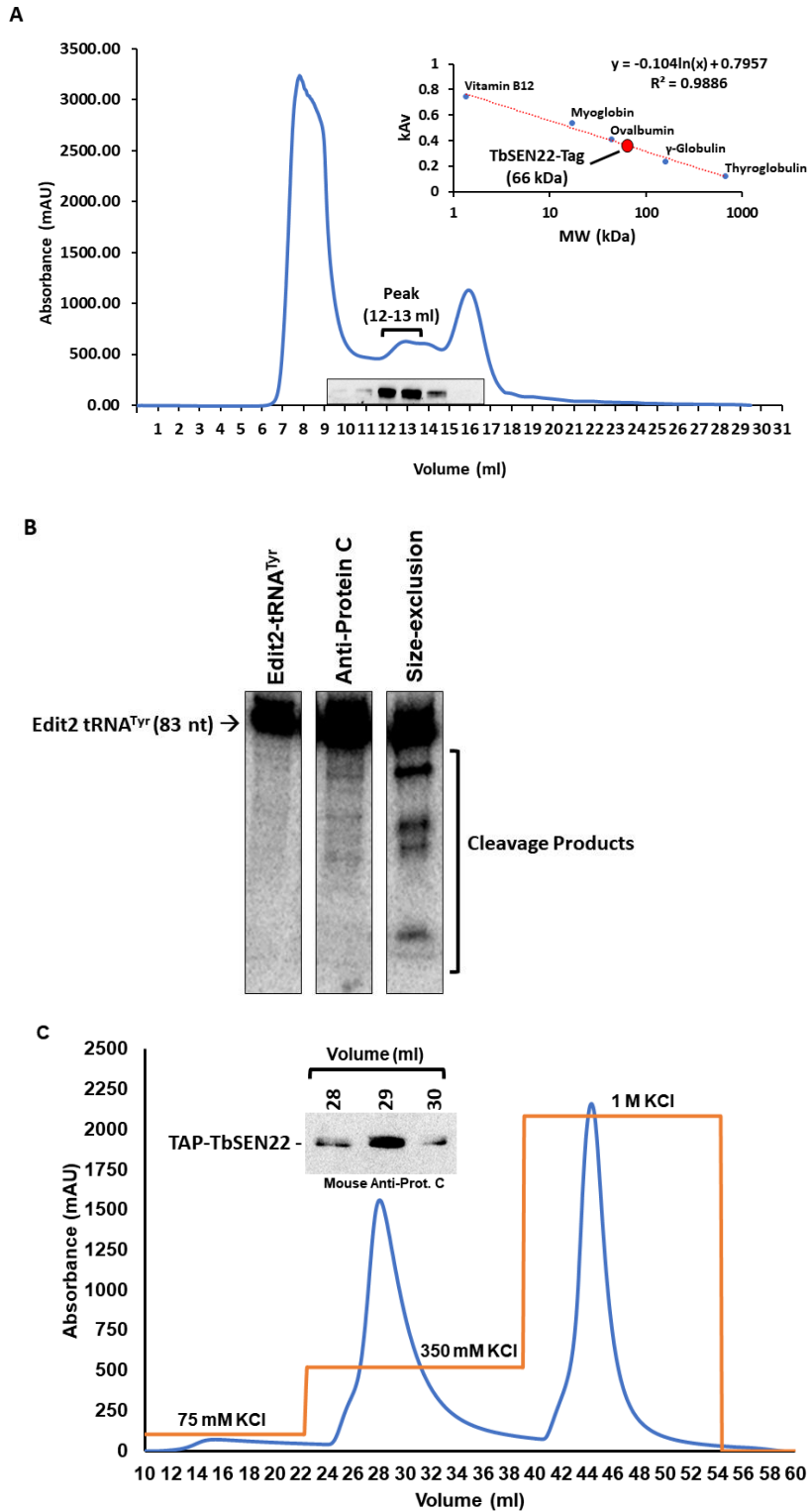


Figure 3.3 Purification of EETbSEN22

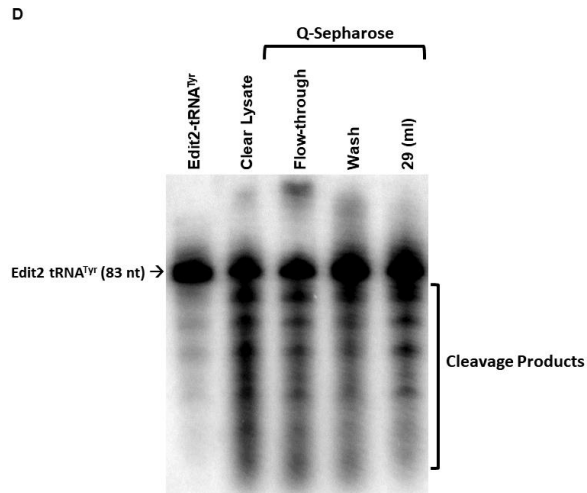


Figure 3.3 Purification of EETbSEN22

Size-exclusion chromatography and *in vitro* activity assay of purified TbSEN from *T. brucei* EETbSEN22. **A.** Chromatogram, linear regression, and western blot analysis (mouse Anti-Protein C HRP) depicting EETbSEN22 elution peak. **B.** *In vitro* activity assay performed with Edit2 tRNA^{Tyr} and size-exclusion purified enzyme. **C.** Chromatogram of Q-Sepharose and western blot analysis (mouse Anti-Protein C HRP) depicting EETbSEN22 elution peak. Peaks at 75 mM and 1 M salt did not contain the protein. **D.** *In vitro* activity assay performed with Edit2 tRNA^{Tyr} and Q-sepharose-purified enzyme.

3.2.3 TbSen22 and TbSen17 contain tRNA endonuclease domains

Considering the TbSEN subunits smaller molecular weights, we wondered whether they presented significant structural variations when compared to other eukaryotes. In order to investigate this, we performed multiple-sequence alignments of the TbSEN subunits and their eukaryotic homologs utilizing the online software Cobalt, and visualized the results with Jalview [97][98][99]. Sequences chosen for this analysis included the well-characterized TSEN homologs from *Homo sapiens*, *Saccharomyces cerevisiae*, *Methanocaldococcus jannaschii*, and *Arapidopsis thaliana* [33][25][100][101]. Our alignments showed that both TbSEN22 and TbSEN17 contain the expected C-terminus tRNA endonuclease domain (accession cd22363) complete with the catalytic triad Tyr/His/Lys, which is described and confirmed in the literature (**Fig. 3.4 A**) [33]. We also note that the difference in molecular weight observed in TbSEN components comes from a shorter N-terminus region, which has no identifiable domain in other eukaryotes (**Fig. 3.4 A**). Alignment of TbSen12 with TSEN15 homologs also denoted structural conservation at the C-terminus, although no specific protein domain could be identified for this molecule (**Fig. 3.4 B**).

B

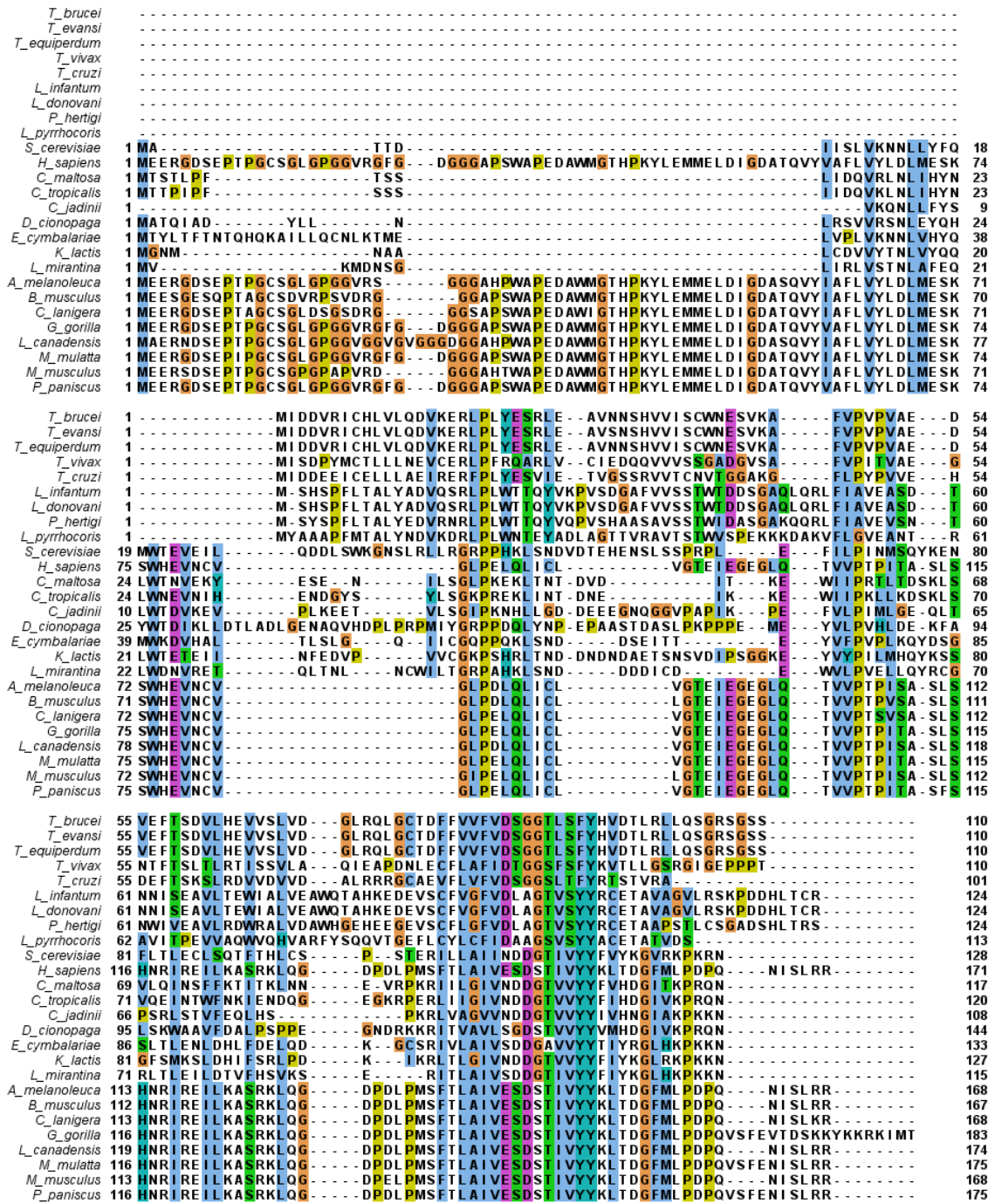


Figure 3.4 Endonuclease Domains of TbSEN

Figure 3.4 Endonuclease Domains of TbSEN

Multiple-sequence alignments of TSEN homologs generated with NCBI Cobalt and visualized with Jalview utilizing Clustal-X default residue coloring: blue (hydrophobic), red (positively charged), magenta (negatively charged), green (polar), pink (cysteine), orange (glycine), yellow (proline), cyan (aromatic), white (non-conserved). **A.** Multiple-sequence alignment of TSEN34 and TSEN2 homologs. The conserved catalytic triad Tyr/His/Lys, inside the C-terminus domain, is denoted by asterisks. **B.** Multiple-sequence alignment of TSEN15 homologs.

The same alignments of these TbSEN sequences were also used to generate phylogenetic trees utilizing the maximum likelihood method on the software MEGA11, with one thousand bootstrap repeats (**Fig. 5 A**) [102][103]. Also added to these trees were TSEN sequence representatives of fungi, protozoans, archaeans, metazoans, and plants, all obtained from National Center for Biotechnology Information (NCBI) BLAST queries [104] (**see Appendix C for full sequences and access numbers**). Our results show that, when full structure similarity is taken into consideration, TbSEN22 is most probably a homolog of TSEN2, and not TSEN34 as previously thought [12], while TbSEN17 is most probably the homolog of TSEN34 (**Fig. 3.5 A**). TbSEN22 and TbSEN12 structures were also more closely related to plant TSEN homologs, while TbSEN17 was more closely related to yeast TSEN34 homologs (**Fig. 3.5 A and B**).

A

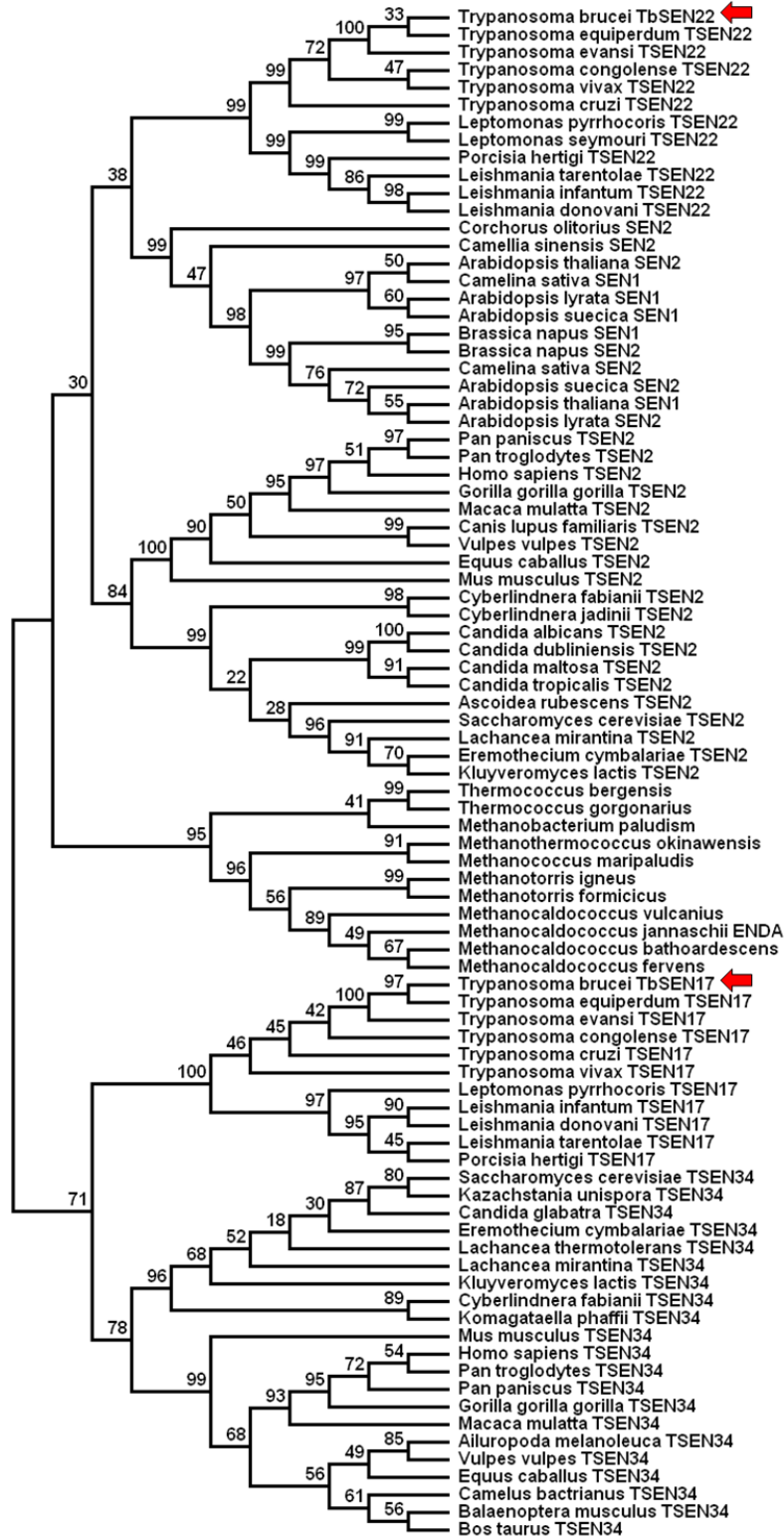


Figure 3.5 Phylogeny of TbSEN

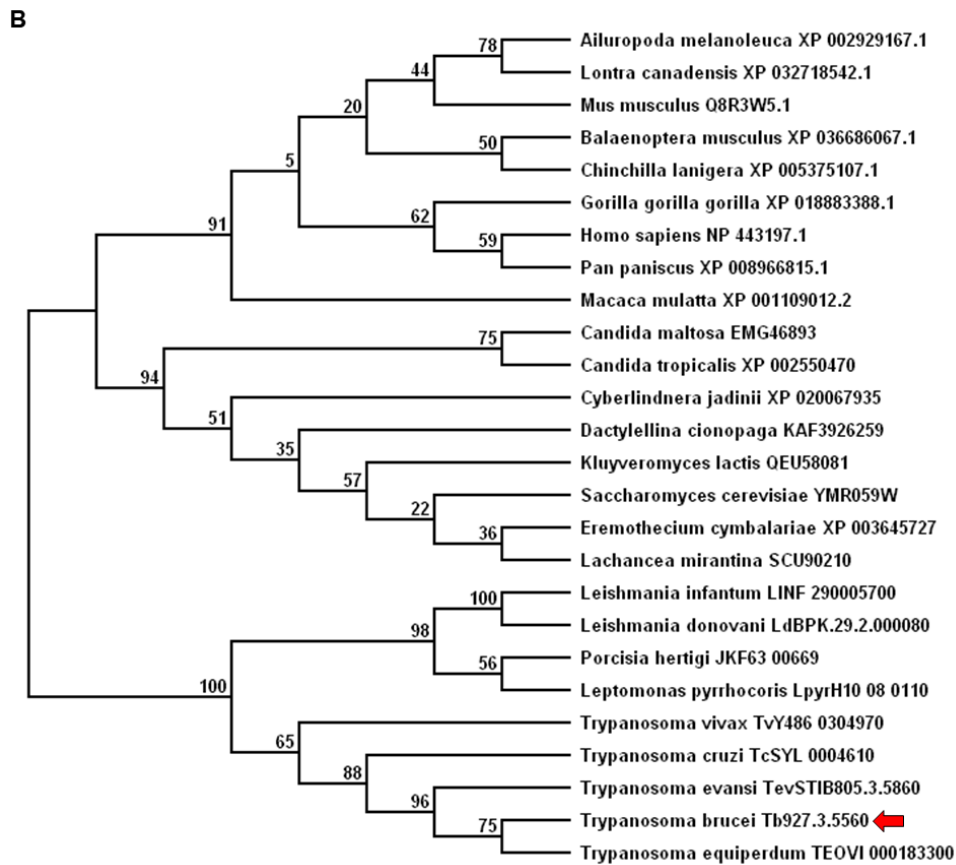


Figure 3.5 Phylogeny of TbSEN

Phylogenetic trees containing homologs of TSEN subunits from representative species generated with MEGA11. The maximum likelihood trees were generated with default parameters and one thousand bootstrap replicates. Bootstrap values are displayed as percentages at each tree node. **A.** TbSEN2 and TbSEN34 homologs tree. **B.** TbSEN15 homologs tree.

3.2.4 TbSEN localizes to the cytoplasm

In vertebrates, tRNA splicing takes place in the nucleus, the compartment where most of tRNA processing enzymes are located, and most tRNAs are thought to be exported to the cytoplasm ready to be used in translation [24][105]. Two notable exceptions are *S. cerevisiae* and *S. pombe*, where TSEN localizes to the surface of the mitochondria [54][106]. In the case of *S. cerevisiae*, tRNA splicing is not only located to the cytoplasm, but TSEN has been implicated in a secondary function of mRNA cleavage, mostly of mitochondrial messages [35]. TbSEN is structurally different from most TSEN homologs, with subunits containing shorter N-terminus, a possible heterotrimeric organization, and a unique preference for edited tRNAs [12]. We wondered, then, whether the enzyme would also present a different subcellular localization when compared to other eukaryotes. To further investigate this, we utilized the pPOT family of plasmids to *in-situ* tag one copy of each one of the TbSEN subunits in *T. brucei* SmOx [107][108]. This resulted in a single strain containing N-terminally tagged loci for TbSEN22 and TbSen17, and a C-terminally tagged locus TbSEN12 (**Fig. 3.6 A**). This strain was then utilized in immunofluorescence microscopy assays, where it was revealed that all three TbSEN subunits localize to the cytoplasm of *T. brucei*, and not to the nucleus or the mitochondrion (**Fig. 3.6 B, see Appendix A11 for protocol**). Moreover, we also show that TbSEN22 and TbSEN12, as well as TbSEN22 and TbSEN17 co-localize, with confident Mander's coefficients (>0.7) [109], indicating the three

subunits are most probably present in a complex that localizes to the cytoplasm
(Fig. 3.6 C).

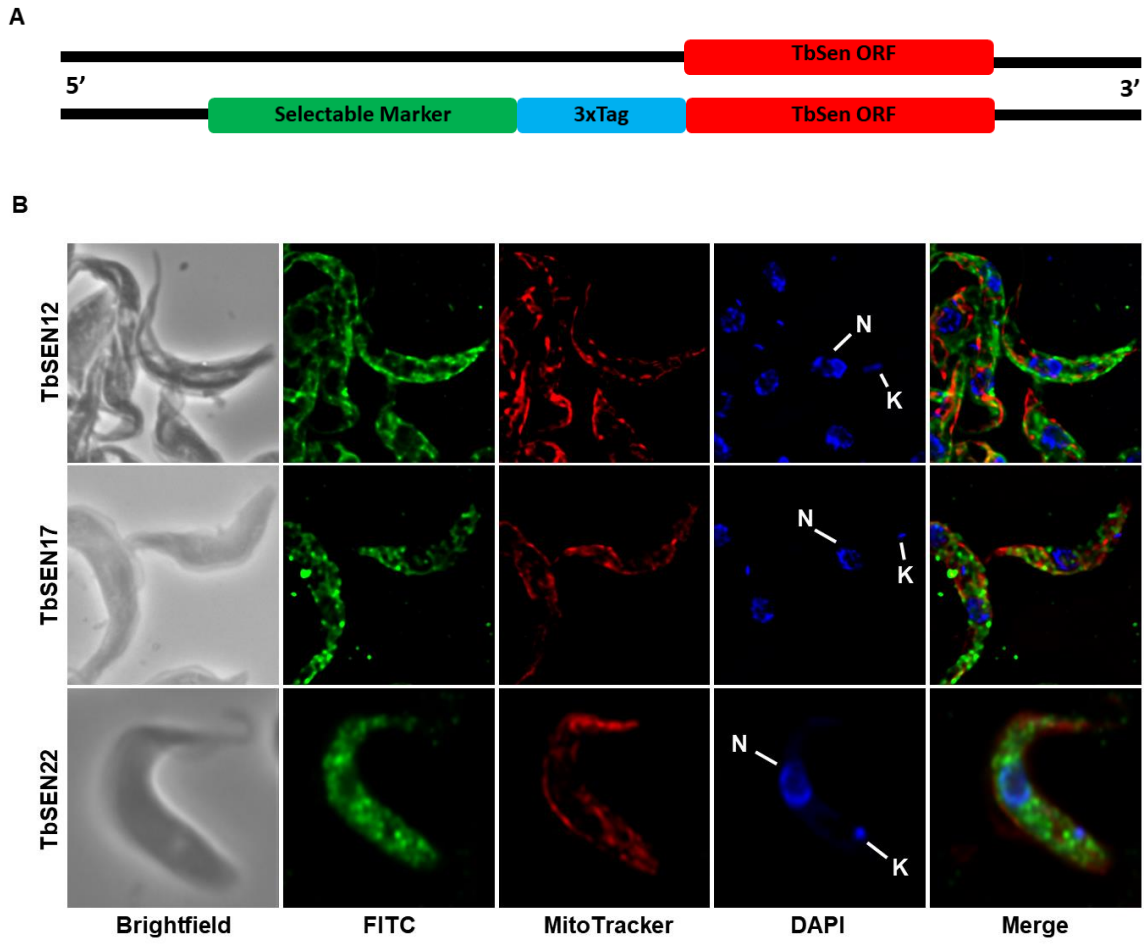


Figure 3.6 Immunofluorescence Microscopy of TbSEN

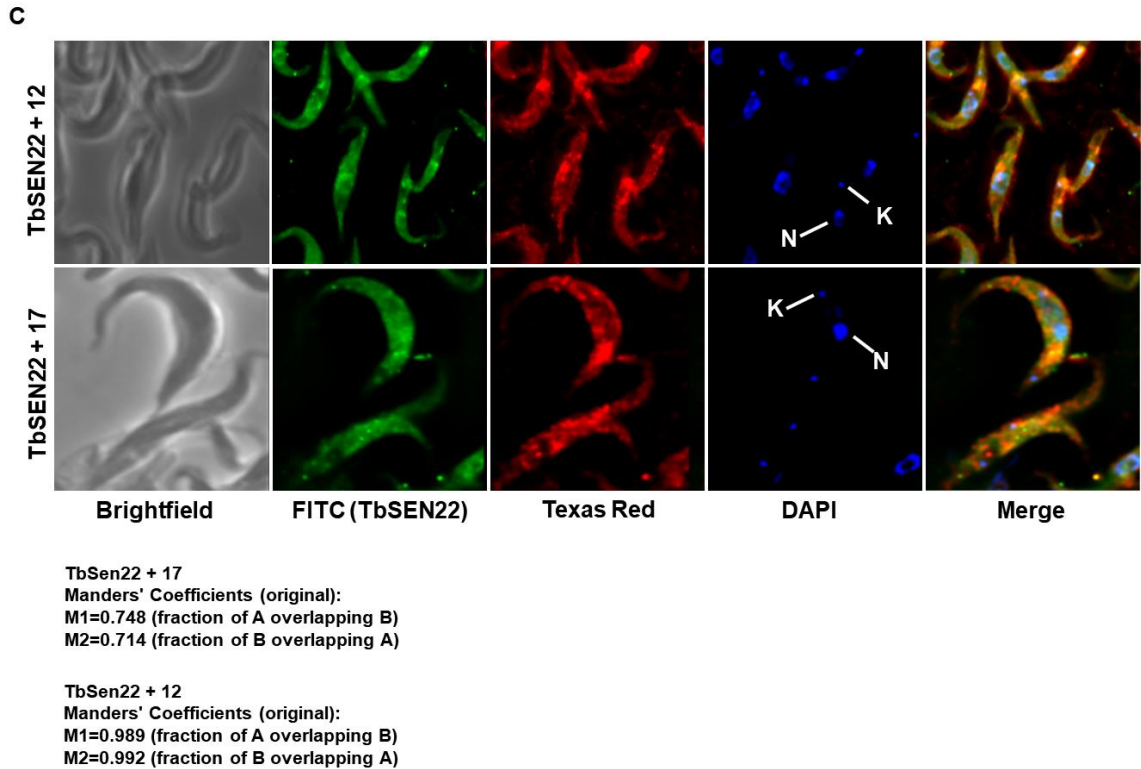


Figure 3.6 Immunofluorescence Microscopy of TbSEN

Immunofluorescence microscopy of *in-situ* tagged TbSEN subunits. **A.** Genomic context of *in-situ* tag-TbSEN *T. brucei* SmOx strain. **B.** Subcellular localization of individual TbSEN subunits. Green reveals the labeled protein, red reveals the mitochondrion, and blue reveals dsDNA (nucleus and kinetoplast denoted). **C.** Co-localization of TbSEN subunits. Green reveals TbSEN22, red reveals TbSEN12 or 17, blue reveals dsDNA.

3.2.5 TbSEN17 is essential for viability

As stated above, tRNA splicing is essential, and knockdowns of TbSEN22 result in growth phenotypes in *T. brucei*, as well as pre-tRNA^{Tyr} accumulation [12]. To assess whether TbSEN12 and TbSEN17 are also essential, and whether they are involved in tRNA splicing, we performed individual RNAi knockdowns of each subunit, followed by northern blot analysis. Our results show that TbSEN17 knockdown generates a growth phenotype in *T. brucei*, similar to the one reported for TbSEN22 (**Fig. 3.7 B**) [12]. A growth phenotype was also detected for TbSEN12 knockdown (**Fig. 3.7 A**), however, this knockdown could not be corroborated by RT-PCR, indicating a possible off-target effect of the plasmid utilized (**Fig. 3.7 A**) [110]. Moreover, northern blot analysis performed on total RNA extracted from the strains showed no accumulation of pre-tRNA under knockdown conditions of TbSEN17 (**Fig. 3.7 C**).

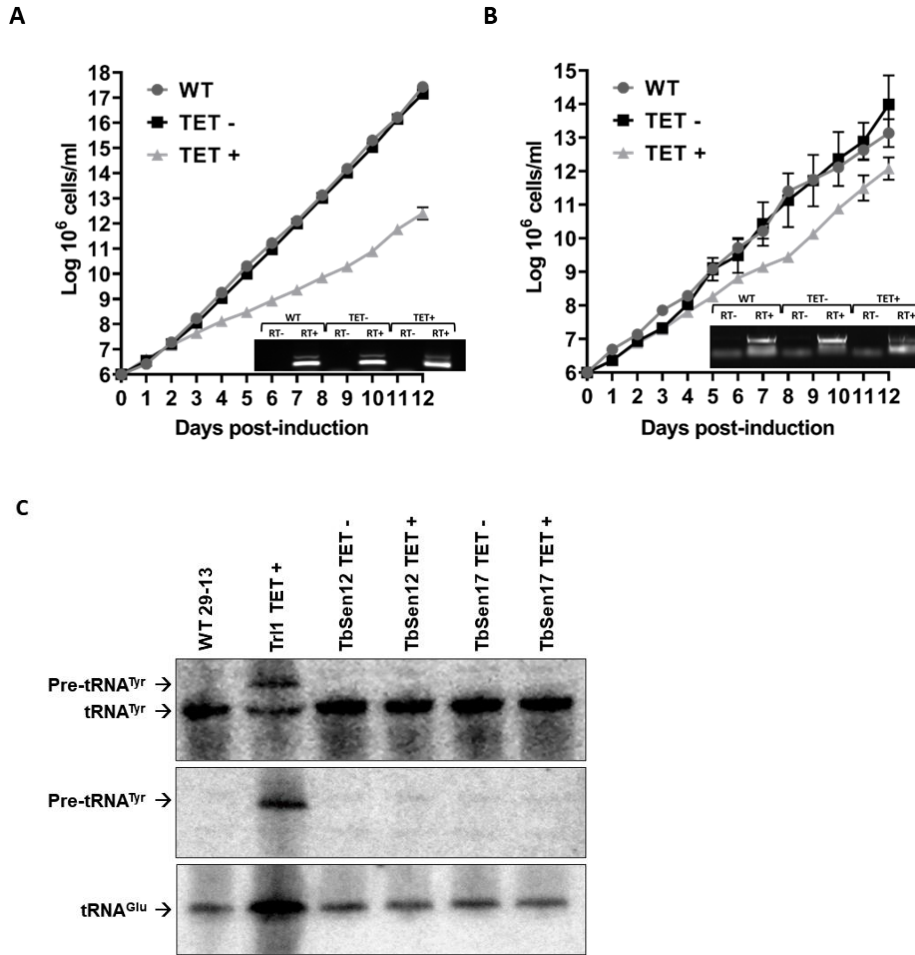


Figure 3.7 Knockdown of TbSEN12 and 17

RNAi knockdown of TbSEN12 and TbSEN17. **A.** TbSEN12 knockdown growth curve and RT-PCR results. Cell concentrations shown on Y axis are cumulative. **B.** TbSEN17 knockdown growth curve and RT-PCR corroboration. **C.** Northern blot analysis of total RNA extracted from day 7 of the knockdowns.

3.2.6 TbSEN activity reconstitution attempts in *E. coli*

Recently, the human TSEN enzyme was reconstituted in both prokaryotic and eukaryotic models utilizing inducible plasmid expression systems [33][34]. This reconstitution allowed for in-depth studies of TSEN characteristics such as substrate preference, assembly, relationship to disease, and the obtention of a crystal structure [34] (reviewed in **section 1.6**). Following those lines, we attempted to reconstitute TbSEN in the prokaryotic model *E. coli* BL21. For this end, an artificial operon was constructed containing the three TbSEN subunits, including a hexa-his N-terminally tagged TbSEN22. We then utilized chromatographic assays including nickel affinity (Ni-NTA), followed by either size-exclusion or anion exchange to further purify 8xHis-TbSEN22. Purified samples were then resolved by SDS-PAGE, which were further stained with silver or utilized in western blot analysis with mouse anti-His antibodies. This purification approach revealed protein bands corresponding to the His-TbSEN22 and five other proteins, including two with sizes consistent with TbSen12 and TbSen17 (**Fig. 3.8 A and B**). No endonuclease activity was detected at any point in the purification process. Interestingly, the recombinant TbSEN behaved similarly to the endogenous TAP-tag TbSEN during size-exclusion analysis and anion-exchanging, including eluting with a size of 55 kDa, consistent with that of a trimer composed of TbSEN12, 17 and 8xHis-TbSEN22, and eluting from Q-Sepharose at 350 mM salt concentration (**Fig. 3.8 C and D**).

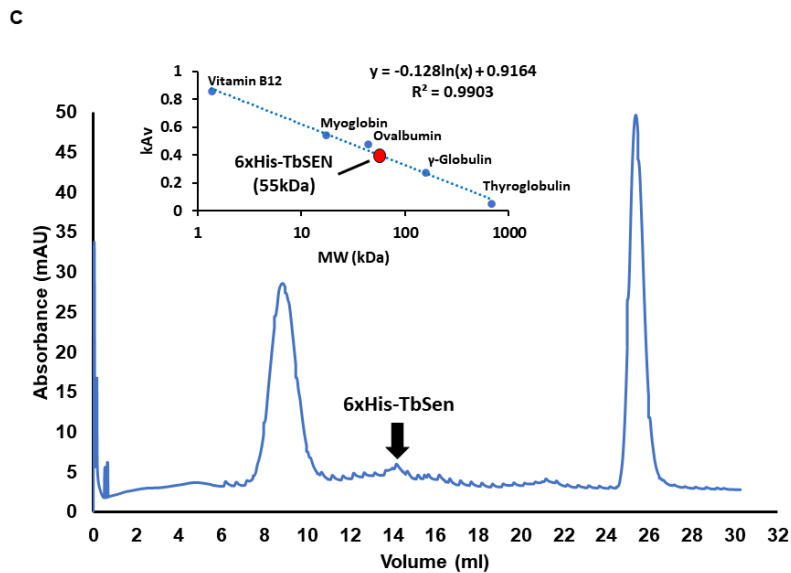
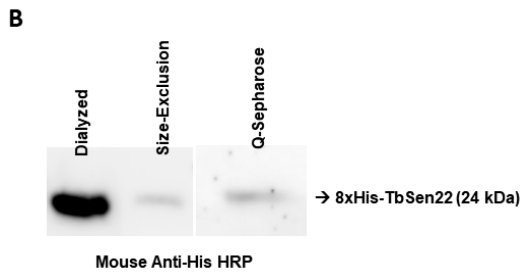
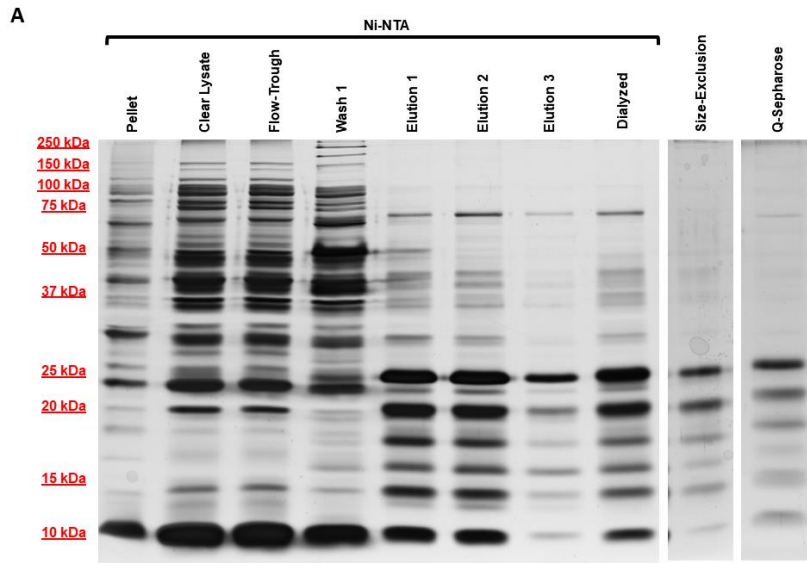


Figure 3.8 Purification of Recombinant TbSEN

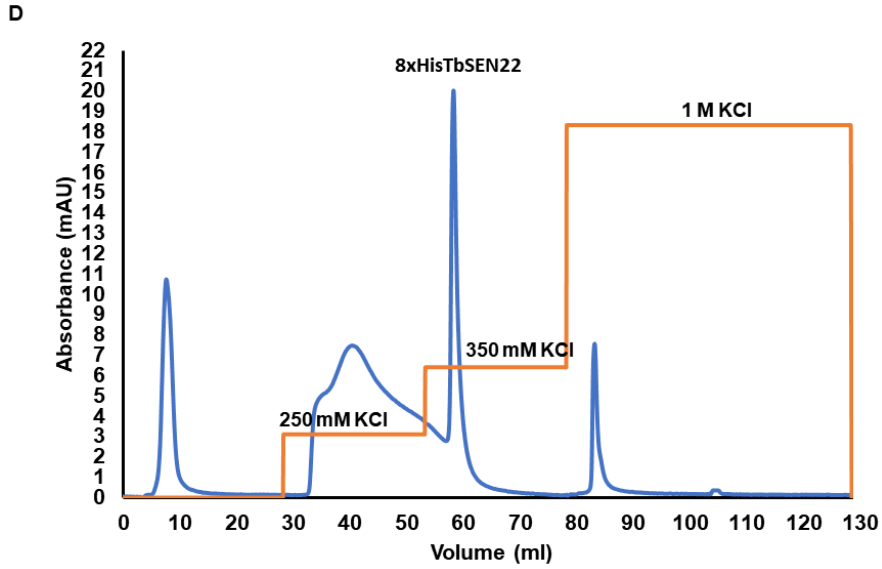


Figure 3.8 Purification of Recombinant TbSEN

Overview of recombinant TbSEN purification steps. **A.** Silver-stained gel containing 15 μg of total protein per lane for every step of purification. **B.** Western-blot analysis with mouse anti-His revealing His-TbSen22. **C.** Chromatogram depicting 8xHis-TbSEN22 elution peak and linear regression analysis. **D.** Chromatogram of Q-Sepharose purification depicting 8xHis-TbSEN22 elution peak. Peaks at 250 mM and 1 M salt did not contain the protein.

3.3 Discussion

Previously, a single homolog for a TSEN subunit had been described in *T. brucei*: TbSEN22 [12]. Throughout this project, utilizing chromatographic methods for protein purification, and bioinformatics tools for structural analysis, we were able to identify two additional *Trypanosoma* homologs of TSEN: TbSEN17 and TbSEN12. TbSEN17 is a 17 kDa protein containing a tRNA endonuclease domain at the C-terminus, complete with the catalytic triad described in the literature for TSEN [33]. The presence of this conserved domain indicates that TbSEN17 may partake in essential pre-tRNA cleavage, however, while a growth phenotype can be observed under knockdown conditions, no pre-tRNA^{Tyr} accumulation could be detected in the northern blot analysis performed on total RNA extracted from TbSEN17 RNAi strains. Interestingly, northern blot analysis also failed to detect pre-tRNA accumulation under TbSEN22 knockdown conditions, and RT-PCR was utilized instead, indicating that the accumulated pre-tRNAs may be short-lived in *T. brucei* [12]. Our attempts at amplifying pre-tRNA^{Tyr} from TbSEN17 RNAi strains via RT-PCR were unsuccessful, so the question of whether TbSEN17 partakes in pre-tRNA cleavage remains unanswered.

Previously, TbSEN22 had been implicated as a TSEN34 homolog in *T. brucei* [12]. Our phylogenetic analysis utilizing the maximum likelihood method and full protein sequences suggests instead, that TbSEN17 is the homolog of TSEN34, and TbSEN22 is the homolog of TSEN2. Interestingly, our analysis also shows that TbSEN22 (as well as TSEN22 of other trypanosomatids), is more closely related

to plant TSEN2 proteins, while TbSEN17 (as well as TSEN17 of other trypanosomatids), is more closely related to fungi TSEN34 proteins. Trypanosomatids have been suggested to possess a “photosynthetic lineage”, as their genomes contain several “plant-like” genes, which includes homologs of proteins that are found in the chloroplast or cytoplasm of plants, algae, and cyanobacteria [111]. Examples include homologs of the chloroplast-localized 6-phosphogluconate dehydrogenase (cp6PGDH) and sedoheptulose-1,7-bisphosphatase (SPBase), as well as the ascorbate-dependent hemoperoxidase (TcAPX) [112][113]. Moreover, it has been suggested that Trypanosomatids had obtained, most probably by endosymbiosis, and subsequently lost, a photosynthetic plastid [112]. Indeed, a functional photosynthetic plastid can be found in the closely-related group of euglenids, which together with trypanosomatids, form the *Euglenozoa* phylum [112]. Trypanosomatids possess, instead, a specialized peroxisome, dubbed “glycosome”, that houses most of the enzymes involved in glycolysis, some of which, are homologous to plastid proteins [114][112]. Our data here suggests, intriguingly, that TbSEN22 may also have a “plant-like” origin.

In eukaryotes, TSEN is an heterotetramer, composed of four subunits, including TSEN2, 12, 34 and 54 (a conformation known as $\alpha\beta\gamma\delta$), and all subunits are required for pre-tRNA cleavage activity [24][33][34]. Our purification assays utilizing a TAP-tagged TbSEN22 produced an enzyme that elutes from size-exclusion columns with a size consistent with that of a 66-kDa trimer of TbSEN12,

17 and TAP-22, but that is still capable of cleaving pre-tRNA *in vitro*. This suggests that, in *T. brucei*, a homolog of TSEN54 is either not required for activity, or not present at all. In the latter case, TbSEN would possess an alternate conformation, being instead, a heterotrimer. A trimeric domain TSEN organization has been previously described in the archaea *Candidatus Micrarchaeum acidiphilum* (ARMAN-2), in stark contrast to other archaeal TSEN, which possess either homotetrameric (α_4), homodimeric (α_2), or heterotetrameric ($\alpha\beta$)₂ conformations [115]. This enzyme is composed of a duplicated catalytic unit bound to a structural subunit, all present in one gene, and is capable of cleaving bulge-helix-bulge (BHB) motifs as a dimer, which is dubbed ϵ_2 , after the fusion of the three domains [115]. A possible heterotrimeric organization of TbSEN would show a similarly stark contrast to eukaryotic TSEN, on which TSEN54 is missing, but is not required for activity.

In vertebrates, TSEN localizes to the nucleus, while in *S. cerevisiae*, it localizes to the surface of the mitochondria, where it performs the secondary function of mRNA cleavage [35]. Indeed, the yeast enzyme has been implicated on a novel mRNA decay pathway, dubbed TSEN-initiated decay pathway [35]. Our immunofluorescence localization shows that TbSEN (in the form of TbSen12, 17 and 22) localizes to the cytoplasm, corroborating previously published data from our group that shows that, in *Trypanosoma brucei*, Trl1, the second enzyme in the tRNA splicing ligase pathway, localizes to this compartment [53]. Whether TbSEN

also possess a secondary function due to this unique subcellular localization, remains to be uncovered.

Our attempts at reconstituting activity of TbSEN in *E. coli* BL21 were unsuccessful. Our tagged TbSEN22 is capable of co-purifying with five other proteins, including two with sizes consistent with TbSEN12 and TbSEN17; it also behaves similarly to the endogenous enzyme when subjected to size-exclusion and anion exchange chromatographic methods, eluting with the size consistent with that of a trimer (55 kDa), and at 350 mM salt concentration, respectively. In spite of this, the recombinant protein shows no *in vitro* pre-tRNA cleavage activity on any step of the purification. One possible explanation is that the recombinant TbSEN is missing essential post-translational modifications (PTMs), which cannot be added in the prokaryotic model utilized for this experiment. In the reconstitution of the human TSEN, purification of a CLP1-TSEN complex was not possible in *E. coli*, requiring instead, a HEK-293 system, indicating that complex formation most probably required PTMs [33]. A search for TSEN PTM sites in the yeast amino acid modifications database (YAAM) reveals that T106 in TSEN2, and S399, S400, and T401, in TSEN54 are phosphorylated [116]. A similar search in the human PTM database reveals that TSEN2 receives 16 PTMs, including phosphorylation and acetylation, with six phosphorylation sites localizing to the tRNA endonuclease domain [117]. Moreover, the human TSEN34 receives a total of 27 PTMs, including methylation, phosphorylation, acetylation, and ubiquitination, with three phosphorylation sites and one ubiquitination site localizing to the tRNA

endonuclease domain [117]. Human TSEN15 also contains four phosphorylation sites, while TSEN54 contains 32 sites for methylation, phosphorylation, acetylation, and ubiquitination, similarly to TSEN34 [117]. PTMs are common in trypanosomatids, with *T. brucei* and *T. cruzi* possessing heavily modified histones as a form of epigenetic control of gene expression [118][119]. Described trypanosomatids PTMs include the aforementioned phosphorylation, acetylation, and ubiquitination, as well as hydroxylation, succinylation, malonylation, and many others [119]. Furthermore, *T. brucei* also acetylates and detyrosinates the α -tubulin components of the flagella and cytoskeleton, potentially as means to discriminate between old and newly synthesized microtubule arrays during cell division [120]. If TbSEN components require any PTMs for pre-tRNA cleavage activity, it is evident that our prokaryotic system cannot provide it. We suggest reconstitution of the enzyme activity may yield better results if performed in a eukaryotic system, such as insect cells [34].

In most eukaryotes, TSEN is a heterotetramer which, in vertebrates, localizes to the nucleus, where it acts on multiple pre-tRNAs. Here, we have described an unusual homolog of TSEN in *T. brucei*, dubbed TbSEN. We furthermore present evidence that: the TbSEN complex contains homologs of TSEN2 and TSEN34 with complete active sites, including the catalytic triad Y/H/K; the tRNA cleavage activity does not require TSEN54, or, rather, TbSEN is possibly a heterotrimer that is missing TSEN54 completely; the complex localizes to the cytoplasm, alongside Trl1 ligase, the next enzyme in the tRNA splicing pathway

[53]. We suggest that TbSEN is a divergent homolog of TSEN, composing a minimalized tRNA splicing system that deals with a single intron-containing tRNA substrate (**Fig. 3.9**).

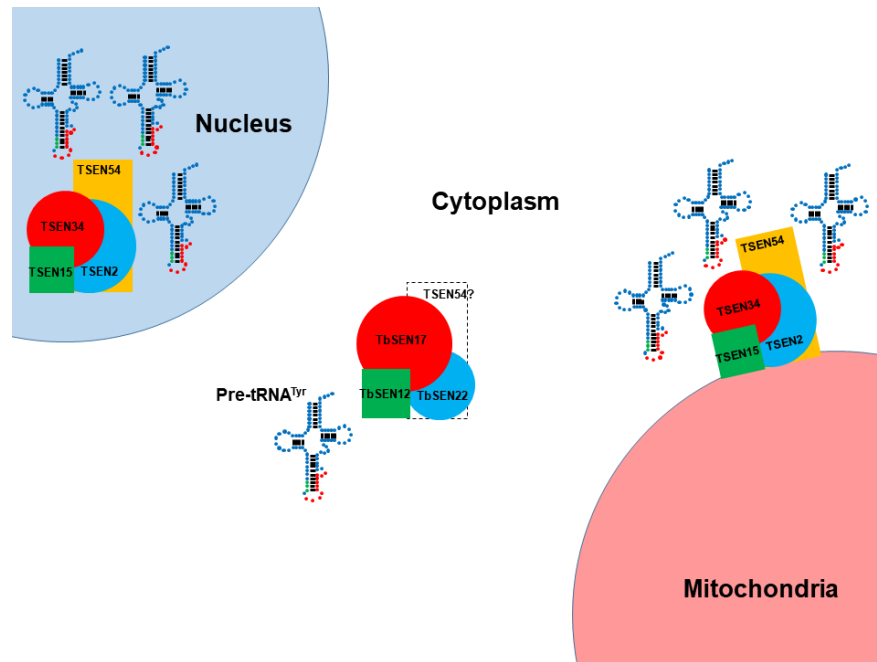


Figure 3.9 Proposed Model for TbSEN

A proposed model for TbSEN: in vertebrates, TSEN localizes to the nucleus; in *S. cerevisiae* and *S. pombe*, it localizes to the surface of the mitochondria, where, in *S. cerevisiae*, it has secondary functions acting on mRNA. In both cases, the enzyme catalyzes pre-tRNA cleavage on a variety of tRNA species. TbSEN localizes to the cytoplasm, and is possibly a heterotrimer of smaller homologs of TSEN2, 34 and 15, composing a minimalized tRNA cleavage system that is enough to recognize and bind its sole tRNA substrate, pre-tRNA^{Tyr}.

3.4 Materials and methods

3.4.1 EETbSEN22 TAP-Tag Purification

EETbSEN22 cells were allowed to grow in 6 liters of SDM-79 media containing 10% fetal bovine serum for 48 hours before being harvested by centrifugation at 1400 g for 10 min. Pellets were either stored at - 80° C, or immediately resuspended in PA-150 buffer (150 mM potassium chloride, 20 mM Tris-HCl [pH 7.7], 3 mM MgCl₂, 0.1% Tween 20) for total protein extraction by sonication followed by centrifugation [96]. Cleared lysates were bound to IgG Sepharose by rotation at 4° C for 4h, washed with PA-150, and eluted by addition of 300 U of TEV protease in PA-150 under rotation at 4°C overnight [96]. Eluted proteins were then bound to Anti-Protein C matrix by rotation at 4° C for 2h, and eluted with EDTA/EGTA elution buffer (5 mM Tris-HCl [pH 7.7], 10 mM EGTA, 5 mM EDTA) [96]. Samples were resolved in 10% acrylamide gels and visualized by silver staining or western-blotting with mouse anti-protein C HRP.

3.4.2 Size-exclusion chromatography

Cleared lysates of EETbSEN22 resuspended in PA-150 were ran through a PA-150 equilibrated Superdex 200 Increase Column attached to an ÄKTA™ Pure system (Cytiva), and 500 µl volume fractions were collected according to manufacturer protocols. For linear regression calculations, Bio-Rad gel-filtration standards (Catalog # 1511901) were run through the column in similar fashion. For

the size-exclusion of recombinant TbSEN, Nickel-purified samples were dialyzed overnight to remove imidazole from buffer prior to injection into the column.

3.4.3 Anion-exchanging

Cleared lysates of EETbSEN22 resuspended in PA-150 were dialyzed to reduce salt concentrations to 50 mM prior being injected into an equilibrated Q-Sepharose Fast Flow column attached to an ÄKTA™ Pure system (Cytiva), and 1000 µl volume fractions were collected according to manufacturer protocols. To determine salt concentrations for TbSEN, a linear gradient was utilized first, where the enzyme was revealed to elute at a predictable 350 mM KCl concentration. Further purifications utilized step gradients. For the purification of recombinant TbSEN, Nickel-purified samples were dialyzed overnight to remove imidazole from buffer prior to injection into the column.

3.4.4 Immunofluorescence microscopy

T. brucei 29-13 procyclic cells were allowed to grow in 50 ml of SDM-79 media containing 10% fetal bovine serum for 24 hours before being harvested by centrifugation at 1400 g for 10 min. Cells were then resuspended in 1 ml of serum-free SDM-79, and incubated with 400 nM final concentration Mitotracker for 30 min at 27° C under agitation. Cells were then harvested by centrifugation, washed with serum-free SDM-79 twice, before being resuspended in 100 µl 1 x PBS. Cells were then fixed and spotted into microscope slides with addition of formaldehyde to a

final concentration of 3.7% (v/v), and allowed to dry overnight. Following that, cells were permeabilized with 0.1 % Triton-X for 20 min, and washed twice with 1 X PBS. Blocking was performed with 1 X PBS containing 5.5 % FBS and 0.05 % Tween-20 for 1h, before washing with 1 X PBS twice. Primary and secondary antibodies were bound according to manufacturer suggested dilutions, performed in 1 X PBS containing 3 % BSA and 0.05 % Tween-20. DNA was stained with addition of 300 nM DAPI in 1 X PBS for 1 min, followed by washing with 1 X PBS twice. Slides were then allowed to dry for 2 h before being mounted with Vecta shield mounting media, according to manufacturer protocols, and sealed before microscopy analysis. Imaging was performed utilizing a Nikon Eclipse TI2 fluorescence microscopy and associated software.

3.4.5 Cell culturing and RNAi knockdowns

T. brucei 29-13 procyclic cells [91] were cultured at 27° C in SDM-79 media supplemented with 10% FBS, and growth was assessed by counting with Neubauer chambers. Gene knockdowns were performed with p2T7-177 plasmids as previously described [75]. RNAi was induced by addition of 1 µg/ml tetracycline to the media, generating a dsRNA from two head-to-head T7 promoters [75].

3.4.6 Northern blot analysis

T. brucei 29-13 procyclic cells at mid to late log (6×10^6 to 1×10^7 cells/ml), were harvested by centrifugation at 1400 g for 10 min and washed twice with PBS.

Total RNA was isolated from pellets using a guanidinium thiocyanate-phenol-chloroform protocol as previously described [92]. Samples containing 5 µg of total RNA were resolved in denaturing 8M urea 8% polyacrylamide gels, electroblotted into Zeta-probe nylon membranes according to manufacturer protocol (Bio-Rad), then UV-cross-linked for 1 min. Northern blot hybridization was performed according to manufacturer specifications using ³²P-labeled oligonucleotides. After hybridization, membranes were exposed overnight to a phosphoimager screen. Blots were analyzed using a Typhoon FLA 9000 scanner and the ImageQuant TL software (GE Healthcare). Probes used for Northern hybridization were as follows (5'–3' orientation); tRNA^{Tyr} CCTTCCGGCCGGAATCGAACCAGCGAC; Edit2 tRNA^{Tyr} (for intron visualization) GATACCTGCAAACCTCTAC.

3.4.7 Western blot analysis

Samples containing up to 15 µg of total protein (per lane) were resolved by SDS-PAGE in 10 % Laemmli gels, at constant 90 V for 1h30min, utilizing the mini-PROTEAN tetra vertical electrophoresis cell (Bio-Rad), according to manufacturer protocols. Transfers to nitrocellulose membranes were performed at constant 200 mA for 2h, utilizing the mini trans-blot cell (Bio-Rad) according to manufacturer protocols.

Chapter 4: Concluding remarks and future directions

4.1 Summary

In eukaryotes, tRNA intron cleavage, the first step in the tRNA splicing pathway, is catalyzed by a heterotetrameric enzyme called TSEN [25][33][24]. The four TSEN subunits form a complex that, in vertebrates, localizes to the nucleus, and all components are required for cleavage activity [25][33][24]. In *S. cerevisiae* and *S. pombe*, TSEN localizes to the surface of the mitochondria, and, in *S. cerevisiae*, has been implicated in secondary functions, including mRNA cleavage and decay [54][35][106]. In these organisms, TSEN must deal with multiple pre-tRNAs, and substrate recognition is broad, not requiring a full tRNA molecule in humans [33]. Following intron cleavage, the intron is quickly degraded, while the tRNA exons are joined by ligase enzymes: Trl1, in most eukaryotes, or a complex containing Archease and RtcB, in vertebrates [26][27]. Finally, after ligation by Trl1, the phosphotransferase TPT1 removes a leftover phosphate group from the molecule, generating a mature tRNA [29]. The genome of *T. brucei* encodes a single intron-containing tRNA, TbtRNA^{Tyr}_{GUA}, a single-copy gene. Splicing of TbtRNA^{Tyr} is therefore, essential. Previously, through a number of published works, we have shown that pre-TbtRNA^{Tyr} is a very particular molecule, with unconventional features, including a small intron composed of only 11 nucleotides that undergoes noncanonical base editing as prerequisite for intron cleavage [12]. We have also shown that the Trl1 ligase, an essential component of tRNA splicing pathway, localizes to the cytoplasm in *T. brucei*, indicating that the pre-tRNA is

exported to the cytoplasm for cleavage [53]. Furthermore, the mature TbtRNA^{Tyr} contains the modified nucleotide queuosine (Q) at the anticodon position 34, and the enzyme responsible for this modification is nuclear, indicating that, after splicing, this tRNA undergoes retrograde transport from the cytoplasm to the nucleus to receive Q, before being exported back into the cytoplasm [55]. Moreover Q-modified and unmodified TbtRNA^{Tyr} co-exist in the cytoplasm and engage in translation, with unmodified tRNA^{Tyr} decoding G-ending codons for tyrosine, while Q-modified tRNA^{Tyr} is necessary for the efficient translation of the U-ending codons [56].

In chapter 2 we expand on TbtRNA^{Tyr} uniqueness, showing that the molecule is present as two isoforms, which can be detected by differential resolving in urea gel electrophoresis followed by northern blot hybridization. These isoforms correspond to the mature-sized TbtRNA^{Tyr} (75 nt), plus an alternative isoform of the molecule, dubbed alt-tRNA^{Tyr} (approx. 120-nt). Our data shows that TbtRNA^{Asp}, but no other tested tRNA, is also present as two distinct isoforms. Furthermore, through transcription arrest assays, we reveal that both isoforms of tRNA^{Tyr} exhibit strikingly short half-lives when compared to other tRNAs, both in the same system, and to what is available in the literature. Interestingly, this short half-life is not shared by any other tested tRNA, including both isoforms of TbtRNA^{Asp}. Our RNAi knockdowns and northern blot hybridization assays indicate the endonuclease RRP44, an exosome component in other eukaryotes, but a stand-alone enzyme in *T. brucei*, is responsible for tRNA^{Tyr} degradation. Protein

representatives of eukaryotic tRNA degradation pathways, including homologs to XRN1, Dis3L2, and RRP6, showed little to no effect on TbtRNA^{Tyr} stability during our assays, implying tRNA^{Tyr} stability to be controlled exclusively by RRP44. Interestingly, the RRP44 canonical function in rRNA maturation has been confirmed in *T. brucei* [121][79], indicating tRNA degradation may be a secondary function, perhaps associated with its standalone status in this organism. Considering these unique aspects of TbtRNA^{Tyr}, we suggest this molecule may be used as a nutrient sensor in *T. brucei*, with the rapid turnover allowing for rapid changes in protein biosynthesis in response to environmental changes.

In chapter 3, we describe the *T. brucei* homolog of TSEN: TbSEN. Previously published data had uncovered a single homolog for the active site-containing TSEN34, dubbed TbSEN22, after the smaller molecular weight [12]. Through the use of chromatographic methods, including tandem affinity purification of a tagged TbSEN22, anion exchanging, and size-exclusion, we were able to describe two other components: the active site-containing TbSEN17, and TbSEN12, a homolog of TbSEN15. While no homolog for TSEN54 could be located throughout our experiments, we showed that this enzyme, which elutes from size-exclusion chromatographic runs with the size of a trimer, is capable of cleaving pre-tRNA^{Tyr} *in vitro*. This implies that a homolog for TSEN54 is either not required for activity, or not present in this system. Through RNAi knockdowns, we showed that TbSEN17 is essential, but northern blot hybridizations failed to depict any relationship to tRNA splicing. Moreover, our phylogenetic analysis show that

TbSEN22 is, in fact, a homolog of TSEN2, while TbSEN17 is the homolog of TSEN34. These enzymes are very closely related structurally, containing a conserved tRNA endonuclease domain, and are thought to have originated from a gene duplication event [24]. Finally, in contrast to recently published data on the human TSEN [33][34], our attempts at reconstituting activity in a prokaryotic system were unsuccessful.

4.2 Further exploring TbtRNA^{Tyr}

While at the end of chapter 2 the identity of alt-tRNA^{Tyr} remains undisclosed, preliminary sequencing data on the molecule suggests it to be a 3'-end polyuridylated tRNA. Polyuridylation is rampant in the *Trypanosoma* mitochondrion, where all transcripts receive poly(U), both at the 3' end, and inside the sequence, assisting with maturation and changing the message of mRNAs [122][123]. The exceptions to this rule are tRNAs, which are absent from the mitochondrial genome, and must be imported from the cytoplasm [124]. The mitochondrial polyuridylation events are catalyzed by two uridylyltransferases (TUTases) called TUT1 and TUT2, which are present inside a larger protein complex [49]. Homologs of these enzymes, called TUT3 and TUT4 can be found in the cytoplasm of trypanosomatids, but have no described function [49]. We wondered whether polyuridylation of tRNAs in the cytoplasm may be the function of TUT3 and 4 in *T. brucei*, and if that activity is related to tRNA^{Tyr} stability. In order to investigate this, we individually knocked down their expression by inducible

RNAi. Induced and mock-treated transgenic RNAi cell lines were grown for 10 days [75]. Total RNA was collected after six days of RNAi induction for northern blot hybridization. Knockdown of TUT3 generated a mild growth phenotype, and a statistically significant effect on both isoforms of tRNA^{Tyr}, while knockdown of TUT4 generated a more pronounced growth phenotype, but no observable effect on tRNA (**Fig. 4.1 A-D**). We wonder whether TUT3 and 4 have redundant roles in the cytoplasm, and if a more severe effect on both growth and tRNA stability would be seen with a depletion of both enzymes. This could be tested with a double RNAi of TUT3/4, which has already been planned and is at preliminary stages in our group.

The only other tested tRNA to show two isoforms in our study was tRNA^{Asp}, which is also a Q-modified tRNA. At first glance, one could be induced to relate Q to both tRNA stability, and the presence of multiple isoforms. However, while tRNA^{Asp} stability was also affected by knockdowns of RRP44, it does not share the tRNA^{Tyr} short half-life, as denoted in our transcription arrest assays, which is puzzling. Moreover, the other two Q-modified tRNAs (Asn and His), exhibit neither isoforms or short half-lives, implying Q is not related to either stability nor the presence of isoforms. A deeper analysis of other *T. brucei* tRNAs, including northern blot hybridizations for at least one representative of each of the 20 isoacceptors, as well as RNA sequencing, could better elucidate the presence of isoform tRNAs in this organism. We have already prepared large amounts of extracted RNA from *T. brucei* cells for RNA-seq analysis for this end.

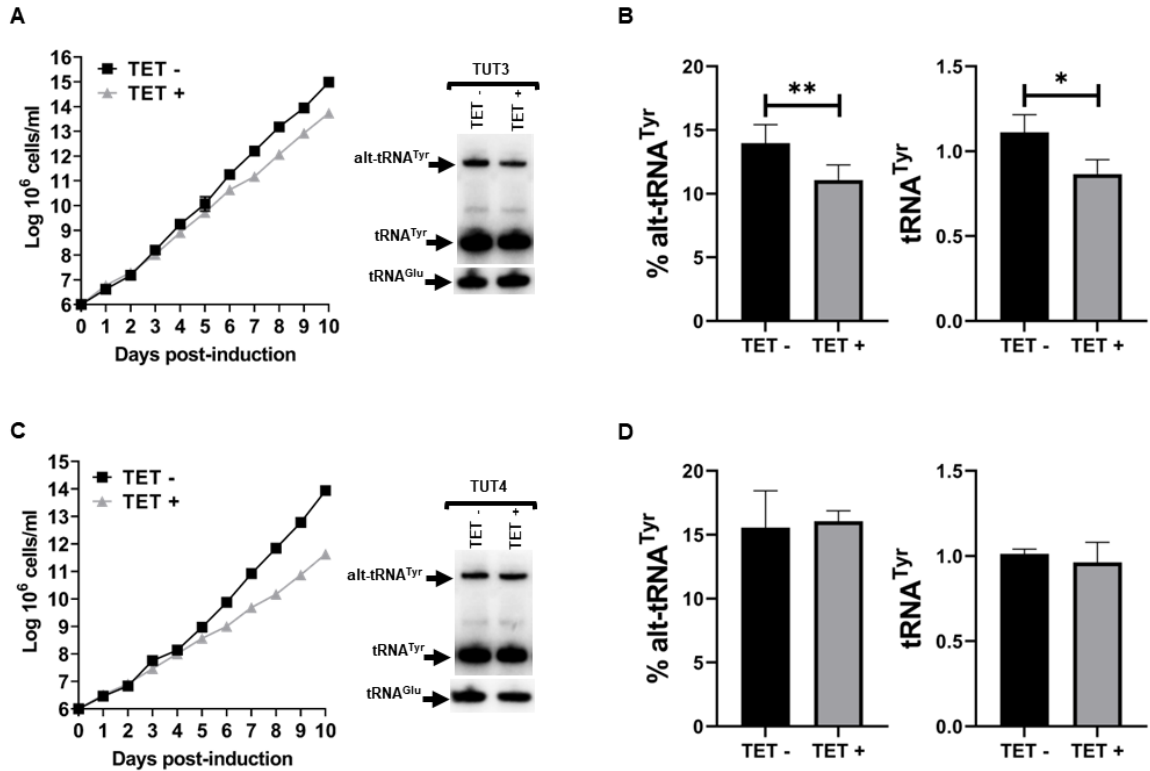


Figure 4.1 Knockdown of TUT3 and 4

Knockdown of *T. brucei* TUT3, but not TUT4 destabilizes tRNA^{Tyr}. **A and C.** Triplicate growth curve of *T. brucei* cells subjected to tetracycline-induced protein knockdown where total RNA was collected on day 6, and Northern blot hybridization performed on the extracted total RNA samples revealing the mature and alternate conformers of tRNA^{Tyr}. Cell concentrations shown on Y axis are cumulative. **B and D.** Relative amounts of alternate conformer tRNA^{Tyr} and mature tRNA^{Tyr} plotted as triplicates.

4.3 Further exploring TbSEN and tRNA splicing

Throughout this project, we were able to describe two additional subunits of TbSEN: TbSEN12 and TbSen17. Whilst we were not able to locate a homolog of TSEN54, we showed that this subunit, if present, is not required for cleavage activity *in vitro*. Our immunofluorescence microscopy assays show that TbSen subunits co-localize to the cytoplasm, the same compartment where the next enzyme in the splicing pathway, TbTrl1, localizes [53]. Puzzling, knockdowns of TbTrl1, but not of TbSen subunits, lead to the accumulation of pre-TbtRNA^{Tyr} to a degree that can be easily detected by northern not hybridization, implying this enzyme is somehow affecting the previous step in the splicing pathway. Our preliminary structural analysis of both TbTrl1, and the phosphotransferase TbTPT1, showed these enzymes exhibit some unique structural characteristics that deviate from other eukaryotes, including the presence of an extra domain in TbTPT1, and multiple putative homologs for TbTrl1. We wonder whether the enzymes for the tRNA splicing pathway all co-localize in the cytoplasm of *T. brucei*. This could be answered by immunofluorescence microscopy assays, not unlike the ones described in this work for TbSEN, and *in-situ* tagged versions of TbTrl1 and TbTPT1 are already being prepared by our group for this end. Furthermore, the same *in situ*-tagged proteins utilized for immunofluorescence microscopy in this study, can also be utilized for co-immunoprecipitation followed by western blot analysis. This could corroborate the subcellular localization of the subunits, and potentially co-purify a novel TbSEN partner, if any. Another technique that can also

be performed to corroborate the proteins subcellular localization, and discover any other proteins that may be interacting with the splicing machinery, is proximity labeling (PL). During PL, a known protein of interest is fused to a biotin ligase protein, and any other molecule that interacts with the resulting fusion protein is labeled with biotin. Tagged molecules can then be enriched and identified by mass spectrometry. The size of the available biotin ligase domains, as well as potential toxicity to the cells, prevented us from attempting this in for the small TbSEN components before. However, a recent publication describes a small but highly efficient biotin ligase domain dubbed “TurboID”, that is capable of PL with little toxicity to the cells [125]. Moreover, this new tool was successfully utilized to PL multiple *Trypanosoma* and *Leishmania* proteins, with no toxicity [126]. We wonder whether this system can be used to tag our known tRNA splicing components in *T. brucei*, leading to the corroboration of their co-localization, as well as the unveiling of any other splicing component not observed by our chromatographic assays. For this end, a plasmid of the pPOT family, the same ones used to *in situ* tag our subunits for immunofluorescence microscopy, was constructed, containing a TurboID [125] domain downstream of a triple HA tag, to be inserted N or C-terminally in an open reading frame. This plasmid was then used to N-terminally tag one allele of TbSen22 in WT 29-13 *T. brucei* cells, with transfection confirmed by both PCR and Western blotting against the HA tag (**Fig 4.2 A-C**). Following that, we performed a pilot experiment comparing the biotinylation patterns of total protein extracts from *T. brucei* 29-13 WT to the TurboID strain (**Fig. 4.3**). For this

end, six 50 ml SDM-79 *T. brucei* cultures were allowed to grow overnight at 27° C: one WT 29-13 culture, one TurboID-TbSen22 culture with no biotin supplementation, and four TurboID-TbSen22 cultures supplemented with biotin at 2 mM final concentration [127]). Cells were then ruptured by sonication to generate a clear lysate by high-speed centrifugation as described above. Twenty µg of total protein per lane were then resolved in 12% Laemmli gels through PAGE for Comassie blue staining and streptavidin blotting (**Fig. 4.3 A-B**). *T. brucei* total protein extracts contain a few endogenously biotinylated proteins (>100 kDa) that are revealed during streptavidin blots [128][129], and we were able to observe those proteins in our control lane (**Fig. 4.3 B**). Moreover, our streptavidin blotting also revealed multiple other biotinylated bands in the TurboID-TbSen22 strain samples, which are not present in the WT control (**Fig. 4.3 B**). These extra bands were present even in the culture that was not supplemented with biotin, indicating that the small amount of biotin supplemented in the SDM-79 media (see **Appendix B1** for recipe) is enough for *in vivo* biotinylation to take place. Experiments utilizing biotin-free media and streptavidin beads for purification of the proteins are underway in the laboratory.

As stated above, reconstitution of activity in a prokaryotic model was unsuccessful during this project. Multiple post-translational modifications (PTMs) have been described in yeast, human, mice and rat TSEN homologs, including some that localize to the interior of the endonuclease domain [116][117]. Furthermore, purification of the human TSEN containing Clp1 was not possible in

a prokaryotic model, but successful in an eukaryotic one, implying additional factors, perhaps PTMs, are required for that interaction [33]. We wonder whether TbSEN receives activity-crucial PTMs that cannot be added by our prokaryotic model, *E. coli* BL21. This could be investigated by expression of recombinant TbSen in an eukaryotic expression model, such as *S. cerevisiae*, or insect cells. Our group has both previously worked on expressing *T. brucei* proteins in *S. cerevisiae* in our facilities, and collaborated with other groups for this matter. Work to express recombinant TbSEN subunits in either *S. cerevisiae*, or insect cells - potentially both - is under consideration.

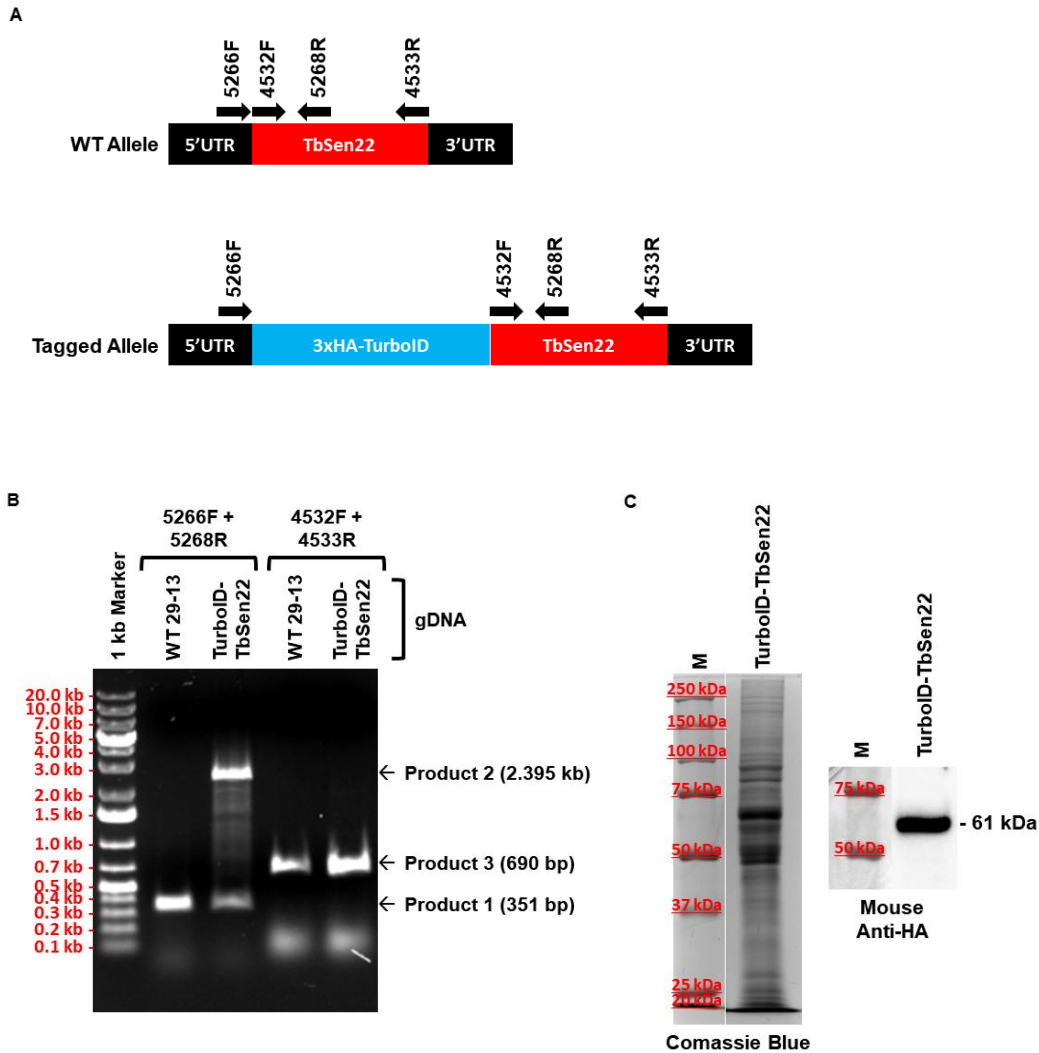


Figure 4.2 N-terminal tagging of TbSen22 with 3xHA-TurbolD

The pPOTv4 plasmid was used to N-terminally tag one allele of TbSen22 *in vivo*. **A.** Diagram representing the genomic context of the generated TurbolD-TbSen22 strain. Annealing sites of primers utilized for confirmation are depicted as arrows. **B.** PCR confirmation of cassette insertion. The larger 2.39 kb product is only generated with the amplification of the TurbolD cassette. **C.** Western blot confirmation of the fusion protein 3xHA-TurbolD-TbSen22 (40 μ g total protein per lane). Left: Coomassie blue staining. Right: Western blot with Mouse Anti-HA o/n.

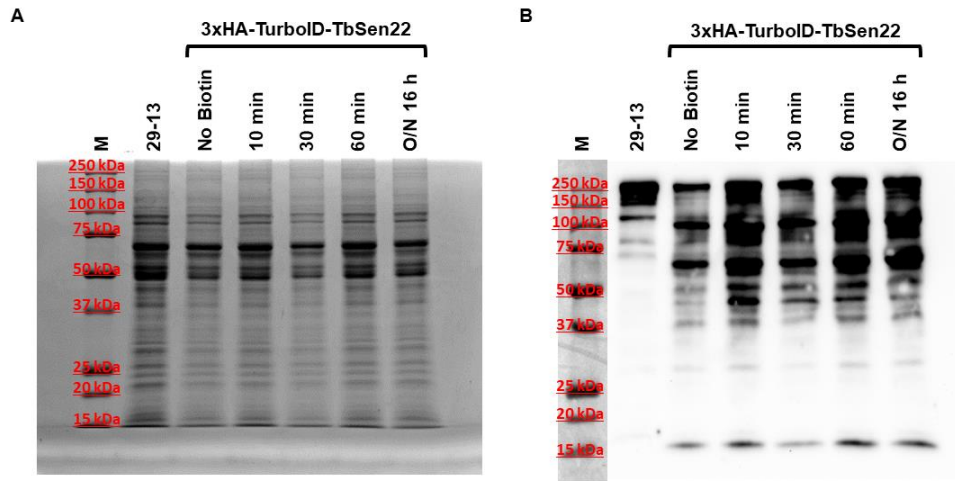


Figure 4.3 Biotinylation assay with 3xHA-TurboID-TbSen22

Gels were 12% Laemmli in both cases, and each lane received 20 μ g of total protein extract. **A.** Coomassie blue staining. **B.** Streptavidin blot revealing all biotinylated proteins in the extracts.

References

1. Zhou Q, Hu H, Li Z: *New insights into the molecular mechanisms of mitosis and cytokinesis in trypanosomes*. Elsevier Inc.; 2014.
2. Simarro PP, Cecchi G, Paone M, Franco JR, Diarra A, Ruiz JA, Fèvre EM, Courtin F, Mattioli RC, Jannin JG: **The Atlas of human African trypanosomiasis: A contribution to global mapping of neglected tropical diseases**. *Int J Health Geogr* 2010, **9**:1–18.
3. Mogk S, Boßelmann CM, Mudogo CN, Stein J, Wolburg H, Duszenko M: **African trypanosomes and brain infection – the unsolved question**. *Biol Rev* 2017, **92**:1675–1687.
4. Brun R, Blum J, Chappuis F, Burri C: **Human African trypanosomiasis**. *Lancet* 2010, **375**:148–159.
5. Deborggraeve S, Koffi M, Jamonneau V, Bonsu FA, Queyson R, Simarro PP, Herdewijn P, Büscher P: **Molecular analysis of archived blood slides reveals an atypical human Trypanosoma infection**. *Diagn Microbiol Infect Dis* 2008, **61**:428–433.
6. Stephens NA, Kieft R, MacLeod A, Hajduk SL: **Trypanosome resistance to human innate immunity: Targeting Achilles' heel**. *Trends Parasitol* 2012, **28**:539–545.
7. Vanhamme L, Lecordier L, Pays E: **Control and function of the bloodstream VSG expression sites in Trypanosoma brucei**. *Int J Parasitol* 2001, **31**:522–530.

8. Borst P: **Antigenic variation and allelic exclusion.** *Cell* 2002, **109**:5–8.
9. Turner CMR: **The rate of antigenic variation in fly-transmitted and syringe-passaged infections of *Trypanosoma brucei*.** *FEMS Microbiol Lett* 1997, **153**:227–231.
10. Berriman M, Ghedin E, Hertz-Fowler C, Blandin G, Renauld H, Bartholomeu DC, Lennard NJ, Caler E, Hamlin NE, Haas B, et al.: **The genome of the African trypanosome *Trypanosoma brucei*.** *Science* 2005, **309**:416–422.
11. Achcar F, Kerkhoven EJ, Barrett MP: ***Trypanosoma brucei*: Meet the system.** *Curr Opin Microbiol* 2014, **20**:162–169.
12. Rubio MAT, Paris Z, Gaston KW, Fleming IMC, Sample P, Trotta CR, Alfonzo JD: **Unusual noncanonical intron editing is important for tRNA splicing in *trypanosoma brucei*.** *Mol Cell* 2013, **52**:184–192.
13. Keren H, Lev-Maor G, Ast G: **Alternative splicing and evolution: Diversification, exon definition and function.** *Nat Rev Genet* 2010, **11**:345–355.
14. Pan Q, Shai O, Lee LJ, Frey BJ, Blencowe BJ: **Deep surveying of alternative splicing complexity in the human transcriptome by high-throughput sequencing.** *Nat Genet* 2008, **40**:1413–1415.
15. Huang J, van der Ploeg LH: **Maturation of polycistronic pre-mRNA in *Trypanosoma brucei*: analysis of trans splicing and poly(A) addition at nascent RNA transcripts from the hsp70 locus.** *Mol Cell Biol* 1991,

- 11:3180–3190.
16. Ullu E, Tschudi C: **Trans splicing in trypanosomes requires methylation of the 5' end of the spliced leader RNA.** *Proc Natl Acad Sci U S A* 1991, **88**:10074–10078.
 17. Ivens AC, Peacock CS, Worthey EA, Murphy L, Aggarwal G, Berriman M, Sisk E, Rajandream M, Adlem E, Aert R, et al.: **The genome of the kinetoplastid parasite, *Leishmania major*.** *Science* 2005, **309**:436–42.
 18. Papasaikas P, Valcárcel J: **The Spliceosome: The Ultimate RNA Chaperone and Sculptor.** *Trends Biochem Sci* 2016, **41**:33–45.
 19. Preußner C, Jaé N, Bindereif A: **MRNA splicing in trypanosomes.** *Int J Med Microbiol* 2012, **302**:221–224.
 20. Reinhold-Hurek B, Shub D a: **Self-splicing introns in tRNA genes of widely divergent bacteria.** *Nature* 1992, **357**:173–176.
 21. Lopes RRS, Kessler AC, Polycarpo C, Alfonzo JD: **Cutting, dicing, healing and sealing: the molecular surgery of tRNA.** *Wiley Interdiscip Rev RNA* 2015, **6**:337–349.
 22. Thompson LD, Daniels CJ: **A tRNA(Trp) intron endonuclease from *Halobacterium volcanii*. Unique substrate recognition properties.** *J Biol Chem* 1988, **263**:17951–17959.
 23. Baldi MI, Mattoccia E, Bufardeci E, Fabbri S, Tocchini-Valentini GP: **Participation of the Intron in the Reaction Catalyzed by the *Xenopus* tRNA Splicing Endonuclease.** *Science (80-)* 1992, **255**:1404–1408.

24. Yoshihisa T: **Handling tRNA introns, archaeal way and eukaryotic way.** *Front Genet* 2014, **5**:1–16.
25. Trotta CR, Miao F, Arn EA, Stevens SW, Ho CK, Rauhut R, Abelson JN: **The Yeast tRNA Splicing Endonuclease: A Tetrameric Enzyme with Two Active Site Subunits Homologous to the Archaeal tRNA Endonucleases.** *Cell* 1997, **89**:849–858.
26. Greer CL, Peebles CL, Gegenheimer P, Abelson J: **Mechanism of action of a yeast RNA ligase in tRNA splicing.** *Cell* 1983, **32**:537–546.
27. Popow J, Jurkin J, Schleiffer A, Martinez J: **Analysis of orthologous groups reveals archease and DDX1 as tRNA splicing factors.** *Nature* 2014, **511**:104–107.
28. Wu J, Hopper AK: **Healing for destruction: TRNA intron degradation in yeast is a two-step cytoplasmic process catalyzed by tRNA ligase Rlg1 and 5'-to-3' exonuclease Xrn1.** *Genes Dev* 2014, **28**:1556–1561.
29. Culver GM, McCraith SM, Consaul SA, Stanford DR, Phizicky EM: **A 2'-phosphotransferase implicated in tRNA splicing is essential in *Saccharomyces cerevisiae*.** *J Biol Chem* 1997, **272**:13203–13210.
30. Popow J, Schleiffer A, Martinez J: **Diversity and roles of (t)RNA ligases.** *Cell Mol Life Sci* 2012, **69**:2657–2670.
31. Paushkin S V., Patel M, Furia BS, Peltz SW, Trotta CR: **Identification of a human endonuclease complex reveals a link between tRNA splicing and pre-mRNA 3' end formation.** *Cell* 2004, **117**:311–321.

32. Hanada T, Weitzer S, Mair B, Bernreuther C, Wainger BJ, Ichida J, Hanada R, Orthofer M, Cronin SJ, Komnenovic V, et al.: **CLP1 links tRNA metabolism to progressive motor-neuron loss.** *Nature* 2013, **495**:474–480.
33. Hayne CK, Schmidt CA, Haque MI, Gregory Matera A, Stanley RE: **Reconstitution of the human tRNA splicing endonuclease complex: Insight into the regulation of pre-tRNA cleavage.** *Nucleic Acids Res* 2020, **48**:7609–7622.
34. Sekulovski S, Devant P, Panizza S, Gogakos T, Pitiriciu A, Heitmeier K, Ramsay EP, Barth M, Schmidt C, Tuschl T, et al.: **Assembly defects of human tRNA splicing endonuclease contribute to impaired pre-tRNA processing in pontocerebellar hypoplasia.** *Nat Commun* 2021, **12**.
35. Hurtig JE, Steiger MA, Nagarajan VK, Li T, Chao TC, Tsai KL, Van Hoof A: **Comparative parallel analysis of RNA ends identifies mRNA substrates of a tRNA splicing endonuclease-initiated mRNA decay pathway.** *Proc Natl Acad Sci U S A* 2021, **118**.
36. Fabbri S, Fruscoloni P, Bufardecì E, Di Nicola Negri E, Baldi MI, Gandini Attardi D, Mattoccia E, Tocchini-Valentini GP: **Conservation of substrate recognition mechanisms by tRNA splicing endonucleases.** *Science* (80-) 1998, **280**:284–286.
37. Tsuboi T, Yamazaki R, Nobuta R, Ikeuchi K, Makino S, Ohtaki A, Suzuki Y, Yoshihisa T, Trotta C, Inada T: **The tRNA splicing endonuclease**

- complex cleaves the mitochondria-localized Cbp1 mRNA. *J Biol Chem* 2015, **290**:16021–16030.**
38. Breuss MW, Sultan T, James KN, Rosti RO, Scott E, Musaev D, Furia B, Reis A, Sticht H, Al-Owain M, et al.: **Autosomal-Recessive Mutations in the tRNA Splicing Endonuclease Subunit TSEN15 Cause Pontocerebellar Hypoplasia and Progressive Microcephaly.** *Am J Hum Genet* 2016, **99**:228–235.
39. Lim J, Ha M, Chang H, Kwon SC, Simanshu DK, Patel DJ, Kim VN: **Uridylation by TUT4 and TUT7 marks mRNA for degradation.** *Cell* 2014, **159**:1365–1376.
40. Kurosaki T, Popp MW, Maquat LE: **Quality and quantity control of gene expression by nonsense-mediated mRNA decay.** *Nat Rev Mol Cell Biol* 2019, **20**:406–420.
41. Navickas A, Chamois S, Saint-Fort R, Henri J, Torchet C, Benard L: **No-Go Decay mRNA cleavage in the ribosome exit tunnel produces 5'-OH ends phosphorylated by Trl1.** *Nat Commun* 2020, **11**:1–11.
42. Vasudevan S, Peltz SW, Wilusz CJ: **Non-stop decay - A new mRNA surveillance pathway.** *BioEssays* 2002, **24**:785–788.
43. Houseley J, Tollervey D: **The Many Pathways of RNA Degradation.** *Cell* 2009, **136**:763–776.
44. Schoenberg DR, Maquat LE: **Regulation of cytoplasmic mRNA decay.** *Nat Rev Genet* 2012, **13**:246–59.

45. Kadaba S, Wang X, Anderson JT: **Nuclear RNA surveillance in *Saccharomyces cerevisiae*: Trf4p-dependent polyadenylation of nascent hypomethylated tRNA and an aberrant form of 5S rRNA.** *Rna* 2006, **12**:508–521.
46. Chernyakov I, Whipple JM, Kotelawala L, Grayhack EJ, Phizicky EM: **Degradation of several hypomodified mature tRNA species in *Saccharomyces cerevisiae* is mediated by Met22 and the 5'-3' exonucleases Rat1 and Xrn1.** *Genes Dev* 2008, **22**:1369–1380.
47. Estévez AM, Kempf T, Clayton C: **The exosome of *Trypanosoma brucei*.** *EMBO J* 2001, **20**:3831–3839.
48. Clayton CE: **Networks of gene expression regulation in *Trypanosoma brucei*.** *Mol Biochem Parasitol* 2014, **195**:96–106.
49. Aphasizhev R, Aphasizheva I, Simpson L: **Multiple terminal uridylyltransferases of trypanosomes.** *FEBS Lett* 2004, **572**:15–18.
50. Manful T, Fadda A, Clayton C: **The role of the 5'-3' exoribonuclease XRNA in transcriptome-wide mRNA degradation.** *Rna* 2011, **17**:2039–2047.
51. Malecki M, Viegas SC, Carneiro T, Golik P, Dressaire C, Ferreira MG, Arraiano CM: **The exoribonuclease Dis3L2 defines a novel eukaryotic RNA degradation pathway.** *EMBO J* 2013, **32**:1842–1854.
52. Tan THP, Bochud-Allemann N, Horn EK, Schneider A: **Eukaryotic-type elongator tRNAMet of *Trypanosoma brucei* becomes formylated after**

- import into mitochondria.** *Proc Natl Acad Sci U S A* 2002, **99**:1152–1157.
53. Lopes RRS, Silveira G de O, Eitler R, Vidal RS, Kessler A, Hinger S, Paris Z, Alfonzo JD, Polycarpo C: **The essential function of the Trypanosoma brucei Trl1 homolog in procyclic cells is maturation of the intron-containing tRNATyr.** *RNA* 2016, doi:10.1261/rna.056242.116.
54. Yoshihisa T: **Possibility of Cytoplasmic pre-tRNA Splicing: the Yeast tRNA Splicing Endonuclease Mainly Localizes on the Mitochondria.** *Mol Biol Cell* 2003, **14**:3266–3279.
55. Kessler AC, Kulkarni SS, Paulines MJ, Rubio MAT, Limbach PA, Paris Z, Alfonzo JD: **Retrograde nuclear transport from the cytoplasm is required for tRNATyr maturation in T. brucei.** *RNA Biol* 2018, **15**:528–536.
56. Dixit S, Kessler AC, Henderson J, Pan X, Zhao R, D’Almeida GS, Kulkarni S, Rubio MAT, Hegedúsová E, Ross RL, et al.: **Dynamic queuosine changes in tRNA couple nutrient levels to codon choice in Trypanosoma brucei.** *Nucleic Acids Res* 2021, **49**:12986–12999.
57. Kulkarni S, Rubio MAT, Hegedusová E, Ross RL, Limbach PA, Alfonzo JD, Paris Z: **Preferential import of queuosine-modified tRNAs into Trypanosoma brucei mitochondrion is critical for organellar protein synthesis.** *Nucleic Acids Res* 2021, **49**:8247–8260.
58. LaCava J, Houseley J, Saveanu C, Petfalski E, Thompson E, Jacquier A,

- Tollervey D: **RNA Degradation by the Exosome Is Promoted by a Nuclear Polyadenylation Complex.** *Cell* 2005, **121**:713–724.
59. Allmang C, Kufel J, Chanfreau G, Mitchell P, Petfalski E, Tollervey D: **Functions of the exosome in rRNA, snoRNA and snRNA synthesis.** *EMBO J* 1999, **18**:5399–410.
60. Mitchell P, Tollervey D: **Musing on the structural organization of the exosome complex.** *Nat Struct Biol* 2000, **7**:843–846.
61. Cesaro G, da Soler HT, Guerra-Slompo EP, Haouz A, Legrand P, Zanchin NIT, Guimaraes BG: **Trypanosoma brucei RRP44: a versatile enzyme for processing structured and non-structured RNA substrates.** *Nucleic Acids Res* 2023, **51**:380–395.
62. Sroga GE: **Half-life of tRNA and the Initial Rate of tRNA Accumulation in Plant Cells from Cell Suspension Cultures of Lupinus angustifolius cv. Turkus and Petroselinum hortense cv. Berlińska Growing at Different Rates.** *J Plant Physiol* 1984, **116**:81–89.
63. Karnahl U, Wasternack C: **Half-life of cytoplasmic rRNA and tRNA, of plastid rRNA and of uridine nucleotides in heterotrophically and photoorganotrophically grown cells of Euglena gracilis and its apoplastic mutant W3BUL.** *Int J Biochem* 1992, **24**:493–497.
64. Smith DWE, Weinberg WC: **Transfer RNA in reticulocyte maturation.** *Biochim Biophys Acta* 1981, **655**:195–8.
65. Abelson HT, Johnson LF, Penman S, Green H: **Changes in Rna in**

- Relation to Growth of Fibroblast .2. Lifetime of Messenger-Rna, Ribosomal-Rna, and Transfer-Rna in Resting and Growing Cells.** *Cell* 1974, **1**:161–165.
66. Hanoune J, Agarwal MK: **Studies on the half life time of rat liver transfer RNA species.** *FEBS Lett* 1970, **11**:78–80.
67. Gudipati RK, Xu Z, Lebreton A, Séraphin B, Steinmetz LM, Jacquier A, Libri D: **Extensive Degradation of RNA Precursors by the Exosome in Wild-Type Cells.** *Mol Cell* 2012, **48**:409–421.
68. Frederick MI, Heinemann IU: **Regulation of RNA stability at the 3' end.** *Biol Chem* 2021, **402**:425–431.
69. Schneider A, McNally KP, Agabian N: **Splicing and 3'-processing of the tyrosine tRNA of Trypanosoma brucei.** *J Biol Chem* 1993, **268**:21868–21874.
70. Kramer S, Queiroz R, Ellis L, Webb H, Hoheisel JD, Clayton C, Carrington M: **Heat shock causes a decrease in polysomes and the appearance of stress granules in trypanosomes independently of eIF2 α phosphorylation at Thr169.** *J Cell Sci* 2008, **121**:3002–3014.
71. Manful T, Fadda A, Clayton C: **The role of the 5'-3' exoribonuclease XRNA in transcriptome-wide mRNA degradation.** *Rna* 2011, **17**:2039–2047.
72. Li CH, Irmer H, Gudjonsdottir-Planck D, Freese S, Salm H, Haile S, Estévez AM, Clayton C: **Roles of a Trypanosoma brucei 5'/3'**

- exoribonuclease homolog in mRNA degradation.** *Rna* 2006, **12**:2171–2186.
73. Alexandrov A, Chernyakov I, Gu W, Hiley SL, Hughes TR, Grayhack EJ, Phizicky EM: **Rapid tRNA decay can result from lack of nonessential modifications.** *Mol Cell* 2006, **21**:87–96.
74. Sakyama J, Zimmer SL, Ciganda M, Williams N, Read LK: **Ribosome biogenesis requires a highly diverged XRN family 5'→3' exoribonuclease for rRNA processing in Trypanosoma brucei.** *Rna* 2013, **19**:1419–1431.
75. LaCount DJ, Bruse S, Hill KL, Donelson JE: **Double-stranded RNA interference in Trypanosoma brucei using head-to-head promoters.** *Mol Biochem Parasitol* 2000, **111**:67–76.
76. Towler BP, Pashler AL, Haime HJ, Przybyl KM, Viegas SC, Matos RG, Morley SJ, Arraiano CM, Newbury SF: **Dis3L2 regulates cell proliferation and tissue growth through a conserved mechanism.** *PLoS Genet* 2020, **16**:1–29.
77. Wilusz JE, Whipple JM, Phizicky EM, Sharp PA: **tRNAs marked with CCACCA are targeted for degradation.** *Science (80-)* 2011, **334**:817–821.
78. Shikha S, Schneider A: **The single CCA-adding enzyme of T. Brucei has distinct functions in the cytosol and in mitochondria.** *J Biol Chem* 2020, **295**:6138–6150.

79. Cesaro G, Carneiro FRG, Ávila AR, Zanchin NIT, Guimarães BG: **Trypanosoma brucei RRP44 is involved in an early stage of large ribosomal subunit RNA maturation.** *RNA Biol* 2019, **16**:133–143.
80. Wek SA, Zhu S, Wek RC: **The histidyl-tRNA synthetase-related sequence in the eIF-2 alpha protein kinase GCN2 interacts with tRNA and is required for activation in response to starvation for different amino acids.** *Mol Cell Biol* 1995, **15**:4497–4506.
81. Raina M, Ibba M: **TRNAs as regulators of biological processes.** *Front Genet* 2014, **5**:1–14.
82. Ren B, Wang X, Duan J, Ma J: **Rhizobial tRNA-derived small RNAs are signal molecules regulating plant nodulation.** *Science* 2019, **365**:919–922.
83. Jeck WR, Sorrentino JA, Wang K, Slevin MK, Burd CE, Liu J, Marzluff WF, Sharpless NE: **Erratum: Circular RNAs are abundant, conserved, and associated with ALU repeats (RNA (156)).** *Rna* 2013, **19**:426.
84. Wilusz JE: **A 360° view of circular RNAs: From biogenesis to functions.** *Wiley Interdiscip Rev RNA* 2018, **9**:1–17.
85. Jeck WR, Sorrentino JA, Wang K, Slevin MK, Burd CE, Liu J, Marzluff WF, Sharpless NE: **Circular RNAs are abundant, conserved, and associated with ALU repeats.** *RNA* 2013, **19**:141–157.
86. Capel B, Swain A, Nicolis S, Hacker A, Walter M, Koopman P, Goodfellow P, Lovell-Badge R: **Circular transcripts of the testis-determining gene**

- Sry in adult mouse testis.** *Cell* 1993, **73**:1019–1030.
87. Lu Z, Filonov GS, Noto JJ, Schmidt CA, Hatkevich TL, Wen Y, Jaffrey SR, Gregory Matera A: **Metazoan tRNA introns generate stable circular RNAs in vivo.** *Rna* 2015, **21**:1554–1565.
88. Noto JJ, Schmidt CA, Matera AG: **Engineering and expressing circular RNAs via tRNA splicing.** *RNA Biol* 2017, **14**:978–984.
89. Schmidt CA, Giusto JD, Bao A, Hopper AK, Gregory Matera A: **Molecular determinants of metazoan tricRNA biogenesis.** *Nucleic Acids Res* 2019, **47**:6452–6465.
90. Blanc V, Alfonzo JD, Aphasizhev R, Simpson L: **The mitochondrial RNA ligase from *Leishmania tarentolae* can join RNA molecules bridged by a complementary RNA.** *J Biol Chem* 1999, **274**:24289–24296.
91. Wirtz E, Leal S, Ochatt C, Cross GM: **A tightly regulated inducible expression system for conditional gene knock-outs and dominant-negative genetics in *Trypanosoma brucei*.** *Mol Biochem Parasitol* 1999, **99**:89–101.
92. Chomczynski P, Sacchi N: **Single-step method of RNA isolation by acid guanidinium thiocyanate-phenol-chloroform extraction.** *Anal Biochem* 1987, **162**:156–159.
93. Cozen AE, Quartley E, Holmes AD, Hrabeta-Robinson E, Phizicky EM, Lowe TM: **ARM-seq: AlkB-facilitated RNA methylation sequencing reveals a complex landscape of modified tRNA fragments.** *Nat*

- Methods* 2015, **12**:879–884.
94. Huppertz I, Attig J, D'Ambrogio A, Easton LE, Sibley CR, Sugimoto Y, Tajnik M, König J, Ule J: **iCLIP: Protein-RNA interactions at nucleotide resolution.** *Methods* 2014, **65**:274–287.
 95. Upton HE, Ferguson L, Temoche-Diaz MM, Liu XM, Pimentel SC, Ingolia NT, Schekman R, Collins K: **Low-bias ncRNA libraries using ordered two-template relay: Serial template jumping by a modified retroelement reverse transcriptase.** *Proc Natl Acad Sci U S A* 2021, **118**:1–10.
 96. Schimanski B, Nguyen TN, Günzl A, Gu A: **Highly Efficient Tandem Affinity Purification of Trypanosome Protein Complexes Based on a Novel Epitope Combination.** *Eukaryot Cell* 2005, **4**:1942–1950.
 97. Papadopoulos JS, Agarwala R: **COBALT: Constraint-based alignment tool for multiple protein sequences.** *Bioinformatics* 2007, **23**:1073–1079.
 98. Troshin P V., Procter JB, Barton GJ: **Java bioinformatics analysis web services for multiple sequence alignment-JABAWS:MSA.** *Bioinformatics* 2011, **27**:2001–2002.
 99. Troshin P V., Procter JB, Sherstnev A, Barton DL, Madeira F, Barton GJ: **JABAWS 2.2 distributed web services for Bioinformatics: Protein disorder, conservation and RNA secondary structure.** *Bioinformatics* 2018, **34**:1939–1940.
 100. Akama K, Junker V, Beier H: **Identification of two catalytic subunits of**

- tRNA splicing endonuclease from *Arabidopsis thaliana*.** *Gene* 2000, **257**:177–85.
101. Li H, Trotta CR, Abelson J: **Crystal structure and evolution of a transfer RNA splicing enzyme.** *Science* 1998, **280**:279–84.
102. Tamura K, Stecher G, Kumar S: **MEGA11: Molecular Evolutionary Genetics Analysis Version 11.** *Mol Biol Evol* 2021, **38**:3022–3027.
103. Pattengale ND, Alipour M, Bininda-Emonds ORP, Moret BME, Stamatakis A: **How many bootstrap replicates are necessary?** *J Comput Biol* 2010, **17**:337–54.
104. Altschul SF, Gish W, Miller W, Myers EW, Lipman DJ: **Basic local alignment search tool.** *J Mol Biol* 1990, **215**:403–10.
105. Englert M, Latz A, Becker D, Gimple O, Beier H, Akama K: **Plant pre-tRNA splicing enzymes are targeted to multiple cellular compartments.** *Biochimie* 2007, **89**:1351–1365.
106. Wan Y, Hopper AK: **From powerhouse to processing plant: conserved roles of mitochondrial outer membrane proteins in tRNA splicing.** *Genes Dev* 2018, **32**:1309–1314.
107. Dean S, Sunter J, Wheeler RJ, Hodgkinson I, Gluenz E, Gull K: **A toolkit enabling efficient, scalable and reproducible gene tagging in trypanosomatids.** *Open Biol* 2015, **5**:140197.
108. Poon SK, Peacock L, Gibson W, Gull K, Kelly S: **A modular and optimized single marker system for generating *Trypanosoma brucei***

- cell lines expressing T7 RNA polymerase and the tetracycline repressor.** *Open Biol* 2012, **2**:110037.
109. Aaron JS, Taylor AB, Chew TL: **Image co-localization - co-occurrence versus correlation.** *J Cell Sci* 2018, **131**.
110. Wickstead B, Ersfeld K, Gull K: **Targeting of a tetracycline-inducible expression system to the transcriptionally silent minichromosomes of *Trypanosoma brucei*.** *Mol Biochem Parasitol* 2002, **125**:211–6.
111. Hannaert V, Saavedra E, Duffieux F, Szikora JP, Rigden DJ, Michels PAM, Opperdoes FR: **Plant-like traits associated with metabolism of *Trypanosoma* parasites.** *Proc Natl Acad Sci U S A* 2003, **100**:1067–1071.
112. Martin W, Borst P: **Secondary loss of chloroplasts in trypanosomes.** *Proc Natl Acad Sci U S A* 2003, **100**:765–767.
113. Wilkinson SR, Obado SO, Mauricio IL, Kelly JM: ***Trypanosoma cruzi* expresses a plant-like ascorbate-dependent hemoperoxidase localized to the endoplasmic reticulum.** *Proc Natl Acad Sci U S A* 2002, **99**:13453–13458.
114. Opperdoes FR, Borst P: **Localization of nine glycolytic enzymes in a microbody-like organelle in *Trypanosoma brucei* : The glycosome.** *FEBS Lett* 1977, **80**:360–364.
115. Fujishima K, Sugahara J, Miller CS, Baker BJ, Di Giulio M, Takesue K, Sato A, Tomita M, Banfield JF, Kanai A: **A novel three-unit tRNA splicing endonuclease found in ultrasmall Archaea possesses broad**

- substrate specificity.** *Nucleic Acids Res* 2011, **39**:9695–9704.
116. Ledesma L, Sandoval E, Cruz-Martínez U, Escalante AM, Mejía S, Moreno-Álvarez P, Ávila E, García E, Coello G, Torres-Quiroz F: **YAAM: Yeast Amino Acid Modifications Database.** *Database* 2018, **2018**:1–8.
117. Li Z, Li S, Luo M, Jhong JH, Li W, Yao L, Pang Y, Wang Z, Wang R, Ma R, et al.: **DbPTM in 2022: An updated database for exploring regulatory networks and functional associations of protein post-translational modifications.** *Nucleic Acids Res* 2022, **50**:D471–D479.
118. Maree JP, Tvardovskiy A, Ravensborg T, Jensen ON, Rudenko G, Patterson H-G: **Trypanosoma brucei histones are heavily modified with combinatorial post-translational modifications and mark Pol II transcription start regions with hyperacetylated H2A.** *Nucleic Acids Res* 2022, **50**:9705–9723.
119. de Almeida RF, Fernandes M, de Godoy LMF: **An updated map of Trypanosoma cruzi histone post-translational modifications.** *Sci Data* 2021, **8**:1–10.
120. Sasse R, Gull K: **Tubulin post-translational modifications and the construction of microtubular organelles in Trypanosoma brucei.** *J Cell Sci* 1988, **90 (Pt 4)**:577–589.
121. Okuda EK, Gonzales-Zubiate FA, Gadal O, Oliveira CC: **Nucleolar localization of the yeast RNA exosome subunit Rrp44 hints at early pre-rRNA processing as its main function.** *J Biol Chem* 2020,

- 295:11195–11213.
122. Simpson L, Shaw J: **RNA editing and the mitochondrial cryptogenes of kinetoplastid protozoa.** *Cell* 1989, **57**:355–66.
 123. Adler BK, Harris ME, Bertrand KI, Hajduk SL: **Modification of Trypanosoma brucei mitochondrial rRNA by posttranscriptional 3' polyuridine tail formation.** *Mol Cell Biol* 1991, **11**:5878–5884.
 124. Tan THP, Pach R, Crausaz A, Ivens A, Schneider A: **tRNAs in Trypanosoma brucei: genomic organization, expression, and mitochondrial import.** *Mol Cell Biol* 2002, **22**:3707–3717.
 125. Branon TC, Bosch JA, Sanchez AD, Udeshi ND, Svinkina T, Carr SA, Feldman JL, Perrimon N, Ting AY: **Efficient proximity labeling in living cells and organisms with TurboID.** *Nat Biotechnol* 2018, **36**:880–898.
 126. Geoghegan V, Mottram JC, Jones NG: **Tag Thy Neighbour: Nanometre-Scale Insights Into Kinetoplastid Parasites With Proximity Dependent Biotinylation.** *Front Cell Infect Microbiol* 2022, **12**:1–14.
 127. Hertz HL, Price IF, Tang W: **Visualization and Purification of Caenorhabditis elegans Germ Granule Proteins Using Proximity Labeling.** *Bio-protocol* 2022, **12**:1–10.
 128. Soto-Gonzalez F, Tripathi A, Cooley A, Paromov V, Rana T, Chaudhuri M: **A novel connection between Trypanosoma brucei mitochondrial proteins TbTim17 and TbTRAP1 is discovered using Biotinylation Identification (BioID).** *J Biol Chem* 2022, **298**:102647.

129. Morriswood B, Havlicek K, Demmel L, Yavuz S, Sealey-Cardona M, Vidilaseris K, Anrather D, Kostan J, Djinović-Carugo K, Roux KJ, et al.: **Novel bilobe components in *Trypanosoma brucei* identified using proximity-dependent biotinylation.** *Eukaryot Cell* 2013, **12**:356–367.

Appendix A: Protocols

A1: Total RNA Preparation from *Trypanosoma brucei*

Table A.1: Solution D Components

Components	Instructions
4M Guanidinium isothiocyanate,	23.6 g Guanidinium Isothiocyanate powder
25 mM Sodium Citrate pH 7,	12.5 ml 100 mM Citrate pH 7 buffer
0.5% Sarkosyl	Add 250 mg Sarkosyl powder
0.1M β -mercaptoethanol**	354 μ l β -mercaptoethanol
-	↑ 50 ml MiliQ water

Filter sterilize, then keep refrigerated at all times.

*We keep frozen stocks of Solution D in the large freezer in Room 232.

**Add β -mercaptoethanol to solution right before using it (do not freeze stock with β -mercaptoethanol)

Steps:

1. Pellet Cells (1500 x g, 10m, cold) then remove supernatant.
2. Resuspend pellet in 2 ml ice-cold 1 X PBS, then transfer to 2ml centrifuge tube.
3. Pellet Cells (1500 x g, 10m, cold) then remove supernatant.
4. Resuspend pellet completely in 100 μ l 1x ice-cold PBS.
5. Add the following components, mixing well by pipetting up and down on every step:
 - 500 μ l Solution D.

- 50 µl 2M NaOAc pH 4.
 - 500 µl Water-Phenol.
 - 100 µl Chloroform:Isoamyl alcohol.
6. Cool sample on ice at least 15 min.
 7. Spin down cell debris (16000 x g, 10 min, cold).
 8. Transfer about 80% of supernatant to a new 2 ml tube.
 9. Add equal volume of isopropanol to supernatant, mix well.
 10. Incubate from 1 h to overnight at -20° C.
 11. Spin down nucleic acids (16000 x g, 30 min, cold).
 12. Resuspend pellet in 1 ml MiliQ water.
 - Nucleic acid pellet is transparent and can take a few minutes to resuspend.
 13. Add 1 ml of Water-phenol, mix well.
 14. Spin down sample (16000 x g, 10 min, cold).
 15. Transfer about 80% of supernatant to a new 2 ml tube.
 16. Add components for ethanol precipitation: 100 µl 3M NaOAc, 2 µl 20 mg/ml Glycogen, 2.5 volumes of 100% Ethanol.
 17. Incubate samples from 30 min to overnight on ice or -20° C.
 18. Spin down sample (16000 x g, 30 min, cold).
 19. Wash pellet with 70% ethanol.
 20. Spin down sample (16000 x g, 10 min, cold).
 21. Remove all liquid and allow pellet to air dry for about five min.

22. Resuspend in water, or 1x TE pH 8.0 (usually 20 - 100 μ l).
23. Measure concentration with nano-drop or spectrophotometer.
24. RNA samples must be stored at -20° C, and kept on ice at all times during use.

A2: Polyacrylamide Gel Electrophoresis for RNA Separation

1. Pour 8% 8M urea polyacrylamide gel (60 μ L APS + 10 μ L TEMED for 10mL)
2. Typical RNA loading 8 – 12 μ g RNA per well. EtOH + glycogen precipitate to obtain small volume for loading. Resuspend pellet in 7 μ L urea load dye
3. Heat samples 90°C for 10 min in urea loading dye. Brief centrifuge before loading gel.
4. Electrophoresis in 1x TBE or 1x TAE to correlate with polyacrylamide gel.
5. Carefully wash wells with buffer filled syringe multiple times.
6. Dispense sample slowly so dye forms thin layer on bottom of well and does not spread out.
7. Run gel at 85-100V until bromophenol blue dye is at the bottom of the gel (1-2 hour). For better separation, run bromophenol blue off the gel and proceed until xylene cyanol is near the bottom.
8. To visualize RNA, add gel to small dish containing buffer + EtBr for 10 min.
9. Gel can be washed in buffer to remove traces of EtBr before visualization.

A3: Northern Blot Analysis

Day 1:

1. Pour an 8% urea polyacrylamide gel (10 ml gel mix, 60 μ L 10% APS, 10 μ L TEMED)
 - Gel mix, APS and TEMED solutions are stored at 4° C.
 - Running buffer for this gel is 1x TBE or TAE.
 - It is advisable to pre-run the gel for 30 min at 80-90 V.
2. Prepare RNA samples by ethanol precipitating the desired amount of RNA in a new tube.
 - Use 8 - 12 μ g of total RNA per lane (2.5 μ g if using mitochondrial RNA).
 - Bring sample volume up to 300 μ l with MiliQ water, then add 30 μ l of 3M NaOAc, 750 μ l of 100% ethanol and 2 μ l 20 mg/ml glycogen. Mix well, then spin 30 min at 16000 g.
 - Remove supernatant, and after allowing the pellet to dry for 5 min, resuspend it directly in 6 - 8 μ l of 1x urea loading dye. Lower volumes generate sharper bands.
3. Heat samples at 90°C for 10 min, then use a quick spin to collect liquid at the bottom of the tube.
4. Carefully wash gel wells with syringe multiple times right before loading.
 - This will remove precipitated urea that interferes with the run.

5. Load samples into wells slowly, so that the dye forms a thin layer at the bottom of the well.
6. Run gel at 80 - 90 V so that the bottom dye (bromophenol blue) is at the bottom of the gel (usually 2h - 2h30min). For better separation of intron containing tRNA, run bottom dye off the gel, keeping the top dye (xylene cyanol) right above wire.
7. Cut bottom right corner of gel to remember orientation.
8. Add gel to small dish for Ethidium Bromide (10 mg/ml EtBr) staining to assay RNA quality. EtBr staining for 10 min should reveal rRNA bands (M1 - M6) and tRNA band. If better picture is desired, let gel rinse in water for a few minutes before imaging to remove background.
9. Assemble the transfer components while staining is taking place. Electroblotting is performed in 0.5 x TBE (or TAE if used previously). The same TBE used for the gel run can be used here. Wet sponges, filter paper, and zeta probe membrane before assembling. Cut the bottom right corner of the membrane before placing on gel (mimicking the cut in the gel).
10. Transfer can be done at 80 V for 1h30min to 2h.
 - During this step, make sure the boiling bath and the heat block are at the correct temperature (90° C) for the SSDNA and the probe (if reusing).
11. After transferring, write identifying information on upper left corner of membrane with a pencil (don't use a pen).

12. UV crosslink RNA to membrane for 1 min. Many times, the EtBr stain is also transferred to the membrane and can be observed. We can use the BioRad gel doc for this step: take a 1 min picture for EtBr with the membrane gel face down in the machine.
13. *Optional step* - the membrane can be baked under negative pressure in the oven for 20 minutes.
14. Pre-hybridization: transfer membrane to glass cylinder, then add 5 ml of pre-hyb to it. Denature the SSDNA for 10 min at 90°C, chill it on ice for < 1 min, and then add 10 µl to the pre-hyb (final concentration of 20 µg/ml). Allow pre-hybridization in rotating oven for 30 minutes at the same temperature as the probing step.
15. Probing: denature labeled probe for 10 min at 90°C. Quick spin, then chill on ice for < 1 min. Add 10 µl of probe to the pre-hyb + SSDNA solution in the cylinder. Allow hybridization over night at correct temperature (generally the probe T_m minus 20° C is a good starting place). Hybridization temperatures for tRNA probes usually range from 42°C to 55°C.

Day 2:

1. Pour out labeled probing solution into a small 15 mL conical tube. Label (using tape) with name, date probe was labeled and what the probe is for. Place tube in hot box in small -20° C freezer for later use or decay.

- If reusing old probe in solution for hybridization of a new membrane, use boiling water bath at 90° C to heat probe for 10 min before use. Membrane should still be pre-hybridized with pre-hyb + SSDNA for 30 min before this.
2. Add 5 ml of oligo Rinse. Rotate and swirl in hand to rinse. Dump down hot sink.
 - This will remove the leftover of the pre-hyb + SSDNA + probe.
 3. Add 5 ml of wash 1. Place back in rotating oven and wash for 20 min at the same temperature as probing.
 4. Dump wash down in the hot sink (room 226).
 5. Add 5 ml of wash 2. Place back in rotating oven and wash for 20 min at the same temperature as probing.
 6. Dump wash down in the hot sink (room 226).
 7. Cut filter paper slightly larger than membrane. Wet with water. Place membrane on top of wet filter paper (Do not let membrane with probe dry out)
 8. Place this in a plastic bag or surround in saran wrap.
 9. Place in P-imager cassette overnight. Screen should be blanked for 10 min just before use.
 10. To strip membrane – boil in 50 mL conical with stripping solution once 20 min

Solutions Adapted From Bio-Rad Zeta-Probe

100x Denhardt's solution:

2% BSA

2% PVP

2% Ficoll

Pre-hybridization:

5x SSC

20 mM Na_2HPO_4 , pH 7.2

7% SDS

1x Denhardt's

*SS DNA added separately before hybridization.

Wash 1:

3x SSC

10x Denhardt's

5% SDS 25 mM NaH_2PO_4 , pH 7.5

Wash 2:

1x SSC

1% SDS

Stripping Solution:

0.1x SSC

0.5% SDS

A4: Preparing And Labeling Stocks of Northern blot Probes

Our probes are usually 25-30 nt-long DNA oligos in reverse complementarity to the tRNA (Ex: "4343R"). A list of all Northern probes can be found in the lab online data sheet.

Steps:

1. Spin down lyophilized pellets at 13200 RPM for 2 min in the microcentrifuge.
2. Resuspend pellets in autoclaved MiliQ water to a concentration of 200 μM .
Use the nmol concentration of the primer x 5 for the volume of water to be added in microliters (ex: 25 nmol \rightarrow 125 μl of water).
3. Allow pellet to resuspend at room temperature for at least 15 min, then homogenize with pipette.
4. Dilute oligos 1:10 for labeling (work concentration should be 20 μM).
5. Always store tubes at -20 $^{\circ}\text{C}$.

Labeling Northern blot Probes with ^{32}P γ -ATP

Wear lab coat, gloves and goggles the whole time. Radioactive γ -ATP is kept at -20 $^{\circ}\text{C}$, inside the acrylic box. Half-life is 14.29 days, so the volume used in the reaction must be adjusted to the number of half-lives that have passed. Usually we use 1 μl when the γ -ATP is brand new, adding 1 μl extra for every 10 days that have passed (so use 2 μl from 10 days-old ATP and 3 from 20 days-old). The PNK enzyme catalyzes the transfer and exchange of P_i from the γ position of ATP to the 5'-hydroxyl terminus of DNA and RNA.

Steps:

1. Thaw all reagents for 30 min behind an acrylic shield.
2. Assemble reaction in a 1.5 ml microfuge tube, **identified** and **dated** (with labeling date):

Table A.2: End-label Reaction

Reagent	Volume (μ l)
20 μ M Oligo	2
32 P γ -ATP	1-3
10X PNK Buffer	1
T4 Polynucleotide Kinase (PNK)	1
MiliQ Water	\uparrow to 10

3. Incubate at 37 °C for 1-2h (heat block, never water).
4. Add 60 μ l of autoclaved MiliQ water to bring volume up.
5. Purify labeled probe with a G-25 column to get rid of the excess γ -ATP.
6. Store at -20 °C (freezer door, acrylic container).

→ For Northern blot probing: measure 0.3 μ l from the probe in the scintillation counter. We use 2.5×10^6 CPM per 1 blot (1 membrane). 2020 Update: we use 10 μ l of probe per 5 ml of pre-hyb.

A5: Preparation of Plasmid DNA (Alkaline Lysis)

Table A.3: Plasmid DNA Preparation Solutions

Solution 1	Solution 2	Solution 3
1.25 ml 1M Tris-HCl pH 8	2.5 ml 20% SDS	14.8g potassium acetate (CH ₃ CO ₂ K)
1 ml 0.5M EDTA	1 ml 10N NaOH	5.75 ml acetic acid (C ₂ H ₄ O ₂)
↑ 50 ml with MiliQ Water	↑ 50 ml with MiliQ Water	↑ 50 ml with MiliQ Water

Autoclave solutions 1 and 3 (do not autoclave solution 2 with SDS) and store them at RT (15 to 25° C).

Steps:

1. Grow cells in 2 ml 2x YT culture o/n.
2. Transfer culture to 2 ml microcentrifuge tube and spin down cells for 1 min at 13200 RPM.
 - Discard supernatant by pouring.
 - Remove residual liquid with P200.
3. Add 150 µl of solution 1.
 - Resuspend cells using rack.
 - Incubate tube for 5 min at room temperature.
4. Add 150 µl of solution 2.
 - Invert tube 5 times to mix (do not use the vortex mixer, as it will break the genomic DNA, contaminating the plasmid preparation).

- Incubate tube for 5 min at room temperature.
5. Add 150 μ l of solution 3.
 - Invert tube 5 times to mix.
 - Incubate tube for 5 min at room temperature.
 6. Spin down cell debris for 15 min at 13200 RPM.
 - Transfer supernatant to new 1.5 ml tube with P200.
 7. Phenol extract plasmid DNA.
 - Add equal volume of Tris-phenol (usually 400 μ l).
 - Tap and invert tube to mix.
 - Spin down proteins for 15 min at 13200 RPM.
 - Transfer supernatant to new 1.5 ml tube.
 8. Chloroform extract plasmid DNA (optional)
 - Add equal volume of chloroform:Isoamyl alcohol 49:1 (usually 300 μ l).
 - Tap and invert tube to mix.
 - Spin down phenol for 15 min at 13200 RPM.
 - Transfer supernatant to new 1.5 ml tube.
 9. Ethanol precipitate plasmid DNA.
 - Add 2.5 volumes of 100% Ethanol (no 3M NaOAc or glycogen necessary).
 - Tap and invert tube to mix.
 - Spin down plasmid DNA for 35 min at 13200 RPM.

- Remove supernatant and wash pellet with 70% ethanol.
- Leave pellet air-drying for at least 15 min.

10. Resuspend plasmid DNA in desired volume of 1X TE buffer or water (usually 50-100 μ l).

- Measure concentration and write it on the side of the tube (in μ g/ μ l).

IMPORTANT: This protocol generates a high salinity sample, so a G-25 purification is required for plasmid digest and sequencing assays.

Detailed Solutions 1 – 3 (50 ml Volume)

Table A.4: Detailed Solution 1

Component	Lab Stock	Final []	For 50 ml Solution
Tris-HCl pH 8.0	1 M	25 mM	1.25 ml
EDTA	0.5 M	10 mM	1 ml
MiliQ Water	-	-	↑ 50 ml

Table A.5: Detailed Solution 2

Component	Lab Stock	Final []	For 50 ml Solution
SDS	20 %	1 %	2.5 ml
NaOH	10 N	0.2 N	1 ml
MiliQ Water	-	-	↑ 50 ml

Table A.6: Detailed Solution 3

Component	Lab Stock	Final []	For 50 ml Solution
Potassium Acetate	Powder	3 M	14.8 g
Acetic Acid	100 %	11.5 %	5.75 ml
MiliQ Water	-	-	↑ 50 ml

A6: Reverse Transcription-PCR

1. Isolate RNA by guanidine isothiocyanate protocol
2. RQ1 DNase treatment
 - a. 5 μ l of 10x RQ1 DNase buffer
 - b. 1 μ l of RQ1 DNase
 - c. 5 μ g of RNA
 - d. Bring volume to 50 μ l with water
3. Incubate reaction at 37°C for 1hr to overnight
4. Add 50 μ l of water, then phenol extract with tris saturated phenol
5. Ethanol precipitate with 2x volume ethanol, 1/10th volume 3M NaOAc, 1 μ l glycogen
6. Resuspend pellet in 20 μ l of water
7. Recommended step: attempt a PCR to check the DNase treatment. If successful there should be no product. Be sure to include a positive control.
8. Anneal RT primer. (make sure to calculate how many reactions you need)
 - a. 1 μ l of 2 pmol RT oligo
 - b. 5 μ l of RNA
 - c. 5 μ l of water
9. 70°C for 10 min followed by chill on ice 15 sec.
10. Add the following master mix to the reaction tube:
 - a. 4 μ l of 1st strand buffer

b. 2 μl of 0.1 M DTT

c. 1 μl of dNTP's (10 mM)

11. Set reaction for 2 min at 42°C

12. Add 1 μl of Reverse Transcriptase to the RT+ tubes. (You will need an RT+ and RT- tube for each sample)

13. Leave reaction 42°C for minimum of 1hr

14. 2 μl of reaction can be used as template for a 100 μl PCR reaction

A7: SDS Polyacrylamide gel electrophoresis for protein analysis

1. Pour bottom of stacking gel first:

4 mL H₂O

3.3 mL 30% acrylamide mix

2.5 mL 1.5 M Tris pH 8.8

0.1 mL 10% SDS

0.1 mL APS

0.01 mL TEMED

2. After pouring, layer 0.2 mL of 0.1% SDS on top of gel to level the bottom layer

3. Once polymerized, pour off the 0.1% SDS, dry remaining liquid with paper towel.

4. Pour, then layer the top of the stacking gel:

2.1 mL H₂O

0.5 mL 30% acrylamide mix

0.38 mL 1.5 M Tris pH 6.8

0.03 mL 10% SDS

0.03 mL APS

0.003 mL TEMED

5. After polymerized, gel can be run in 1x SDS-PAGE buffer

6. Gels are run for 1-2 hr at 100V, depending on the separation required

7. If doing a western blot, see "Western blot" A10 protocol, if staining,

continue below:

- a. Add gel to Fixing solution overnight (50% MeOH, 10% acetic acid v/v)
- b. Stain gel in Staining solution 30 min to 1 hr. (0.025% Coomassie brilliant blue, 10% acetic acid w/v)
- c. Transfer gel to De-staining solution and leave with agitation until desired level of destaining (10% acetic acid v/v).

10x SDS PAGE buffer

30.0 g Tris base

144.0 g glycine

10.0 g SDS

Bring final volume to 1 L with water

A8: Silver Staining of Protein Gels

For these steps, do not use the same containers we usually use for Coomassie blue staining. Instead, use a clean container, reserved only for silver staining. All components for the solutions A, B and C are found in the “Silver Staining” cabinet close to the gel doc area. Use MiliQ water, not distilled water from the tap. Manipulate gel carefully, as any small contaminant will appear with the silver staining procedure.

Table A.7: Silver Staining Solutions

Solution	Components	Instructions
Fixative	40% Ethanol 10% Acetic Acid	(i.e. Coomassie Destaining Solution)
Solution A	0.02% Na ₂ S ₂ O ₃ -5H ₂ O	50 mg Na ₂ S ₂ O ₃ -5H ₂ O in 250 mls H ₂ O
Solution B	0.1% AgNO ₃	50 mg AgNO ₃ in 50 mls H ₂ O
Solution C	6 % Na ₂ CO ₃ 0.02% Formaldehyde 0.0004% Na ₂ S ₂ O ₃ -4H ₂ O	6 g Na ₂ CO ₃ in 100 mls H ₂ O + 50 ul of 37% Formaldehyde + 2.0 mls of Solution A (0.02% Na ₂ S ₂ O ₃)
Quencher	1% Acetic Acid	-

(make all solutions fresh in the same day!)

Steps:

1. Fix proteins in gel

- Incubate gel in Fixative Solution for 30 min - o/n (**no o/n agitation**).
- Rinse gel 4 x 5 minutes in MilliQ water to remove acid.

2. Sensitize gel

- Incubate gel in Solution A for 5 minutes under agitation.
- Rinse gel 3 x 5 minutes in MilliQ water.

3. Stain gel

- Incubate gel in Solution B for 20-40 minutes under agitation.
- Pour off silver stain into silver-waste container.
- Rinse gel BRIEFLY 3 times in MilliQ water.
(i.e. no incubation time on the washes or it will remove the silver).

4. Develop stain

- Incubate gel in Solution C until staining develops.
 - Monitor staining development closely until desired darkness of bands is obtained.
 - Usually: about 4 min for stonger bands to appear; 10 min for a good picture.

5. Quench staining

- Remove staining solution.
- Wash gel 2x in Fixative or 1% Acetic acid.

Sensitivity of silver staining is approximately 5-10 ng per band

We usually take a picture after 10 min developing and then another at 20 min (very dark).

A9: Western blot with Primary/Secondary Antibodies

While proteins are transferring to membrane, prepare a 5% milk solution (1g milk in 20 ml 1X PBS-Tween 20) in a 50 ml falcon tube. Once the milk is dissolved, aliquot 4 ml from it for the primary and secondary antibodies into two 15 ml falcon tubes (4 ml milk each). Keep the three solutions on ice until needed.

Keep protein side of the membrane up at all times inside the plastic container. Perform all steps at room temperature under agitation.

Steps:

1. Block membrane for at least 1h with milk solution.
2. Save milk back into 50 ml falcon tube.
3. Incubate membrane with PRIMARY ANTIBODY for at least 1h.
 - 1:4000 dilution.
 - 1 μ l antibody stock in 4 ml milk solution.
4. Save antibody into two 2 ml microfuge tubes and freeze it at -20°C .
 - This antibody can be reused several times.
5. Wash membrane with 1X PBS-Tween 20 4 x 5 min.
 - No specific volume, pour enough liquid to cover membrane.
6. Block membrane for at least 30 min with milk solution.
7. Incubate membrane with SECONDARY ANTIBODY for at least 1h.
 - 1:4000 dilution.

- 1 μ l antibody stock in 4 ml milk solution (can be diluted more).
 - Do not save antibody.
8. Wash membrane with 1X PBS-Tween 20 4 x 5 min.
 9. Visualize with Clarity Western for 5 min.
 - Mix equal volumes of luminol and H_2O_2 .
 - 400 μ l each for large membranes, 200 μ l for small membranes.
 - Distribute evenly on surface of membrane with P1000.
 10. Pour liquid and wrap membrane in plastic.

A10: C-labeled *in vitro* Transcription

The order of the components is important. Add template last, right before the enzyme.

Table A.8: 50 μ l C-labeled *in vitro* Transcription Reaction

Component	Volume (μ l)
10X Transcription Buffer	5
1% NP-40	5
25 mM rNTPs (G, A, U)	2.5
25 mM CTP	1
Hot CTP	4
ddWater	\uparrow 50 (calculate)
Template	1-5 μ g (calculate)
T7 RNA Polymerase	2
Total	50 μl

Steps:

1. Mix components in 1.5 ml microfuge tube.
 - Add template **last**, right before the enzyme.
2. Incubate at 37° C for 3h.
 - Use water bath.
3. Phenol extract.
 - Bring volume up to 300 μ l with ddwater.

- Add equal (300 μ l) volume of phenol.
 - Spin down at 13200 RPM for 15 min.
 - Transfer supernatant to new tube.
4. Ethanol precipitate.
- Add 1/10 volume of 3M NaOAc.
 - Add 2.5 volumes of 100% Ethanol
 - Spin down at 13200 RPM for 30 min
 - Air-dry pellet for 10-15 min
 - Resuspend sample in 20 – 50 μ l ddwater.
5. Run sample in 8% acrylamide gel (8M Urea) for gel extraction.
- Same gel we use for Northern blots.
 - Load samples with urea buffer with **NO dye**.
 - Load extra lane with dye as marker.
 - Run gel 85-100V so the bottom dye is at the bottom of the gel (1-2 hours).
6. Cut band from the gel with UV-shadowing and transfer it to 1.5 ml microfuge tube.
7. Add 0.3 M NaOAc to cover the slice (usually 1ml) to extract the tRNA.
- We can add phenol to prevent nucleases from degrading the RNA
- 8. Incubate overnight at 4° C.**
9. Spin down sample at 13200 RPM for 10 min.

10. Transfer aqueous supernatant to new 1.5 ml microfuge tube (if using phenol, leave phenol behind).

11. Ethanol precipitate sample

- Add 3 volumes of ethanol (already has NaOAc)
- 2-3 μ l of glycogen.
- Spin at 13200 RPM for 30 min.

12. Once the pellet is air-dried, resuspend it in 20 – 50 μ l ddwater.

- This is our tRNA sample for activity assays. Store at -20° C.

A11: Endonuclease (TbSen) Cleavage Assay

To test activity of our purified TbSen samples (both recombinant and endogenous) using *in vitro* transcribed, labeled tRNA^{Tyr} (usually EDIT3) as template.

Table A.9: 10x Cleavage Buffer

Stock	1x	10x	For 1 ml 10x
1M Tris-HCl pH 7.5	50 mM	500 mM	500 μ l
1M MgCl₂	5 mM	50 mM	50 μ l
1M DTT	1 mM	10 mM	10 μ l
1M Spermidine	1 mM	10 mM	10 μ l
3M KCl*	50 mM	500 mM	166.67 μ l
MiliQ Water	-	-	↑ 1 ml

* Our preparations of TbSen already have KCl at 100 mM, so we don't usually add it to the buffer.

Steps:

1. Prepare 10x buffer on the same day. The spermidine is inside the T7 polymerase box at -20° C.

2. Chill buffer and other components on ice, including the MiliQ water and empty tubes.
3. Prepare the reactions as following:

Table A.10: *In Vitro* Cleavage Reaction

Component	1 Reaction (50 μl)
10x Cleavage Buffer	5 μ l
Enzyme Sample	1 – 10 μ g
Radiolabeled tRNA	10 – 20k CPM (usually 1 μ l from stock)
MiliQ Water	↑ 50 μ l

4. Incubate reactions at 37° C for 10 – 30 min (use dry bath since this is radioactive).
5. Transfer tubes back to ice.
6. Extract tRNA with 20 μ l of **cold** Tris-Phenol.
7. Ethanol precipitate tRNA with **cold** 1/10 volume 3M NaOAc, 2 μ l of 20 μ g/ μ l Glycogen and 2.5x volumes of 100% ethanol. Samples can also be stored at -20° C and spun later.
8. Resuspend tRNA in 10 μ l of urea loading dye.
9. Resolve samples on 8% acrylamide gel (usually 1 h 30 min run).
10. Dry gel and expose it to the phosphoimager screen o/n.

A12: Procyclic *Trypanosoma brucei* Immunofluorescence

Required Materials

1. 1X PBS (chemicals room)
2. SDM-79 Medium (hemin, antibiotic and serum-free)
3. Fetal Bovine Serum (FBS) (bottle is at 4°C in our side)
4. Bovine Serum Albumin (BSA) (powder is at 4°C with FPLC machine)
5. Tween 20 (with detergents in chemicals room)
6. Triton-X (small -20°C in our side)
7. 37% Formaldehyde (under the fume hood, in our side)
8. Primary and Secondary Antibody bound to FITC (small -20°C in our side)
9. DMSO (stock is at RT in chemicals room)
10. 1 mM Mitotracker Stock Solution (from powder, diluted in DMSO, small -20°C in our side)
11. 300 µM DAPI 1xPBS Solution (small -20°C in our side)
12. Slides and coverslips
13. Dark box to store slides during incubation (we use a P1000 box with a foil cover)

Fluorescent Stains (Stored at -20° C)

1. 4',6-diamidino-2-phenylindole (DAPI): binds AT-rich genomic regions, stains DNA in **BLUE**.
2. Mitotracker: stains live cells, active mitochondria in **RED** or **GREEN** (must be applied before fixing cells).
3. Alexa Fluor®488: bound to secondary antibody, reveals our protein in **GREEN**
4. Alexa Fluor®594: bound to secondary antibody, reveals our protein in **RED**

Solutions (Prepare 10 ml from each a Day Ahead, store at 4° C)

1. 1x PBS
2. 7.4% Formaldehyde in 1x PBS.
3. 5.5% FBS; 0.05% Tween-20 in 1x PBS.
4. 3% BSA; 0.05% Tween-20 in 1x PBS.
5. 0.1% Triton-X in 1x PBS

Preparing the Samples

Staining with Mitotracker

1. Pipette the volume containing 10×10^6 cells into 15 ml conical tubes
2. Harvest the cells for 10 min at 2300 rpm
3. Resuspend in 1 mL of serum free media and transfer to 1.5 mL tubes
 - Pour out supernatant carefully, leave a little bit of liquid behind.
4. Add Mitotracker to a final concentration of 400 nM
 - Make an intermediate 100 μ M Mitotracker solution in DMSO (never use PBS)
 - Simply dilute the 1 mM stock 1:10 with DMSO, keeping the volume low (ex: 1 μ l in 9 μ l DMSO)
 - For a 1 ml volume, add 4 μ l.
5. Incubate tubes for 30 min at 27 °C with agitation.
 - During this step, the Mitotracker will diffuse into the cells and accumulate in the mitochondria
 - Place 1.5 ml tubes sealed inside a 50 ml conical, covered in foil. Place conical tube in the shaker.
 - During this time, prepare the slides (cleaning with 70% ethanol)
6. Spin down cells for 4 min at 4000 rpm
7. Pour supernatant carefully and resuspend in 1 mL of serum-free media

- Serum-free media has no hemin, no serum and no antibiotics
8. Spin down cells for 4 min at 4000 rpm
 9. Pour supernatant carefully and resuspend cells in 100 μ l of 1X PBS kept at room temperature

Fixing the Cells on a Slide

10. Add 100 μ l of 7.4% Formaldehyde in 1x PBS to the cells
 - 1:2 Dilution will bring final concentration to 3.7% Formaldehyde in 1x PBS
 - Mix gently by pipetting up and down with P200
11. Transfer 40 μ l of the cell solution to a glass slide (can do multiple slides with 40 μ l each)
 - Slide should contain important information including date
 - Pipette, then smear it to the size of a quarter with a pipette tip
12. Incubate slides until the drop is dry at room temperature **IN THE DARK**
 - Place inside P1000 box with a foil cover
 - Can take up to 2 hours to dry. **CAN DRY OVERNIGHT IN THE DARK.**

Permeabilizing the Cells

13. Wash smear with 100 μ l 1x PBS three times

- Use tape or wax pencil to mark the location of dried smears, it will be difficult to see after washes
 - Pipette the PBS on the smear and tilt the slide to let it run to a paper.
14. Cover the smear with 100 μ l of 0.1% Triton-X in 1x PBS for 20 minutes
- This is what permeabilizes the cells
15. Wash smear with 100 μ l 1x PBS three times
- Pipette the PBS on the smear and tilt the slide to let it run to a paper.

Block the Cells

16. Cover the smear with 100 μ l of 5.5% Fetal Bovine Serum (FBS) and 0.05% Tween 20 in 1x PBS
17. Incubate IN THE DARK for at least 1h
18. Wash smear with 100 μ l 1x PBS two times
- Pipette the PBS on the smear and tilt the slide to let it run to a paper.

Primary Antibody (Anti-Protein or Anti-tag)

19. Cover the smear with 40 μ l primary antibody solution
- Antibody dilution in: 3% BSA, 0.05% Tween 20 in 1x PBS.
 - The dilution depends on the antibody and has to be optimized (for DHFR-TS I do 1:1000, for HD2 1:500 and for HMG-CoA Synthase 1:2400).

- Antibody manuals/documentation may have a recommended concentration for microscopy, which is usually **10x** the concentration used in Western blot.

20. Incubate IN THE DARK for at least 1h

- Place inside P1000 box with a foil cover

21. Wash smear with 100 μ l 0.05% Tween 20 in 1x PBS three times

- Pipette the PBS on the smear and tilt the slide to let it run to a paper.

22. Wash smear with 100 μ l 1x PBS two times

- Pipette the PBS on the smear and tilt the slide to let it run to a paper.

Secondary Antibody (fluorophore-conjugated)

23. Cover the smear with 40 μ l secondary antibody solution (ALEXA antibody dilutions for Trypanosomatids is usually 1:40)

24. Incubate IN THE DARK for at least 1h

- Place inside P1000 box with a foil cover

25. Wash smear with 100 μ l 0.05% Tween 20 in 1x PBS three times

- Pipette the PBS on the smear and tilt the slide to let it run to a paper

26. Wash smear with 100 μ l 1x PBS two times

- Pipette the PBS on the smear and tilt the slide to let it run to a paper

Staining DNA with DAPI

27. Cover the smear with 100 μ l of 1x PBS containing 300 nM DAPI

- DAPI stock solution from -20° C is 300 µM, so final concentration on slide is 300 nM
- Dilute DAPI 1:1000 with 1x PBS

28. Incubate IN THE DARK for 5 min

29. Wash smear with 100 µl 1x PBS two times

- Pipette the PBS on the smear and tilt the slide to let it run to a paper

30. Incubate IN THE DARK (let it dry completely)

- Can take up to 2 hours to dry, but don't leave it overnight

Mounting the Cells

31. Cover the smear with 7 µl of Vecta shield mounting media

- Pipette the drop right in the middle of the smear

32. Carefully place the coverslip and seal all the edges with nail polish

- Similar to placing a coverslip for a wet mount

33. Place slides in the P1000 box with foil cover and allow the nail polish to dry overnight

Microscopy and Z-Stack Acquisition

For the acquisition of images, we use the Ruiz's lab microscope **Nikon Eclipse Ti**. We should always save a Z-stack file (.nd2) containing the image of the 3 dyes (DAPI, Mitotracker and FITC), and a separate TIF file containing the image of the parasites under phase-contrast. Always sign your name in the sign-

off sheet in the room (Room 216 – Microscopy). Their software, NDS elements, DOES NOT have the package to deconvolve the images, so we use ImageJ and Hyugens in our office computer for that (Windows XP machine).

Steps:

1. Turn ON all 5 switches marked by yellow stickers
 - From most distant to the closest of the computer
2. Turn ON computer
 - User: microscope1
 - Password: micronikon1
3. Open the software NDS elements
4. Position slide in the microscope
 - Slide goes upside down in this microscope
 - Light source can be pushed back if necessary
 - Start with 100x (Ph3) using oil (single drop on top of the objective)
5. Operating the microscope
 - White buttons in front of the microscope control where the image goes: top button (eye) sends the image to the eye piece, left button (L100) sends it to the computer
 - Find the parasites with the eye piece first, using DAPI
 - The joystick on the left side of the computer controls the focus and the stage, make sure to have them set to fine or extra fine

- Find an area with a good amount of cells (not too many) before sending the image to the computer

6. Operating the software

- To see the live image: button with a camera and play symbol
- Acquiring Z-Stack: Application → Define/Run ND Acquisition → Define Top/Bottom
- We used: DAPI (800 ms); Mitrotracker/Texas Red (2s); FITC (800 ms)
- Use the best DAPI focus point as “Home” (ex: 2315.125 μm)
- Move the micrometer and click button to set your “Top” and “Bottom” (ex: 2317.125 μm / 2311.125 μm) for the stacks. Top and bottom should be the points on which the DAPI image is blurred
- Steps should be 0.2 μm , aim at a total of 30 layers
- Save file as .nd2 in the Alfonzo lab folder

Deconvolution of Images

For the deconvolution, we use Image J and Hyugens (both installed in the Windows XP computer in the lab office).

Cropping the Image with Image J

1. Open the .nd2 file with Image J

2. Metadata will open. Write down information for your records (size in pixels, vertical slice distance, numerical aperture, etc.)
 - For our images: Size “X”, Size “Y”: our amount of pixels; Size Y: our number of stacks; Step: should be 0.2 μm ; Numerical aperture: 1.45.
3. 3 Channels will open: DAPI, MITO, FITC
4. MERGE the channels: Image \rightarrow Color \rightarrow Merge Channels
 - ID each channel(c=2; c=0; c=1; etc.)
 - Create a composite (this is what we will crop)
5. Use “rectangular selection” tool to select the desired area
6. Right-click on desired area and choose “duplicate”
 - Check box with “duplicate hyperstack” to save the stacks
 - If you don't, this will generate a 2D image
7. Save image in .ids or .ics format, so it can be opened with our Hyugens 3.4 copy: Plugins \rightarrow Bioformat Exporter
 - Save file in desired folder, keep name simple (ex: for figure 1, parasites, use 1A, 1B, 1C, etc.)
 - In the bioformats exporter “multiple files” leave all boxes unchecked, then click OK
 - Process takes a few seconds. Creates both an .ids file and a calendar file we don't use (but save it anyway)

Deconvolving the Image with Hyugens Essentials 3.4

1. Open the .ids image: File→open (the .ids file, not the calendar)
 - In the workspace: add information obtained from the Image J
 - Numerical Aperture: 1:45 (from the side of 100x objective in the microscope)
 - Lens immersion Refr. Index: 1.515
 - Medium Refractive Index: 1.515 (from the side of the tube of immersion oil)
2. Click “next”, then give the software the wavelengths of all channels.

Table A.11: Nikon Microscope Settings

	0 (FITC)	1 (DAPI)	2 (Mitotracker)
Excitation Wavelength (nm)	490	350	579
Emission Wavelength (nm)	525	470	599
Excitation Photon Count	1	1	1

*I saved all these values as a file for “**Ruiz Lab Microscope**” Template

3. Click “next” in between channels.
4. The program will show us the dimensions:
 - X Sample Size (nm) 64.5700
 - Y Sample Size (nm) 64.5700
 - Z Sample Size (nm) 200 nm

5. Review everything and “accept”. We do not launch the “crop tool”, so “skip” this step.
6. Import microscope template (we can use this with our Ruiz template), otherwise “skip”
7. We can now deconvolve each channel separately. We keep everything the same, except for the last screen:
 - Maximum Iterations: 100 (default is 50)
 - Signal to noise ratio: 40 (increase if background is too much)
 - Quality Treshold: 0.1
8. Click on “Deconvolve”, then select “correct original”
9. Takes a few moments. The deconvolved file will show up on top of the original, double click on the images if you want to check them.
10. We can now either “accept” to go to the next channel, or “resume iterations” to deconvolve the same file again. We deconvolved it again several times. When the software asks, select to use the existing image as reference. This creates “Channel 0-1”, “Channel 0-2”, and so on. Once the image looks good (deconvolving it doesn’t increase its quality), click “accept”, then select which ones to use, and click “accept. Once all channels are done deconvolving, the merged file will be created.
11. Save the file: File → Save Deconvolved As... → .ics Image file. This creates two files: .ics and .ids

12. Now that we have the image, we must adjust contrast, color, brightness, etc. and generate a .TIF for publication.

Treating the Image with Image J

1. Open .ics file
2. Select the slices you want (in our case, 8-10 gave us a good image). Write down which ones you are using.
3. Image → Stacks → Z-Project
4. Enter slices, select either “Standard Deviation” or “Sum Slices”. If you want to see specific things like granules, use “Max Intensity”.
5. Repeat these steps for every channel.
 - Good DAPI images should show the nucleolus
 - To reduce background: Process → Math → Subtract (value is 25. The higher the number, the more background you subtract from the image)
6. Merge the channels: Image → Color → Merge Channels
 - Select pictures
 - This will generate our picture in 32-bit. To be able to open it in another program like Photoshop, we can change that to RGB: Image → Type → RGB Color (save both formats!)
7. Export image: File → Save As... → TIF

- We name this RGB file with all the pertinent info. Ex: 2C Composite (RGB) (Green 1-9 std dev -40 background – blue 1-11 std dev)

8. Crop the pictures to the same dimensions

- Open all desired pictures
- Select the smallest one
- Use “Rectangular selection”
- Cover all the small image, then click on “duplicate”
- Select the next image (just click on it), then hit “Shift + E”
- This will transfer the selection size to the new image.
- Again, “duplicate”
- Repeat for all images. Save as TIF

9. Generate Separate Channels: Image → Color → Split Channels

- LUT to add color, then save as TIF (one by one)
- Name files as DAPI, FITC, etc.

10. Adjust brightness and contrast: can be done with either Image J or Photoshop (or Gimp!)

- We use photoshop in the lab computer: open the merge files
- Menu to the right shows the channels (check/uncheck boxes)
- Adjust brightness and contrast individually
- Write down all adjustments done

11. Save final TIF version (merged)

12. Repeat adjustment with individual channels RGBs and save them

- Use the same values for all of them: ex. DAPI Bright + 150

13. Crop and save the Phase-contrast picture (Image J)

- Open phase-contrast file, then open one of the RGB cropped for sizing
- Zoom to 100 % in the phase contrast using + and –
- Select the RGB image
- Use the rectangular box tool to select all of it (all area), then click “duplicate”
- Select the phase-contrast image (just click on it), then hit “Ctrl + E”.
Use the box to select the cell that you want in the picture
- Click “duplicate, then select the new image and make it an RGB: Image → Type → RGB Color.
- Save as TIF
- After this, this image can be treated in Photoshop/Gimp as well (brightness, orientation and contrast).

14. Make the composite Image with Image J

- Copy final files into new folder
- Name them in the order they should appear:
 - “A” for the phase-Contrast
 - “B” for Mitrotracker
 - “C” for FITC
 - “D” for DAPI

- “E” for Merge (all channels)
- Open Image J
- File → Import → Image Sequence
- Select only the first image
- Check the box “convert to RGB (if not, they will appear grey)
- Images will open on Image J
- Click on Image → Stacks → Make Montage
- Determine columns x rows (usually 5x1) Border width should be = 1,
click “OK”
- Save image as TIF
- Titles for the pictures are added with another program
(Photoshop/Gimp)

Appendix B: Recipes

B1: SDM-79 Medium Recipe

Table B.1: SDM-79 Medium for PCF Trypanosomes (Recipe)

Lab #	Component	Source	Catalog Number	Molecular Weight (g)	Amount/Liter	Amount/10 Liters	Amount/20 Liters
1	MEM (Earl's Powder)	Gibco-BRL	61100-061	N/A	7.0 g	70 g	140 g
2	Grace's Insect Media	Gibco-BRL	21200-076	N/A	2.0 g	20 g	40 g
3	50X MEM Essential Amino Acids	Gibco-BRL	11130-051	N/A	8.0 ml	80 ml	160 ml
4	100X MEM Non-Essential Amino Acids	Gibco-BRL	11140-050	N/A	6.0 ml	60 ml	120 ml
5	Glucose (Anhydrous)	Fisher	D16	180.16	1.0 g	10 g	20 g
6	HEPES (Sodium Salt)	Fisher	BP410	260.3	8.0 g	80 g	160 g
7	MOPS (Free Acid)	Fisher	BP308	9.26	5.0 g	50 g	100 g
8	Sodium Bicarbonate	Fisher	S233	84.01	2.0 g	20 g	40 g
9	Sodium Pyruvate	Fisher	BP356	110.04	0.1 g	1 g	2 g
10	DL-Alanine	SIGMA	A-7502	89.09	200 mg	2 g	4 g
11	L-Arginine	SIGMA	A-3909	210.7	100 mg	1 g	2 g
12	L-Glutamine	SIGMA	G-8540	146.15	300 mg	3 g	6 g
13	DL-Methionine	SIGMA	M-2768	149.2	70 mg	700 mg	1.4 g
14	L-Phenylalanine	SIGMA	P-2126	165.2	80 mg	800 mg	1.6 g
15	L-Proline	SIGMA	P-0380	115.1	600 mg	6 g	12 g
16	DL-Serine	SIGMA	S-4375	105.1	60 mg	600 mg	1.2 g
17	Taurine	SIGMA	T-0625	125.1	160 mg	1.6 g	3.2 g
18	DL-Threonine	SIGMA	T-1520	119.1	350 mg	3.5 g	7 g
19	L-Tyrosine	SIGMA	T-3754	181.2	100 mg	1 g	2 g
20	Guanosine	SIGMA	G-6264	283.2	10 mg	100 mg	200 mg
21	Folic Acid	SIGMA	F-8758	441.4	4 mg	40 mg	80 mg
22	D(+) Glucosamine Hydrochloride	SIGMA	G-1514	215.6	50 mg	500 mg	1 g
23	p-Aminobenzoic Acid	SIGMA	A-9878	137.1	2 mg	20 mg	40 mg
24	Biotin	SIGMA	B-4639	244.3	0.2 mg	2 mg	4 mg

Add all ingredients in approximately half of the final volume. Allow medium to stir for a couple of hours (3h+) to completely dissolve all components. Add water to final volume and make sure the pH is set to 7.3 (pH with 2M NaOH if necessary). When preparing 20 L (for the lab main stock) the pH can be adjusted using NaOH pellets: 18.5 g of NaOH, or about 180 pellets, will bring the pH up from the initial

6.4 to 7.3. Filter sterilize the media with a 0.2 µm filter and store it at 37° C overnight to assess contamination. After that, medium can be stored at 4° C for up to three months.

Two sealed packets can be made to expedite preparation of the medium: components 5 to 9 (Glucose to Sodium Pyruvate) and components 10 to 19 (Alanine to Tyrosine) can be combined and stored in a sealed desiccated container, ready to use when medium needs to be made. All other components must be weighted out individually each time.

Personal stocks for culturing must receive 10% heat inactivated fetal bovine serum or newborn serum and 0.38% hemin (info on next page).

Table B.2: Culture Media for *Trypanosoma brucei* (Personal Stock)

Component	Volume		
	200 ml	500 ml	1 L
Heat-Inactivated Fetal Bovine Serum	20 ml	50 ml	100 ml
Hemin	760 µl	1.9 ml	3.8 ml
SDM-79 Media	↑ 200 ml	↑ 500 ml	↑ 1 L

Table B.3: Available *T. brucei* Selection Drugs in the Alfonzo Lab

Name	Origin	Class / Mechanism	Concentrations		Volume to Add per Medium/Culture Volume				
			Stock []	Final []	5 ml	50 ml	200 ml	500 ml	1 L
G418/Geneticin	<i>Micromonospora rhodorangea</i>	Aminoglycoside. Protein synthesis inhibitor.	100 mg/ml	12 µg/ml	0.6 µl	6 µl	24 µl	60 µl	120 µl
Hygromycin B	<i>Streptomyces hydroscopicus</i>	Aminoglycoside. Protein synthesis inhibitor.	100 mg/ml	50 µg/ml	2.5 µl	25 µl	100 µl	250 µl	500 µl
Phleomycin	<i>Streptomyces verticillus</i>	Glycopeptide. DNA intercalating agent.	20 mg/ml	2.5 µg/ml	0.625 µl	6.25 µl	25 µl	62.5 µl	125 µl
Puromycin	<i>Streptomyces alboniger</i>	Nucleoside. Protein synthesis inhibitor.	10 mg/ml	1 µg/ml	0.5 µl	5 µl	20 µl	50 µl	100 µl
Blasticidin S*	<i>Streptomyces griseochromogenes</i>	Nucleoside. Protein synthesis inhibitor.	10 mg/ml	10 µg/ml	5 µl	50 µl	200 µl	500 µl	1 ml
Nourseothricin	<i>Streptomyces noursei</i>	Aminoglycoside. Protein synthesis inhibitor.		100 µg/ml					
Penicillin-Streptomycin (100x)	<i>Penicillium chrysogenum</i> <i>Streptomyces griseus</i>	β-lactam. Cell wall biosynthesis inhibitor. Aminoglycoside. Protein synthesis inhibitor	5000 U - 5 mg /ml	50 U - 50 µg / ml	50 µl	500 µl	2 ml	5 ml	10ml
Tetracycline	<i>Streptomyces rimosus</i>	Polyketide. Protein synthesis inhibitor.	1 mg/ml (1000x)	1 µg/ml (1x)	5 µl	50 µl	N/A	N/A	N/A
Cycloheximide (non inhib.)	<i>Streptomyces griseus</i>	Fungicide. Eukaryotic protein synthesis inhibitor.	10 µg/ml (1000x)	10 ng/ml (1x)	5 µl	50 µl	N/A	N/A	N/A

*SmOx cells are naturally resistant to Blasticidin S, but the drug will work for selection at twice the normal working concentration (20 µg/ml).

Appendix C: TSEN Homolog Sequences

C1: TSEN2 Homolog Sequences

>Trypanosoma_brucei_Tb927.11.9740

MASGSGRGEGVGEHRPNPIVRVVG VNGPLFVCE DSSVLSKFPQMYKKDYSGP
HLGVEELEYLSEFVSIEFITAEDRQYWASLRMRHEFSCR VYRH LTKMGLFLRH
GSQFGAAFIGYRDLKDHGNCLVYFGPLSQLSATAAARVAASVGKEAWVVEEFP
IKATGCLSVSKIESYWGPSGQGGNSVCGDKGGKCVKKRRLSYTPIVQL

>Trypanosoma_evansi_TevSTIB805.11_01.10040

MASGSGRGEGVGEHRPNPIVRVVG VNGPLFVCE DSSVLSKFPQMYKKDYSGP
HLGVEELEYLSEFVSIEFITAEDRQYWASLRMRHEFSCR VYRH LTKMGLFLRH
GSQFGAAFIGYRDLKDHGNCLVYFGPLSQLSATAAARVAASVGKEAWVVEEFP
IKATGCLSVSKIESYWGPSGQGGNSVCGDKGGKCVKKRRLSYTPIVQL

>Trypanosoma_equiperdum_TEOVI_000184400

MASGSGRGEGVGEHRPNPIVRVVG VNGPLFVCE DSSVLSKFPQMYKKDYSGP
HLGVEELEYLSEFVSIEFITAEDRQYWASLRMRHEFSCR VYRH LTKMGLFLRH
GSQFGAAFIGYRDLKDHGNCLVYFGPLSQLSATAAARVAASVGKEAWVVEEFP
IKATGCLSVSKIESYWGPSGQGGNSVCGDKGGKCVKKRRLSYTPIVQL

>Trypanosoma_congolense_TcIL3000.A.H_000955700

MAASGDTGEEGDEGCLACTIRVTGLFGPLFVCHNASVFLSKFPQMYKRDYSSA
YLSIEELEYLSSSFRIEFDNEIDARYRVRLRERHEFSCRVYRHLTEEMGIALRHG
GRFGAAFIGYRDINGHGDCLVYFGPLSSMALIAATRVAASSVGKEAWIVEKSANC
SFDQPLVTRVERGHRSLAQQVDGCKGESQAFRKKRRLSRTQSA

>Trypanosoma_vivax_TvY486_1110380

MDGSPIPKEVSVTEGNKKDQSSPLLRVIGSFGPLFVCHDTSVFLPQFPQMLKKD
YGSAHLSIEELNYLSLSFRVVFDRQEDEGRHVAMSRQHRFSCDAYRQLTDKW
GLSLRHGSKFGAAFIGYHNVSGHSDYLIFFGPLSRLAAIAAVRVASSVGKEAWS
VEKRPDSTCGYHGELSFARIENSKLTCSKRNAASSEEDTRAQRHVYNGAVI

>Trypanosoma_cruzi_TcYC6_0007120

MENLEDGDPRQRRHFGGDAAPATRKADKCGEEGGGEANDDENIILRIIRTHGP
LFVCENPSLFLQTLQPARKKHYS DHLSIEELEYLGHSDILFKNEQDSHRRACL
RERHATSCRVYRYLTDEMGLRLRHGSQFGAAFIGYRDVNGHGEYLVYLGPLSR
LEEVA AVRVAR SVAKEAWVAEEQQDGSGFSFTRLSPSVSGRASRET PRQLVM
GTNGPKTVS

>Leishmania_infantum_LINF_360046200

MLVIEGTNGPLFRVAESAAAIAYLSTHYPQCKKRGSGWHLSVEEV SLLQSQRRL
ADGVH FASADTKEQFEVLRKRYARDCAVYAALTTDHGYRLRHGSQFGANYIGY

QDVGTHGECLLFTGPLAELERVRAVRIARSVGKRAMLVTVQEGDSGCSSTVTV
TDLMADSLADLRRPHKSCRKA

>Leishmania_tarentolae_LtaPh_3638500

MRTDGTNPNAHEGFILVIEGTDGPLFSVAESAAAIAYLSTHYPQCKKRSSGWQLS
VEEVSLLQSQLGSTDGVHFAAADTREKFEELRKRYARDCAVYAALTTDHGYKL
RHGSQFGANYIGYQDVETHGECLMFTGPLAELEQVRAVRIARSVGKRAMLVTV
QQDDNGCSSTVTVTDLMTTEFFADLRRPHKACRKE

>Leishmania_donovani_LdBPK_363920.1

MLVIEGTNGPLFRVAESAAAIAYLSTHYPQCKKRGSGWHLSVEEVSLLQSQLRR
ADGVHFASADTKEQFEVLRKRYARDCAVYAALTTDHGYRLRHGSQFGANYIGY
QDVGTHGECLLFTGPLAELERVRAVRIARSVGKRAMLVTVQEGDSGCSSTVTV
TDLMADSLADLRRPHKSCRKA

>Porcisia_hertigi_JKF63_00384

MCTDKKAGCAYEETALFIDGTNGPLFSVAESSAAMAYLATNYPQCKKRGLGW
QLSVEEVHFLQSQLHQSGGVHFMASAVTKDQYEVLRKRYARDCLVYTSLTTKYG
YRLRHGSQFGANYIGYRDVGTHGECLFFTGPLAELEKVRVRIARSVGKRAML
VLLQEGGDDSPCTVTVSELMADSCAGLQRSHKSRRKE

>Leptomonas_pyrrhocoris_LpyrH10_06_1370

MLLTIVGTNGPLFVFRKSTETADFLSSHYPQFAKRSLGWQLSVEEVYCLQSRQ
DSCAEAGPGKAPDFAVSFEAASAVEQYTALRKAYASDCFIYSELTLRHGYKLRH
GSSFGASYIGYRDLNEHGECLEFFTGPLTALEQVRAVRTAHSVGKEAVMLVVA
EEAGVTLTRLGGGRAAPEVAHRRKIRRKE

>Leptomonas_seymouri_Lsey_0172_0010

MQTARQRCAAHVLLHPAYARAQTHMQLTIVGTNGPLFLVDTSAEAVLFLSTHY
PQFAKRLLGWQLSVEEVYCLQSCCKGHDAQAQLGNVSDVAVVFESASAAAQYQ
ELWKTYAIDCCIYSQLTLCHGYKLRHGSSFGANYIGYQDVNRHGECLEFFAGPLT
DLEQVRAVRVAHSVGKDAVQVLVVTGAGVALTRLGGSRAATGATRHRKLRR
KE

>Saccharomyces_cerevisiae_YLR105C

MSKGRVNVKRYKYPLPIHPVDDLPELILHNPLSWLYWAYRYYKSTNALNDKVH
VDFIGDTHLITVQDDKQMLYLWNNGFFGTGQFSRSEPTWKARTEARLGLNDT
PLHNRGGTKSNTETEMTLEKVTQQRRLQRLEFKKERAKLERELLELRKKGHI
DEENILLEKQRESLRKFKLKQTEDVGIVAQQQDISESNLRDEDNLLDENGDLL
PLESLELMPVEAMFLTFALPVLDISPACLAGKLFQFDAQYKDIHSFVRSYVIYHHY
RSHGWCVRSYKIFGCDYLLYKRGPPFQHAFCVMGLDHDVSKDYTWYSSAR
VVGAKKTFVLCYVERLISEQEIALWKSNNFTKLFNSFQVGEVLYKRWVPGR
NRD

>Homo_sapiens_NP_001138864

MAEAVFHAPKRKR RVYETYESPLPIFGQDHGPKLEFKIFRAEMINNVIVRNAE
DIEQLYGKGYFGKGILSRSRPSFTISDPKLVAKWKDMKTNMPIITSKRYQHSVE
WAAELMRRQGQDESTVRRILKDYTKPLEHPPVKRNEEAQVHDKLNSGMVSNM
EGTAGGERPSVVNGDSGKSGGVGDPREPLGCLQEGSGCHPTTESFEKSVRE
DASPLPHVCCCKQDALILQRGLHHEDGSQHIGLLHPGDRGPDHEYVLVEEAEC
AMSEREAAPNEELVQRNRLICRRNPYRIFEYLQLSLEEAFFLVYALGCLSIYYEK
EPLTIVKLWKAFTVVQPTFRTTYMAYHYFRSKGWVVKVGLKYGTDLLLYRKGP
PFYHASYSVIIELVDDHFEGSLRRPLSWKSLAALSRVSVNVSKELMLCYLIK PST
MTDKEMESPECMKRIKVQE VILSRWVSSRERSDQDDL

>Ascoidea_rubescens_XP_020050142

MSKRRRNLNQLYPNLPINVYQFPVLFPHNLISWISYAYSYYRFVTASPKLTKSD
VLIVEGNIHQVKDEQDQKRLWCNGFFGKGILSRSEPTWHERTLVRLGLKENAA
YNSNNKNRNKSKNRDKKNLASEDITKLRNERNLYKKQREKLEQEEVQLRKQL
DLARESVDERKVVQAKL DKLKLKLVSDEQKTLIKEINEEIKELRPEDKKLINAK
EHDVNQLEYLQLMPVETFFLSFSLGCVNVYEKKEIFLKLLSTTEFLKSVKSLKA
DDKFIMKYVVYHNYRSKGWCVRSGIKFGCDFLIYNKGPPF SHAEFCLIVLPNYV
DESKNRHVSKKFSLLSGINRVIGGVRKSMILVYVNIPED EQFN RVINNRNENDLI
DFEKLFLKYKVTEIMYSRWQPSRNRD

>Candida_albicans_RLP64711

MGKKNNKFLNKIYSQPLPITLTSSKHNVSLPNLYPHNPISWIWYIIRYCQINIVYQV
PELHNPPLSVIYENQIFKVIDRESMLKLWRQGFFGKGILSRSEPTWEKRTITRLN
LDNANNGKDLAMEDITKKRREERKLFKLERARFQELELKKRQGIITDEEVEEMN
KLEIQLTELKRTQVRFDKQENGEVKEIHIRDEDEDIITENGELLPLEFLQLQEVET
FFLKFALQRIDIVNVDSLLDLFYKCCSHHSFSPIPTSNNQFIIEYIAYHYFRTNGW
CVRSGIKFGTDFLLYKRGPPFTHAEFCVLVMTKDSKYDWFQIAAKARVIGSVKK
TFVLCYIEYPTQGEFDQILQKQNEEDIDHGLLLKELLSKYKISEVIYKRWNPSRTR
D

>Candida_dublinsiensis_XP_002419914

MGKKNNKLLNKIYSQPLPITLTSSKYNVSLPNLYPHNPISWIWYIMIRYCQINIVYQ
VPELDNPPLSVIYENQIFKVIDPESMLKLWRQGFFGKGILSRSEPTWEKRTITRL
NLDKANSKDLAMEDITKKRREERKFFKLERARFQELELKKRQGIITEKEVDEM
NKLESQTELKRTQVRFDKSENGEVNEVHIRDEDEDIITENGELLPLEFLQLQEV
EAFFLKFALQRVDIVNVDSLLDLFYKCCSHHSFSAIPTSNNQFVIEYIAYHYFRTN
GWCVRSGIKFGTDFLLYKRGPPFTHAEFCVLVMTKDSKYDWFQIAAKARVIGSV
KKTFFVLCYIDYPTQEEFDHILQKQHEKDIDHGLLLKELLNKYKISEVIYKRWNPSR
TRD

>Candida_maltosa_EMG48421

MGKRNNKFLNKIYSRPLPITLTSQKYNVSLPNLYPHNPISWVWYLVRYLQINILY
EVPERHNPPLPVIYEDQIFKVTDRDAMMQLWRQGFFGKGILSRSEPSWYQRTL
TRLSLDDGKSNSSTKKDIAMEDVTKIRRDERKFFKLERARLQGLELKKRQGVITE
EELDEMTKLDAALSCLRKAQIRFNQQGEKVEEEEIRDEDDDIVGENGELLPLEFL
QLQAVEAFFLKFALNRIEFDTIDTISDLFSKCCSQTVPDNKFILDYVVYHYFRSN
GWCVRSGVKFGTDYLLYKRGPPFIHAEYCILIMTKDSKYDWFDIATKARVVGSV
KKAFVLCYVDYPSDTEFHEILNQEDIDEGIKFKLLFTKYKISEIYKRWNPSRTRD

>Candida_tropicalis_XP_002545471

MGKRNNKYLNKLYSQPLPITLTSQKYNVSLPELYPHNPISWIWYLMRYFQINIFY
PVPESTNHPLPVIYDGEIFKVTDESSINNLWRQGFFGKGVLSRSEPTWYQRTL
RLNLDDGGKDSNNLAMEDITKIRRNERKMFKLERARFQELELKKRQGVITDDEL
KDMEKLDKLVLRKADIKFDEKGNQLEEIRDEDEDEDIDEDGKLLPLEYLQLQPV
EAFFLKFALNRIQVDGMNSTFDLFTCCSQYESVVTNNRFIVDYAVYHYFRSN
GWCVRSGVKFGTDFLLYKRGPPFIHAEYCVLVMTKD TDYDWF EIAAKARVIGSV
KKTFFVLCYVDSPSQEVFDEILSQQQS QLDHGLLFKQLFEQYKISEVVYRRWNPS
RTRD

>Cyberlindnera_fabianii_CDR40891

MSKRTPLNVRYRHALPVHPIELPNVPHNPLSWLYCLYVFWTSTVSISSRTTVTC
DENGHFFVNDPQH MNVLWSEGGFFGKGVFSRSDPTW NDR TQKRLGIGEFKNLT
MEEITAIRREERKKFKKERANLESKQAE LKKQGIVDPFLEERLKLKELRDKDISV

KLERETYIREEDSEILDDKGHLINIETLQLQPSEVFFLHFALQATDVYQNSIKLSTS
DLLSILWPSRLADDKFILNYLVYQHYSRSLGWCVRSIGKFGTDWLLYKRGPPFHH
AEFTLLILPNYKDDVKNSNIAKDYVWWSSLNRRVSSVRKNLVLVFDVDPQSAI
DDAKSVSEILNLYKIHEVLYRRWIPNKNRD

>Cyberlindnera_jadinii_XP_020070068

MSKRTSLNAKYPHALPVHPIALPELILHNPISWIWFTICYIKSFPTVSRTVVQFKD
GCFAVDSPEEMMTLWNEGFFGKGTMSRSEPTWYDRTQKRLGLGEFKNLTIEEI
TILRREERKKFKRERAQLEKKQKELKSMGIVDPFIEERLKLKELRDKDITPLERE
TFIRPEDDVLVVKGHLINIEQLQLQPCEVMFLEFALQSVTVVTDGVALSSNQLLE
VLWPTKSADDSFIVKYVVYHYRSLGWCVRSAIKFGTDFLLYNRGPPFHAEFA
LHVVPNYNDTQKNTATAQDFTMLSGLNRVIAGVRKNLVLVFDIPTQEEIDKAG
SFQDILSLYSISEVLLRRWVPPNRNRD

>Eremothecium_cymbalariae_XP_003646155

MAKYISNRRRYEHKLPLELIQLPPLIPHNPVSWLHWIFKYVTAVNYMRQTIPVEID
ASGKIIISDHDHMRYLWERGFFGTGQLSRSEPTWYERTASRLQLDGSKQDGVQ
LEQVTRLRRKQRLEFKKERAKFEEKLHLRMNGVLESEILGEEQAFLKSLRDQE
LQYGSVNESGSGGGSSFEFIRMEDSDILTEDGTGIIKLEKLELMPVEAMFLTFAL
PVLDISMKDLLHSIFVETPSFEQIEALCMKYAAYHHYRSHGWCVRSIGVKFGCDY
MLYRQGPPFHAEFSVMVLHHNQAQHDYTWYSTVARVVGAKKCLVLCYISK
KAADDILMELWSRGSYAQAFALFEVNELVYRRWVPGKNRD

>Kluyveromyces_lactis_QEU62286

MSKRSHRNHLQYKHALPIEAQPVPSVWKHPFQAFSWILDWAMRWSETRIIDVK
VNQLGQILVCDQWQM KYLWEHGFFGTGQLSRSEPNWQTRTMSRLQLNDADG
INLEHVTDVRRKQRLEFKKLRAEFEAKKLEMRQKGIVDEQFIEQERLFLKNQRD
KELAFEKDSMQIRDEDLRLIEGNSVIQLESLQLMPVEAIFLSYAVPVLKITLQQLM
VSLVLEPKSFQDIKKLIHQYVAYHHYRSKGWCVRSGIKFGCEFLLYRRGPPFQH
AEYGIMVLDANQSNDYTWYSSAARVVGAKKQFVLCYVEQLIPEDDLMELWK
QSKYDELFRNFKIHHELLYKRWWAGKNRD

>Lachancea_mirantina_SCV04458

MPKYVRDAYRYKYPLPIHPLDHLPLIPHNPISWAYWLF CYLSGSNEPQVRVHA
EMDDLKRVTVCREQDMRLLWDNGFFGTGRMSRSEATWRQRTAKRLGLESSE
RGLESVTEKRRQRRLQFKRERSKFEEAKLELRQKGD LACEILDQERLFLRSLRD
KELAYDKDDDDVVFREIDHELLDDAGEVMPIEVLELMPVEAIFLSFALPVL DLQV
PTLMSTLVSSNATFADIESLATKYVAYHHYRSRGWCVRSGVKFGCDFLLYRRG
PPFQHAFAVMVLNADETLDYTQYSSTARVVGARKSFVVCYVERQVSERQIL
QFWQNHNYASAFSSFKIGEVTYRRWVPGKNRD

>Canis_lupus_familiaris_XP_013977123.1

MAEAVFRAPKRKR RVYESFESPLPIPFQDCGPKQDFKVFTAEMINNNVIVRNT
EDMEQLYGKGYFGKGILSRSRPNFTISDPKLVAKWKDMKTDMPITSTKYQHSV

EWATKLMQRQGQDESTVRKILQDYTKPLEHSGIKRNEEGQRHDELNSGTVSK
MEGTTDREELSMMNGDSGKSVGMEGPSKPSDHQQQSGPDPLTPDGLDES
VEGATLQHCPLPQIHCGKDDGLLPTPGDTQPGDGSQQADLCARKRGPDEYV
LVEEDVYDVSEQECAPNEELAPKKRLVCRRNPYRILEYLQLSLEEAFLLVYALG
CLSIYYEKEPLTIMKLWKAFTVVQPTFRTTYMAYHYFRSKGWVPKVGLKYGTDL
LLYRKGPFFYHASYSVIIELVDDHFEGSLRRPFSWRSALNRVSVNVSKEML
CYLIKPSTMTDKEMESPECMKQIKVQEVIILSRWVSSRERSDQDEL

>Equus_caballus_XP_001492417.1

MAEAVFHAPKRKRRVYENYESPLPIFGQDCDPRKEFKIFCAEMINNNVIVRGA
EDIEQLYGKGYFGKGILSRSPNFTISDPKLVAKWKDMKTDMPITSKKYQHSIE
WATKLMQRQGQDESTVHRILEDYTKPLEHPCIKRKEEVPLQDELNSKMVSKVE
GTAAGEKVSINGDPGKSTDMEDPSSQSHCLQESSGRDPLAVRSSDEHVVTG
PAPLPQVHCSKQDVPLPLCGTQRDDSSQHGGGLICDRGKGS DHEYVLVEEVVC
DESEREDAPNEQLVQKKRLICRRNPYRIFEYLQLSLEEAFLLVYALGCLSIYYDK
EPLTIVKLWKVFTVIQPTFRTTYMAYHHFRSKGWVPKVGLKYGTDLLLYRKGP
FYHASYSVIVELVDDHFEGPLRRPFSWKSLAALSRSVSVNVSKEMLCYLIKPST
MTDKEMESPECMKRIKQVQEVIILSRWVSSRERSDQDEL

>Gorilla_gorilla_gorilla_XP_018880155.2

MAEAVFHAPKRKRRVYETYYESPLPIFGQDHGGLKEFKIFHAEMINNNVIVRNAE
DIEQLYGKGYFGKGILSRSPSFTISDPKLVAKWKDMKTNMPIITSKRYQHSVE

WAAELMRRQGQDESTVHRILKDYTKPLEHPPVKRNEEAQVHDELNSGMVSNM
EGPAGGERPSVVNGDSGKSGGVGDPREPLGCLQEGSGCHPTTESLEKSVRE
DASPLPHVFCCKQDALILQRGLHHEDGRQHIGLLHPGDRGPDHEYVLVEEAEC
AMSEREAAPNEELVRRNRLICRRNPYRIFEYLQLSLEEAFFLVYALGCLSIYYEK
EPLTIVKLWKAFTVVQPTFRTTYMAYHYFRSKGWVPKVGLKYGTDLLLYQKGP
PFYHASYSVIIELVDDHFEGSLRRPLSWKSLAALSRVSVNVSKELMLCYLIKPS
MTDKEMESPECMKRIKVQAGVQCCDLGSLQPLPPGFKRFSCLSLSSWDYRH
APPRMANFCIFSRDGVSPCWPGWSGTPDLK

>Macaca_mulatta_XP_014985699.2

MAEAVFHAPKRKRVRVYETYESPLPIFGQDHSPQKEFKIFRAEMINNNVIVRNA
EDIEQLYGKGYFGKGILSRSPNFTISDPKLVAKWKDVKTNMPIITSKRYQHSVE
WAAELMRRQGQDESTVCRILKDYTKPLEHPPVKRNEEAQVYDELNSGMVSNM
EGTARGERPSVVNGDSGKSGGMGDPSEPLGSLQEGSGCNPTTDGFEKSVRK
DAAPLPQVCCCKQDALILQCGPHHEDGSQHVGLLHAGDRGPDHEYVLVEEVE
CAMSEREDAPNEELVQRNRLICRRNPYRIFEYLQLSLEEAFFLVYALGCLSIYYE
KEPLTIVKLWKAFTGVQPTFRTTYMAYHYFRSKGWVPKVGLKYGTDLLLYRKG
PPFYHASYSVIIELVDDHFEGCLRRPFSWKSLAALSRVSVNVSKELMLCYLIKPS
TMTDKEMESPECMKRIKVQEVIILSRWVSSRERSDQDDL

>Pan_paniscus_XP_034811714.1

MAEAVFHAPKRKRRVYETYESPLPIFGQDHGPKLKEFKIFRAEMINNNVIVRNAE
DIEQLYGKGYFGKGILSRSRPSFTISDPKLVAKWTKMKNMPIITSKRYQRSVE
WAAELMRRQGQDESTVGRILKDYTKPLEHPPVKRDEEAQVHDELNSGMVSNM
EGTAGGERPSVNGDSGKSGGVGDPREPLGCLQEGSGCHPTTESFEKSVRE
DASPLPHVCCCKQDALILQRGLHHEDGSQHIGLLHPGDRGPDHEYVLVEEAEC
AMSEREAAPNEELVQRNRLICRRNPYRIFEYLQLSLEEAFFLVYALGCLSIYYEK
EPLTIVKLWKAFTVVQPTFRRTTYMAYHYFRSKGWVWPKVGLKYGTDLLLYRKGP
PFYHASYSVIIELVDDHFEGSLRRPLSWKSLAALSRVSVNVSKELMLCYLIKPOST
MTDKEMESPECMKRIKVQEVLRSRWVSSRERSDQDDL

>Pan_troglodytes_PNI53348.1

MAEAVFHAPKRKRRVYETYESPLPIFGQDHGPKLKEFKIFRAEMINNNVIVRNAE
DIEQLYGKGYFGKGILSRSRPSFTISDPKLVAKWKDMKNMPIITSKRYQRSVE
WAAELMRRQGQDESTVGRILKDYTKPLEHPPVKRDEEAQVHDELNSGMVSNM
EGTAGGERPSVNGDSGKSGGVGDPREPLGCLQEGSGCHPTTESFEKSVRE
DASPLPHVCCCKQDALILQRGLHHEDGSQHIGLLHPGDRGPDHEYVLVEEAEC
AMSEREAAPNEELVQRNRLICRRNPYRIFEYLQLSLEEAFFLVYALGCLSIYYEK
EPLTIVKLWKAFTVVQPTFRRTTYMAYHYFRSKGWVWPKVGLKYGTDLLLYRKGP
PFYHA

>Vulpes_vulpes_XP_025872611.1

MAEAVFRAPKRKRRVYESFESPLPIFGQDCGPKQDFKVFTAEMINNNVIVRNT
EDMEQLYGKGYFGKGILSRSRPNFTISDPKLVAKWKDMKTDMPIITSTKYQHSV
EWATKLMQRQGQDESTVRKILQDYTKPLEHSGIKRNEEGQRHDELNSGTVSK
MEGTTDREELSMMNGDSGKSVGMEGPSKPSDRQQQSGPDPLTPDGLDESV
VEGATLQHCPLPQIHCGKDDGLLPTPGDTQPGDGSQQADLCARKRGPDEYV
LVEEDVYDVSEQECAPNEELAPKKRLVCRRNPYRILEYLQLSLEEAFLLVYALG
CLSIYYGKEPLTIMKLWKAFTVVQPTFRTTYMAYHYFRSKGWVPKVGLKYGTDL
LLYRKGPFFYHASYSVIIELVDDHFEGSLRRPFSWRSALAALSRVSVNVSKELML
CYLIKPSTMTDKEMESPECMKQIKVQEVILSRWVSSRERSDQDEL

>Mus_musculus_NP_950198.1

MAEAVFRAPKRKRRVYESYESPLPIFGQDQGPRKEFRIFQAEMISNNVVVRG
TEDMEQLYGKGYFGKGILSRSRPNFTIANPTLAARWKGVQTDMPIITSEKYQHR
VEWARDFLRRQGHDESTVQKILTDYTEPLELPCREEKEETPQHEPLSSKADSS
LEGRVEKDELPTVPGGAGQSDDLPLGLGTHSDCLQEGPGHATLAAASPSSHNG
HVAEDPEVLPQETLVPQGGLWPEASSQAAGEKRAAHEYVLIEEELCGAQEEEA
AAASDEKLLKRKLVLCRRNPYRIFEYLQLSLEEAFLLAYALGCLSIYYEKEPLTIV
KLWQAFTAVQPTFRTTYMAYHYFRSKGWVPKVGLKYGTDLLYRKGPFFYHA
SYSVIIELDDNYEGSLRRPFSWKSLAALSRVSGNVSKELMLCYLIKPSTMTAED
METPECMKRIQVQEVILSRWVSSRERSDQDEL

>Methanocaldococcus_jannaschii_AAB99435

MVRDKMGKKITGLLDGDRVIVFDKNGISKLSARHYGNVEGNFLSLSLVEALYLIN
LGWLEVKYKDNKPLSFEELYEYARNVEERLCLKYLVYKDLRTRGYIVKTGLKYG
ADFRLYERGANIDKEHSVYLVKVPEDSSFLLSELTGFV RVAHSVRKKLLIAIVDA
DGDIVYYNMTYVKP

>Methanocaldococcus_bathoardescens_WP_048201592.1

MSKKIIGLLDGDRVIVFDKNGISKLSARHYGNVEGNFLSLSLVEALYLINLGWLAV
KDKNEKMLSFEELYEYAKNIEERLCLKYLVYKDLRTRGYIVKTGLKYGADFRLYE
RGANIDKEHSVYLVKVFTEDSSFLLSELTGFV RVAHSVRKKLLIAIVDADGDIVYY
NMAYVKP

>Methanocaldococcus_fervens_WP_015791937.1

MGKKIIGSLDGDRVIVFDKNGISKLSKHYGNVEGNFLSLSLVEALYLTNLGWLA
VKDNNKILSFEELYEYAKNIEERLCLKYLVYKDLRSRGYIVKTGLKYGADFRLYE
RGANIDKEHSVYLVKVFTEDSSFLLNELTGFV RVAHSVRKKLLIAIVDADGDIVYY
NMTYVKP

>Methanocaldococcus_vulcanius_WP_015732815.1

MAKKIVGLLDGDRVIVFDKNGISKLSAKHYGNLEGNFLSLSLVEALYLMNLGWIE
VKDKNKIISFEELYEYARTVEEKLCLKYLVYKDLRTRGYIVKTGLKYGADFRLYE
RGANIEKEHSVYLVKVFSEDCSLLLSELTGFV RVAHSVRKKLLIAIVDADGDIVYY
NMSYVKP

>Methanotorris_igneus_WP_015732815.1

MMAKKQIVGILSDDRIVVFDKNGISRLCSRYGKNDFFLSLSLIEALYLTSLGW
LVVKDSNGRLLSFEELYEYARNIEESLCIKYLVYKDLRNRGYTVKTGLKYGTDFR
LYERGADIDKEHSVYLVKVFSEEKPCNISELTGFV RVAHSVRKKLLIAIVDADGD
VVYYDMGFVRP

>Methanotorris_formicicus_WP_173361568.1

MMAKKQIVGILSDERVAVFDKNGISRLCARYGKNDNFLSLSLVEALYLTSLG
WLVVKDSNGKLLSFEKLYEYARNIEESLCIKYLVYRDLRNRGYTVKTGLKYGTD
FRLYERGADIDKEHSIYLVKVFSEEKPCNISELTGFV RVAHSVRKKLLIAIVDADG
DVYYDMGFVRP

>Methanothermococcus_okinawensis_AEH06525.1

MAKKPIIAKLSDDRVLIFNRDGISRLNAKGYGELNDNFLSISLVESLYLVSKKWIK
VKSKKDKFLSFEELYDYAHNIDEKLCIKYLVYKDLRNRGYTVKTGLKYGSDYRLY
SRENIDEIHSEYLVKVFSEDRPCAISELTGFV RVAHSVRKKLLIAIVDDDGDIVYYN
MGYLRL

>Methanococcus_maripaludis_AEK20165.1

MAKPKKTIPAKLSDERIVIYDKDGISRLNEKRYGELHENFLSLSFVEGLYLVSKN
WISLRDKNKLLSFEELFDVAQNIDRKL CIRYLAYKDLRNRGYTVRTGLKYGSDF

RLYERSNIDEIHSRYLVKVFSEEIPCEISEITGFVRVAHSVRKELIIAIVDADGSVVY
YNMGYLKL

>Methanobacterium_paludism_WP_013826255.1

MNSKLSGDLVIIIEENKGAKLHEKSHYGNVTEEGLQLSLIEALYLMEKDKLEILSD
DKELSLDEM FELIRSKNLFTMYIVFRDLKNRGYIVKTGFKYGSEFRLYER GKSPG
DGHSNYLVKVAPENCTMTMFDLSSYVRVAHG VNKLLFAVVDDENDITYYNME
WTRP

>Thermococcus_bergensis_WP_225807062.1

MSEFKFYLSGDRVFSMMESAINKLYNKRHYGEVVNGKLFSLIEAAYLLDKGWI
KVFDGEKELGIQELFEIGRKKDEHFDLKFLVYKDLRDRGYTVKTALKYGSHFRV
YRRGMEEHSQWLIWVVPENLRFSPNDITARVRVAHGVRKNMIMAVVDEDNHIV
YYKIEWVKF

>Thermococcus_gorgonarius_WP_088884383.1

MIVFYLSGNRVFSTDKNAIDGLHNNRHYGKLVNGKVFLSLLEAAYLVERGKIEVR
DGKRRLTLEEVMKLGREEDELFDAYLVYKDLRDRGYTVKSGLKFGSHFRVYR
RGMDEHSQWLWVVPENKTIAPNDITARVRVAHGVRKEMIMAVVDDDGDIVYY
KIEWTKF

>Arabidopsis_thaliana_AT5G60230.1

MAPRWKWKGAEAKALAEPISKSVSELQLSLAETESSGTLSSCNVLLAVEPEQA
ELLDRCCFGRLVLSAEKIKKWIQLSFEEAFFLHYNLKCICKISLQGRCLENEVDTW
LYMKS KRPNFPMFFKAYSHLR SKNWVLR SGLQYGVDFVAYRHHPSLVHSEYS
VLVQSGDSDRLRVWSDIHCAVRLSGSVAKTLLTLYVNGNFKGEDVNLLVCLEN
FTVEEQTISRWSPELSREDQSTNSKQHVPNVSNLNTL

>Arabidopsis_thaliana_AT3G45590.1

MAPRWKWKGAEAKALAEPVSKTVSELRSSLTQTEALGFLSSCNVLLSVESEEA
ELLDRCCFGRLVVGAEKDKRWIQLSFEEAFFLFYKLCIKICLHGRSLENEVDLW
RSMSSFQDFAILYKAYSHLR SKNWIVR SGLQYGVDFVVYRHHPSLVHSEYAV
LVQSIGGNDRLKVWSDIHCSVRLTGSVAKSLLVLYVNRKVNTEKMNLPLCLEDY
TVEEQTIRRWSPELSREDETRT

>Arabidopsis_lyrata_XP_020881742.1

MAPRWKWKGAEAKALAEPVSETVLELQSSFAQTVASGFLSSCNVLLSVEPEQA
DLLDRCCFGRPVSVEKDKRWIQLSFEEAFFLFYKLCVKISLHGCSLENEVDL
WRSMSSFKNFAISYKAYSHLR SKNWIVR SGLQYGVDFVVYRHHPSLVHSEYA
VLVQSIGIDRLKVWSDIHCSVRLTGSVAKTLLVLYVNGIVKTENMNLPLCLEDYI
VEEQTIRRWSPELSREDKTRT

>Arabidopsis_lyrata_XP_002866377.2

MAPRWKWKGAEKALAEPIKSVSELQLSLAETESSGTLSSSNVLLAVEPEQA
ELLDRCCFGRLVLSAEKVKKWIQLSFEEAFYLLYNLKCICKISLQGRCLENEVDTW
LYMKSKRPNFPMFFKAYSHLRSKNWWLRSGLQYGVDVAVYRHHPSLVHSEYS
VLVQSGDSDRLRVWSDIHCAVRLSGSVAKTLLTLYVNGKFKGEDLNLPVCLENF
TVEEQTISRWSPELSREDNPQIQNKMLPM

>Arabidopsis_suecica_KAG7564586.1

MAPRWKWKGAEKALAEVSKTVSELQSSLAQIEVSGFLSSCNVLLSVEPEQA
EVLDRCCFGRPVVSAEKDKRWIQLSFEEAFFLYKLCIKISLRGRSLENEVALW
RSMRSFKTNFAISYKAYSHLRSKNWIWRSGLQYGVDVAVYRHHPSLVHSEYAV
LVQFICGNDRLKVWSDIHCSVRLTGSVAKTLLVLYINGNVNTENMNLPLCLEDYT
VEEQTIRRWSPELGREDETRT

>Arabidopsis_suecica_KAG7538649.1

MNFTRGTTISAARVATVFPRERDPNLAPILDLTHDFDELLVVDLRHLYLSTGSLK
HSSPLLTLPESSISSVFSSKPKRQLNFMAPRWKWKGAEKALAEPIKSVSEL
QLSLAETESSGTLSSSNVLLAVEPEQAELLDRCCFGRLVLSAEKVKKWIQLSFE
EAFYLHYNLKCICKISLQGRCLENGVDTWLYMKSKRPNFPMFFKAYSHLRRLKNW
VLRSGLQYGVDVAVYRHHPSLVHS
EYSVLVQSSDSDRLRVWSDIHCAVRLSGSVAKTLLTLYVNGNFKGEDLKLPMC
LENFTVEEQTISRWSPELSREDETTNSKQNVTVNSNLKTL

>Brassica_napus_XP_013682163.1

MAPRWKWKGAEKALAEPIKSVSELQLSLAKTESSGSLSSCNVLLAVEPEQA
ELLDRC CFGKLVLSAEKVKKWIQLSFEEAFYLLYILKCIKLSLRGRCLENEVDTW
MYMRSKRPNFPAFFKTYSHLRSKNWVLRSGLQYGVDVAVYRHHPSLVHSEYS
VLVQSGDSDRLRVWSDVHCAVRLSGSVAKTLLTLHVSGNSNREDLNLPTCLEN
YRVEEQTISRWSPELSREDETTSPKVTNVS NLKTP

>Brassica_napus_XP_013715851.2

MAPRWKWKGAEKALAEPIKSVSELQLSLAKTESTGSLSSCNVLLAVEPEQA
ELLDRC CFGRLVLSAEKVKKWIQLSFEEAFYLLYILKCIKLSRQGRFLESEVEIW
MYMRTKRPNFPVFFKAYSHLRSKNWVLRSGLQYGVDVAVYRHHPSLVHSEYS
VLVQSGDSDRLRVWSDVHCAVRLSGSVAKTLLALHVSGNSNREDLNLPTCLGN
YRVEEQTISRWSPELSREDETTSPKPKVTNVS NLKTP

>Camelina_sativa_XP_010503178.1

MAPRWKWKGAEKALAEPVSETVSELQSSLAQTEASGFLSSCNVLLLVEVEQA
ELLDRC CFGKLVVSSEKDKRWIQLSFEEAFFLFYKLNKIKISPHGRSLEDEVDLW
RSMRSFKPNFAILYKAYSHLRLKNWIVRSGLQYGVDVAVYRHHPSLVHSEYAVL
VQSIGENDGLKAWSDVHCSVRLTGSVAKTLLFLYVNGQVNTENMNLPFCLEDY
TVEELTIRRWSPELCREDETRT

>Camelina_sativa_XP_010456153.1

MAPRWKWKGAEKALAEPISSVSELQLSLAKTESSGTLSSSNVLLAVEPEQA
ELLDRCCFGRLILSAEKVKKWIQLSFEEAFFLFYNLKCIFLQGRCLENEVDTW
MYMKS KRPNFPMFYKAYSHLR SKNWVLRSGLQYGVDVFVAYRHHP SLVHSDYS
VLVQSGDSDRLRVWSDIHCTVRLSGSVAKTLLTLYVNGNFKGEDLNLPLCLENF
TVEEQTISRWSPQLSREDETTNSKPNVTTVSNLCTL

>Camellia_sinensis_XP_028094683.1

MGPRWKKGKSGEGKALADPMSKIVSQLKSSLIQSDSHGLLSGCSVLLEVETEQT
ALLNRSCFGRPIITAQKDKQWFQLGMEEAFYLCYNLCLKIVSYDECTKNDDEL
WNYMKS KRETFFDLFKAYSHLRTRNWWVVRSGPQYGVDVFIAYRHHPALVHSEY
AVLVLSGGDGNANGRLRVWSDFQCTLRRLCGSVAKTLLVLCIDKNGVGAGSPTC
LESYSVEESTITRWSPEQSREDKTVAENGTKQEIFFEHEPRDWVQP

>Corchorus_olitorius_OMO77242.1

MKPRWKKGKSGEAKAIADPMSKIVSQLQSSLMQSEAHGLLSSCSVLVEVDAEVA
DLLNRACFGRPRITAEKEQQWFQLDMEEAFYLCFSLKCLKVVS KDGCTKSDEE
LWEYMKS KKEVFPISYKAYSHLRNKNWVVRSGLQYGVDVFVAYHHHPALVHSE
YAVLALSEGENDLNGRLRVWSDVHCTVRLCGSVAKTLLILNVNNDGQGAISPS
CLEHYTVEERTITRWNPEQSRENQGVLENQTNRSESDLLLLTCVSVVEIRKMRS

C2: TSEN15 Homolog Sequences

>Trypanosoma_brucei_Tb927.3.5560

MIDDVRICHLVLQDVKERLPLYESRLEAVNNSHVVISWCWNEVKAFVPPVAED
VEFTSDVLHEVVSLVDGLRQLGCTDFFVVFVDSGGTLSFYHVDLRLLLQSGRS
GSS

>Trypanosoma_evansi_TevSTIB805.3.5860

MIDDVRICHLVLQDVKERLPLYESRLEAVSNSHVVISWCWNEVKAFVPPVAED
VEFTSDVLHEVVSLVDGLRQLGCTDFFVVFVDSGGTLSFYHVDLRLLLQSGRS
GSS

>Trypanosoma_equiperdum_TEOVI_000183300

MIDDVRICHLVLQDVKERLPLYESRLEAVNNSHVVISWCWNEVKAFVPPVAED
VEFTSDVLHEVVSLVDGLRQLGCTDFFVVFVDSGGTLSFYHVDLRLLLQSGRS
GSS

>Trypanosoma_vivax_TvY486_0304970

MISDPYMCTLLLNEVCERLPFRQARLVCIEDQQVVVSSGADGVSAFVPITVAEG
NTFTSLTLRTISSVLAQIEAPDNLECFLAFIDTGGSFYKVTLLGSRGIGEPPT

>Trypanosoma_cruzi_TcSYL_0004610

MIDDEEICELLAEIRERFPLYESVIETVGSSRVVTCNVTGGAKGFLPYPVVEHD
EFTSKSLRDVVDVVDALRRRGCAEVFLVFVDSGGSLTFYRTSTVRA

>Leishmania_infantum_LINF_290005700

MSHSPFLTALYADVQSRLPLWTTQYVKPVSDGAFVVSSTWTDDSGAQLQRLFI
AVEASDTNNISEAVLTEWIALVEAWQTAHKEDEVSCFVGFVDLAGTVSYRCET
AVAGVLRSPDDHLTCR

>Leishmania_donovani_LdBPK.29.2.000080

MSHSPFLTALYADVQSRLPLWTTQYVKPVSDGAFVVSSTWTDDSGAQLQRLFI
AVEASDTNNISEAVLTEWIALVEAWQTAHKEDEVSCFVGFVDLAGTVSYRCET
AVAGVLRSPDDHLTCR

>Porcisia_hertigi_JKF63_00669

MSYSPFLTALYEDVRNRLPLWTTQYVQPVSHAASAVSSTWIDASGAKQQRLFI
AVEVSNTNWIVEAVLRDWRALVDAWHGEHEEGEVSCFLGFVDLAGTVSYRC
ETAAPSTLCSGADSHLTRS

>Leptomonas_pyrrhocoris_LpyrH10_08_0110

MYAAAPFMTALYNDVKDRPLWNTEYADLAGTTVRAVTSTWVSPEKKKDAKVF
LGVEANTRAVITPEVVAQWVQHVARFYSSQVTGEFLCYLCFIDAAGSVSYAC
ETATVDS

>Saccharomyces_cerevisiae_YMR059W

MATTDIISLVKNNLLYFQMWTEVEILQDDLSWKGNLRLLRGRPPHKLSNDVDT
EHENSLSSPRPLEFILPINMSQYKENFLTLECLSQTFFTHLCSPSTERILLAIINDDG
TIVYYFVYKGVKPKRN

>Homo_sapiens_NP_443197.1

MEERGDSEPTPGCSGLGPGGVRGFGDGGGAPSWAPEDAWMGTHPKYLEMM
ELDIGDATQVYVAFLVYLDLMESKSWHEVNCVGLPELQLICLVGTEIEGEGGLQT
VVPTPITASLSHNRIREILKASRKLQGDPDLMSFTLAIVESDSTIVYYKLTGFM
LPDPQNISLRR

>Candida_maltosa_EMG46893

MTSTLPFTSSLIDQVRLNLIHYNLWTNVEKYESENILSGLPKEKLTNTDVDITKEW
IIPRTLTDKLSVLQINSFFKTITKLNNEVRPKRIILGIVNDDGTVVYYFVHDGITKP
RQN

>Candida_tropicalis_XP_002550470

MTTPIPFSSSIIDQVKLNLIHYNLWNEVNIHENDGYSYLSGKPREKLINTDNEIKK
EWIIPKLLKDSKLSVQEINTWFNKIENDQGEGKRPERLIIGIVNDDGTVVYYFIHD
GIVKPRQN

>Cyberlindnera_jadinii_XP_020067935

VKQNLLFYSLWTDVKEVPLKEETVLSGIPKNHLLGDDEEEGNQGGVPAPIKPEF
VLPIMLGEQLTPSRLSTVFEQLHSPKRLVAGVVNDDGTVVYYIVHNGIAKPKKN

>Dactylellina_cionopaga_KAF3926259

MATQIADYLLNLRSVVRSNLEYQHYWTDIKLLDTLADLGENAQVHDPLPRPMIY
GRPPDQLYNPEPAASTDASLPKPPPEMEYVLPVHLDEKFALSKWAAVFDALPS
PPEGNDRKKRITVAVLSGDSTVVYYVMHDGIVKPRQN

>Eremothecium_cymbalariae_XP_003645727

MTYLTFTNTQHQAILLQCNLKTMELVPLVKNNLVHYQMWKDVHALTSLGQII
CGQPPQKLSNDDSEITTEYVFPVPLKQYDSGSLTLENLDHLFDELQDKGCSRIV
LAIVSDDGAVVYYTIYRGLHKPKKN

>Kluyveromyces_lactis_QEU58081

MGNMNAALCDVVYTNLVYQQLWTETEINFEDVPVCGKPSHRLTNDNDNDA
ETSNSVDIPSGGKEYVYPILMHQYKSSGFSMKSLDHIFSRLPDKIKRLTLGIVND
DGTVVYYFIYKGLRKPKKN

>Lachancea_mirantina_SCU90210

MVKMDNSGLIRLVSTNLAFEQLWDNVRETQLTNLNCWILTGRPAHKLSNDDDDI
CDEWVLPVELLQYRCGRLTLEILDTVFHSVKSERITLAIVSDDGTIVYYFIYKGLH
KPKKN

>Ailuropoda_melanoleuca_XP_002929167.1

MEERGDSEPTPGCSGLGPGGVRSGGGAHPWAPEDAWMGTHPKYLEMMELDI
GDASQVYIAFLVYLDLMESKSWHEVNCVGLPDLQLICLVGTEIEGEGGLQTVVPT
PISASLSHNRIREILKASRKLQGDPDLMSFTLAIVESDSTIVYYKLTDFMLPDP
QNISLRR

>Balaenoptera_musculus_XP_036686067.1

MEESGESQPTAGCSDVRPSVDRGGGAPSWAPEDAWMGTHPKYLEMMELDIG
DATQVYIAFLVYLDLMESKSWHEVNCVGLPDLQLICLLGTEIEGEGGLQTVVPTPV
SASLSHNRIREILKASRKLQGDPDLMSFTLAIVESDSTIVYYKLTDFMLPDPQ
NISLRR

>Chinchilla_lanigera_XP_005375107.1

MEERGDSEPTAGCSGLDSGSDRGGGSAPSWAPEDAWIGTHPKYLEMMELDI
GDATQVYIAFLVYLDLMESKSWHEVNCVGLPELQLICLVGTEIEGEGGLQTVVPT
SVSASLSHNRIREILKASRKLQGDPDLMSFTLAIVESDSTIVYYKLTDFMLPDP
QNISLKR

>Gorilla_gorilla_gorilla_XP_018883388.1

MEERGDSEPTPGCSGLGPGGVVRGFGDGGGAPSWAPEDAWMGTHPKYLEMM
ELDIGDATQVYVAFLVYLDLMESKSWHEVNCVGLPELQLICLVGTEIEGEGGLQT
VVPTPITASLSHNRIREILKASRKLQGDPDLMSFTLAIVESDSTIVYYKLTDFGM
LPDPQVSFEVTDSKKYKKRKIMT

>Lontra_canadensis_XP_032718542.1

MAERNDSEPTPGCSGLGPGGVGGVGVGGGDGGAHPWAPEDAWMGTHPKYL
EMMELDIGDASQVYIAFLVYLDLMESKSWHEVNCVGLPDLQLICLVGTEIEGEG
LQTVVPTPISASLSHNRIREILKASRKLQGDPDLMSFTLAIVESDSTIVYYKLTDF
GFMLPDPQNISLRR

>Macaca_mulatta_XP_001109012.2

MEERGDSEPIPGCSGLGPGGVVRGFGDGGGAPSWAPEDAWMGTHPKYLEMM
ELDIGDATQVYIAFLVYLDLMESKSWHEVNCVGLPELQLICLVGTEIEGEGGLQTV
VPTPITASLSHNRIREILKASRKLQGDPDLMSFTLAIVESDSTIVYYKLTDFFML
PDPQVSFENISLRR

>Mus_musculus_Q8R3W5.1

MEERSDSEPTPGCSGPGPAPVRDGGGAHTWAPEDAWMGTHPKYLEMMELDI
GDATQVYIAFLVYLDLMESKSWHEVNCVGIPELQLICLLGTEIEGEGGLQTVVPTPI

SASLSHNRIREILKASRKLQGDPELPMSFTLAIVESDSTIVYYKLTDFMLPDPQ
NISLRR

>Pan_paniscus_XP_008966815.1

MEERGDSEPTPGCSGLGPGGVRFVGDGGGAPSWAPEDAWMGTHPKYLEMM
ELDIGDATQVYVAFLVYLDLMESKSWHEVNCVGLPELQLICLVGTEIEGEGGLQT
VVPTPITASFSHNRIREILKASRKLQGDPLPMSFTLAIVESDSTIVYYKLTDFM
LPDPQVSFENISLRR

C3: TSEN34 Homolog Sequences

>Trypanosoma_brucei_Tb927.6.4790

MGVALRVITYFRRGPLWGHHRKPSKRPRSNSFDVNNKNCTSTEYDKGALAVN
ENTRDEDEGVTSLLAMRVMMSGADGATEVPLCRAVLRGSSVEGAYGCHYHAYP
SESPHGAHGTSLCWSLEKSSIKLYELLCLCRLANSCRKDVVLFDDGREGLLFSYR
ATL

>Trypanosoma_evansi_TevSTIB805.6.4960

MGVALRVITYFRRGPLWGHHRTPSKRPRSNSFDVNNKNCTSTEYDKGALAVN
ENTRDEDEGVTSLLAMRVMMSGADGATEVPLCRAVLRGSSVEGAYGCHYHAYP
SESPHGAHGTSLCWSLEKSSIKLYELLCLCRLANSCRKDVVLFDDGREGLLFSYR
ATL

>Trypanosoma_equiperdum_TEOVI_000595500

MGVALRVITYFRRGPLWGHHRKPSKRPRSNSFDVNNKNCTSTEYDKGALAVN
ENTRDEDEGVTSLLAMRVMMSGADGATEVPLCRAVLRGSSVESAYGCHYHAYP
SESPHGAHGTSLCWSLEKSSIKLYELLCLCRLANSCRKDVVLFDDGREGLLFSYR
ATL

>Trypanosoma_congolense_TcIL3000_6_4260

MGVVLGLLNSLRSGYARAPSRTREKRLRSPTAAHDRGGGFFEVEGDNTVEVR
GPVPAGSGELQSLTMQIVDGNALGTPLCHSALCGPSVEGTYGCHYHLYPTP

FPQDTHGTYLCWSLRKSPIKCHELVCLCRLANSCRKDMVLVDGDVGLALFFRA
TL

>Trypanosoma_vivax_TvY486_0604160

MGAALRVLCNRSTLILNRAGNESRKRRRSVRDVQGADAGALCKGNNTPPVVV
RAATEALTDGAQSLMRMELLGFTAGVS
APLCRTVLHGTAVEDTYGCHYHAYSSSESPNEAHGTSLCWNLQRSPIGTHELLC
LGRLANNCRKNVFLFDNGGGIMLSYRA
SL

>Trypanosoma_cruzi_C4B63_18g158

MGGSLRVLKEHLACDEGWGQKFWLWRRRKRRRVSNVDDDCGVTTVGMDEE
DRTMVDPEAQSLFRLRVVGTGVASVPLFRSALCGPAVEDTYACHYHLYPSVS
PGDAHGTALCWSLRRSSLKIHALMCLGRVANSCRKEMVLFDDDIGVLLSYTTTP

>Leishmania_infantum_LINF_300040200

MGTYLSELLVRKRPREDGSDASSAAGCSASHAASLPPSSLHLLRSLRYRCAS
PSRIGSEVCRSVAEDEATRRTYGCHAHVYETDTVDGSHGVALAWRVDEFASPL
SALSLLSLCRVANSCRKKTLVTTPKGEAVVLAYAAAL

>Leishmania_tarentolae_LtaP30.3490

MGTYLSLLMRKRPREDAPDDASSAGGCNACDVASLPPSSLSRLLLLNLRYSCAS
PSRIGLEVCRSITEDEATRLTYGCHAHVYEADTLDESHGVALAWRVDESASPLS
ALSLLSLCRVANSCRKKTLVTTTPNGEAVVLAYTATL

>Leishmania_donovani_LdBPK_303500.1

MGTYLSLLVRKRPREDGSDASSAAGCSASHAASLPPSSLSHLLRSLRYRCAS
PSRIGSEVCRSVAEDEATRRTYGCHAHVYETDTVDGSHGVALAWSVDEFASPL
SALSLLSLCRVANSCRKKTLVTTTPKGEAVVLAYAAAL

>Porcisia_hertigi_JKF63_03137

MGTHLSLLVRKRPREGVPESASSQDGCSSPSLAASPPSSLSHLLLSLRYRSSS
PSRAGSKVCRCVLEDERTRHIYGCHAHVYEAKDENKNHGVALAWRIDDSAAPL
STLSLLSLCRVANSSHKKVLVTTQNGEAVLLTYTAAL

>Leptomonas_pyrrhocolis_LpyrH10_04_6520

MGALLSSLLFPRKRCRDNGGGGGEDIATVSREPRSPRACGGGAPANMVDPSP
SLLAKHLCRLRYRCTSSEKVGSLVCRHVAEDATTRQTYGCHAHLYETVTAEES
HGVALAWCVDEADPISALSLLSLCRVANSCRKTTLLTSPLGDALILTYTATL

>Saccharomyces_cerevisiae_YAR008W

MPPLVFDIDHIKLLRKWGICGVLSGTLPTAAQQNVFLSVPLRLMLEDVLWLHLN
NLADVKLIRQEGDEIMEGITLERGAKLSKIVNDRLNKSFEYQRKFKKDEHIAKLKK

IGRINDKTTAEELQRLDKSSNNDQLIESSLFIDIANTSMILRDIRSDSDSLSRDDIS
DLLFKQYRQAGKMQTYFLYKALRDQGYVLSPGGRFGGKFIAYPGDPLRFHSHL
TIQDAIDYHNEPIDLISMISGARLGTTVKKLWVIGGVAEETKETHFFSIEWAGFG

>Homo_sapiens_NP_001070914.1

MLVVEVANGRSLVWGAEAVQALRERLGVGGRTVGALPRGPRQNSRLGLPLLL
MPPEARLLAEIGAVTLVSAPRPDSRHSLALTSFKRQQEESFQEQSALAAEARE
TRRQELLEKITEGQAAKKQKLEQASGASSSQEAGSSQAAKEDETSDGQASGE
QEEAGPSSSQAGPSNGVAPLPRSALLVQLATARPRPVKARPLDWRVQSKDWP
HAGRPAHELRYSIYRDLWERGFFLSAAGKFGGDFLVYPGDPLRFHAHYIAQCW
APEDTIPLQDLVAAGRLGTSVRKTLLLCSPQPDGKVVYTSLQWASLQ

>Candida_glabatra_KAH7586698

MENEGTVDGKVKVVISVVLDEDGVPGSGLVFDLESIRYLRELGIAGVLSGTLPS
ATQQNLFLTVPRLMIEEVLWLFINNLCEVKIIPANSGDYMASIIRKLELADMN
KKNMEKMFALQRDYKRALHKQKLEKLGIKEKKTANEELINSSLFVETPNTSLIT
PEAIKSHQRDHVLDLLKSAFSKYNTYLLYQQLRNQNYVLAPGARFGGKYIAYPG
DPLRYHSHLTIQDAIDYEEPIDLLQLLSGARLGTTVKKLWVFGGVKDKEKNKPV
SFYSVEWAGFG

>Kazachstania_unispora_KAG0654988

MSESKICIKLVVHDLNDPESVICPMIFNLDDMVKLRRLGVCILAGTLPFAAQQNI
FLTIPLKLMVEETIWLVLNGYAELQLIQGPMTSLMTNILETKGDELFLKARDKLLR
SFDLQRQYKKEQHALKLQKLGIDPARDNSSANNKLISSLFVETPNDSLTLQYC
HQGKSPIDPTLDSMLLNLLISNYSNWNNYLLYQSLKSQNYVMSPGGRFGGLFIA
YPGDPLRYHSHLTIDNALDYNDPIDFISLTSGARLGTAVKKLWVIGGVKDENS
TNKANDIQLNQPETLLTKRNDTSFFSIEWAGFG

>Lachancea_thermotolerans_XP_002553827

MVGSKVAIVLLQRDGEAGTPLVFDIASIEKLRSIGVAGILTGTLP SATQQNAFLSV
PLRLMAEEALWLVEKQLGYLVHGGGVVHTAAEAVKAEDMKEARNELEERSFEA
QREFKRQQHLEKLRRLGVKAENSSGTETDYSRLLESSLFIETCDSSALISQRQR
EFDKPEIQARLAQQLRTGCKCKGDFHVYKALREQGYFLSPGSRFGGRFIAYPG
DPLRYHSHMTVQPAMDYRRDPLDLLQVVSGGRLGTGVKKLWVVGGVKDDYD
STDAESGRVSFFSVEWAGFG

>Cyberlindnera_fabianii_ONH67189

MTWPQPAAYMTHTKASGALFAKHKHIDQALIHISLVAGKPLLFSLDDIKKARELGI
VGTLVGTLPAAPQQNLFQGVPLQLMLEECAWLIHHGHAFIVPDKQFIKDLLASLT
DDEIAEMEALRQQQLDQERKIKAKEYQQKMVCRGVVNPKNQNDALLEQALPVTI
PDTASHLPNHALLERVYSNSTSTQERIIRQLGISSLSYAVFDTLKSRGYFLASGL
RFGTHFIAYPGDPLRFHAHLIVNPIDYDEDIGLMNVVGGGRLATGVKKLLTIGST
DDEEEVKFFSIEWAGFG

>Eremothecium_cymbalariae_XP_003647366

MPSGKVAISVSSKLA VPLVFNIEDVKRLRERGAVGILCGTLPTAAQQNLFLTVPL
RLMAEEAVWLVASGYAYFLGDDVLLQEALEGVGSKTVEQWGREERRQKEQQL
AWRRQQRKEREAYGGGGDGGDRGDLAAEGGDGDGARRLEEEQSLFIETCN
ESRLTSEKVRAFSEDAVLQQGLVNAVIARYLKIGDYLMFKSLREQNYFLSPGAR
FGARFIAYPGDPLRYHSHMAVQPAIDYYTEAVDLQQVVC GGRLGTGVKKLWIL
GGVRYREVEAGADQLLECGAPVSFFSIEWAGFG

>Kluyveromyces_lactis_QEU58616

MGHRESFTKAMSAKAKIYLVGSHLEDGDDDASSVVPVLYDVDDIAKIREHGVAG
VLIGTLGGAPQQNVFLGVPLRLMMEEALWLVEVGHAVFRHVTGQDLIKSLKGL
DGEKLQKFKDDRANDVAQQLEWKRANFLRKMKTLRSASAVAVPSDVINEKDE
QLMKQSIFIETKDTSAVIELSLNDQTIDQRKICEQILGQDEKLRLNYKVYKKLREM
GYFMSPGARFGGRYVAYPGDPLRYHSHLTVQDARSKDEDIDLLNMINGARLGT
SVKKTWVLPGINENGDAEFYSVEWAGFG

>Komagataella_phaffii_AOA62092

MNKLPISRNEGLIFDIQTIKNLRLLGIVGYLSGTLPLSTQQNNFLGVPLRLLFEELL
YVVVHHSEYYIVPDDVMFQGLYASLTNNDLQQIRQFAEKEHNQRLETKKKEFQ
AKMSQLRTNGKKIPDSAMIYNTEKEPVFHEIKNTSSHLPNVNTWNDHFNQPEV
QTKLLFQLLQSRPNLSHSLADYLIFSHLRKNGYFITAGLRFGGKFVAYPGDPLRY

HSHLIVKPVYNGEKIELKKLVNGGRLATAVKKVYVIAGLTNKIDVDGVPEQLELD
PKEFITSLEASPVKTFSFEWAGFG

>Lachancea_mirantina_SCU87439

MEALEGENDSKIEISVVGNGNRFEDGVCLVFDIESIRRLRRLGITGILTGTLP
SAAQQNVFLTVPLRLMAEEAVWLVENGFVAVLVSDREALEMGVSDLTASD
WDEMDKQQEALFEEQRRFKREQHFELRAVGKTVANVDANLESSLFVETR
NESSVIQRQRYDFDTPPELQKRLVDQLLHSETLKSNYLVYKALRAQGYC
VSPGSRFGGRYIAYPGDPLRYHSHLTVPPALRYRDEPLDLLQLVGGGRL
GTGVKKLWVLGGVDDDESDEGVTFSSVEWAGFG

>Ailuropoda_melanoleuca_XP_019664253.2

MLVVEVANGRSLVWGAEAVQALRERLGVGGRTVGALPRGPRQNSRLGLPL
LLMPEEARLLAEIGAVTLVSAPRPDPRQHSLALASFKRQQEQGFQEQSAL
AAEARETRQELLEKIAEGQAQKQKLEQASGASESQEAGANPAVFENEAGAS
QAPGEPPEAGSSSPQPGPSNGVAPLPRSALLVQLATARPRPIKAKPLDWR
VQSKDWPHAGRPAHELRYSIYRDWERGFFLSAAGKFGGDFLVYPGDPLRF
HAHYIAQCWAPGDPIPLQDLVSAGRLGTSVRKTLTLLCSPQPDGKVYTS
LQWASLQ

>Balaenoptera_musculus_XP_036688565.1

MGWGWRKQRVARYVRGWLRRDCELVFTRRMLVVEVANGRSLVWGAEAVQA
LRERLGVGGRTVGALPRGPRQNSRLGLPLLLMPEEARLLAEIGAVTLVS
APRPD

PRQHSLALASFKRQQEQGFQEQSALAAEARETRRQELLEKIAEGQAAKKQKLE
QKSGTSGSQEAGGNQAAEENEASAGQAAGEREEAGEGSSSPQPGPSNGVAP
LPRSALLIQLSTARPRPIKARPLDWRVQSKDWP HAGRPAHELRYSIYRDLWER
GFFLSAAGKFGGDFLVYPGDPLRFHAHYIAQCWAPGDPIPLQDLVSAGRLGTS
VRKTL LLLCSPQPDGKVVYTSLQWASLQ

>Bostaurus_NP_001029423.1

MLVVEVANGRSLVWGAEAVQALRERLGVGGRTVGALPRGPRQNSRLGLPLLL
MPEEARLLAEIGAVTLVSAPRPDPRQHSLALASFKRQQEQGFQEQSTLAAEAR
ETRRQELLEKITEGQAAKKLEQESGTSGSQEAGGKQAAEENEASAGQAAGE
HEEAHEGSSPQPGPSNGVAPLPKSALLIQLATARPRPIKARPLDWRVQSKDWP
HAGRPAHELRYSIYRDLWERGFFLSAAGKFGGDFLVYPGDPLRFHAHYIAQCW
APEDPIPLQDLVSAGRLGTSVRKTL LLLCSPQPDGKVVYTSLQWASLQ

>Camelus_bactrianus_XP_010960156.1

MLVVEVANGRSLVWGAEAVQALRERLGVGGRTVGALPRGPRQNSRLGLPLLL
MPEEARLLAEIGAVTLVSAPRPDPRQHSLALASFKRQQEQGFQEQSALAAEAR
ETRRQELLEKIAEGQAAKKQKLEQESGTSGSQEPGGNQAAEENEASASQAAG
EHEEAGEGSSSPQPGPSNGVAPLPRSALLVQLATARPRPIKARPLDWRVQSKD
WPHAGRPAHELRYSIYRDLWERGFFLSAAGKFGGDFLVYPGDPLRFHAHYIAQ
CWAPGDPIPLQDLVSAGRLGTSVRKTL LLLCSPQPDGKVVYTSLQWASLQ

>Equus_caballus_XP_023506137.1

MLVVEVANGRSLVWGAEAVQALRERLGVGGRTVGALPRGPRQNSRLGLPLLL
MPEEARLLAEIGAVTLVSAPRPDPRQHSLTLASFKRQQEQGFQEQSALAAEAR
ETRRQELREKIAESQAACKQRLEQDSGAGESQEASGNPAAGENEASASQASG
EQEEAGSSSPQPGPSDGVAPLPRSALLVQLATARPRPIKARPLDWRVQSKDW
PHAGRPAHELRYSIYRDLWERGFFLSAAGKFGGDFLVYPGDPLRFHAHYIAQC
WAPGDPIPLQDLVSAGRLGTSVRKTLLLCSPQPDGKVVYTSLQWASLQ

>Gorilla_gorilla_gorilla_XP_018870339.1

MRRMLVVEVANGRSLVWGAEAVQALRERLGVGGRTVGALPRGPRQNSRLGL
PLLLMPEEARLLAEIGAVTLVSAPRPDSRHSLALTSFKRQQEESFQEQSALAA
EARETRRQELLEKITEGQAAKKQKLEQASGASSSQEAGSSQAAKEDETSQGQA
SGEQEEAGPSSSQAGPSNGVAPLPRSALLVQLATARPRPVKARPLDWRVQSK
DWPHAGRPAHELRYSIYRDLWERGFFLSAAGKFGGDFLVYPGDPLRFHAHYIA
QCWAPEDTIPLQDLVAAGRLGTSVRKTLLLCSPQPDGFKSQEVSINLLYKCS

>Macaca_mulatta_NP_001248694.1

MLVVEVANGRSLVWGAEAVQALRERLGVGGRTVGALPRGPRQNSRLGLPLLL
MPEEARLLAEIGAVTLVSAPRPDPQHSLALTAFAFKRQQEESFQEQSALAAEARE
TRRQELLEKITEGQAAKKQKLEQASGASSSHEAGSSQAAKENETSQGQASGE
QEEAGPSSSQAEPSNGVAPLPRSALLVQLATARPRPVKARPLDWRVQSKDWP

HAGRPAHELRYSIYRDLWERGFFLSAAGKFGGDFLVYPGDPLRFHAHYIAQCW
APEDIPLQDLVAAGRLGTSVRKTLTLLCSPQPDGKVVYTSLQWASLQ

>Pan_paniscus_XP_034802344.1

MRRMLVVEVANGRSLVWGAEAVQALRERLGVGGRTVGALPRGPRQNSRLGL
PLLLMPEEARLLAEIGAVTLVSAPRPDSRHSLALTSFKRQQEESFQEQSALAA
EARETRRQELLEKITEGQAAKKQKLEQASGASSSQEAGSSQAAKEDETSQGQA
SGEQEEAGPSFSQAGPSNGVAPLPRSALLVQLATARPRPVKARPLDWRVQSK
DWPHAGRPAHELRYSIYRDLWERGFFLSAAGKFGGDFLVYPGDPLRFHAHYIA
QCWAPEDTIPLQDLVAAGRLGTSVRKTLTLLCSPQPDGKVVYTSLQWASLQ

>Pan_troglodytes_XP_009434637.1

MRRMLVVEVANGRSLVWGAEAVQALRERLGVGGRTVGALPRGPRQNSRLGL
PLLLMPEEARLLAEIGAVTLVSAPRPDSRHSLALTSFKRQQEESFQEQSALAA
EARETRRQELLEKITEGQAAKKQKLEQASGASSSQEAGSSQAAKEDETSQGQA
SGEQEEAGPSSSQAGPSNGVAPLPRSALLVQLATARPRPVKARPLDWRVQSK
DWPHAGRPAHELRYSIYRDLWERGFFLSAAGKFGGDFLVYPGDPLRFHAHYIA
QCWAPEDTIPLQDLVAAGRLGTSVRKTLTLLCSPQPDGKVVYTSLQWASLQ

>Vulpes_vulpes_XP_025841117.1

MLVVEVANGRSLVWGAEAVQALRERLGVGGRTVGALPRGPRQNSRLGLPLLL
MPEEARLLAEIGAVTLVSAPRPDPRQHSLALASFKRQQEQDFQEQSALAAEAR

ETRRQELLEKIAEGQAAKKQKLEQESVASESQEASANPAAAESEAGASQAPGE
PEEAGSSSPQPGPSNGVAPLPRSALLVQLATARPRPIKARPLDWRVQSKDWP
HAGRPAHELRYSIYRDLWERGFFLSAAGKFGGDFLVYPGDPLRFHAHYIAQCW
APGDPIPLQDLVSAGRLGTSVRKTLLLCSPQPDGKVVYTSLQWASLQ

>Mus_musculus_NP_001157676.1

MLVVEVANGRSLVWGAEAVQALRERLGVGGRTVGALPRGPRQNSRLGLPLLL
LPEEARLLAEIGAVTLVSAPRPDPRNHGLALASFKRQQEQSFQDQNTLAAEARE
TRRQELLEKIVEGQAAKKQKLEQDSGADEGGQEAGGSEATQGSETSDDGQPS
AEQEGAAPSLDSSSPQPGPSNGVTPLPRSALLIQLATARPRPVKAKPLDWRVQ
SKDWPHAGRPAHELRYSIYRDLWERGFFLSAAGKFGGDFLVYPGDPLRFHAH
YIAQCWSAEDPIPLQDLVSAGRLGTSVRKTLLLCSPQPDGKVVYTSLQWASLQ

Appendix D: Actinomycin D Uncropped Northern blot Membranes

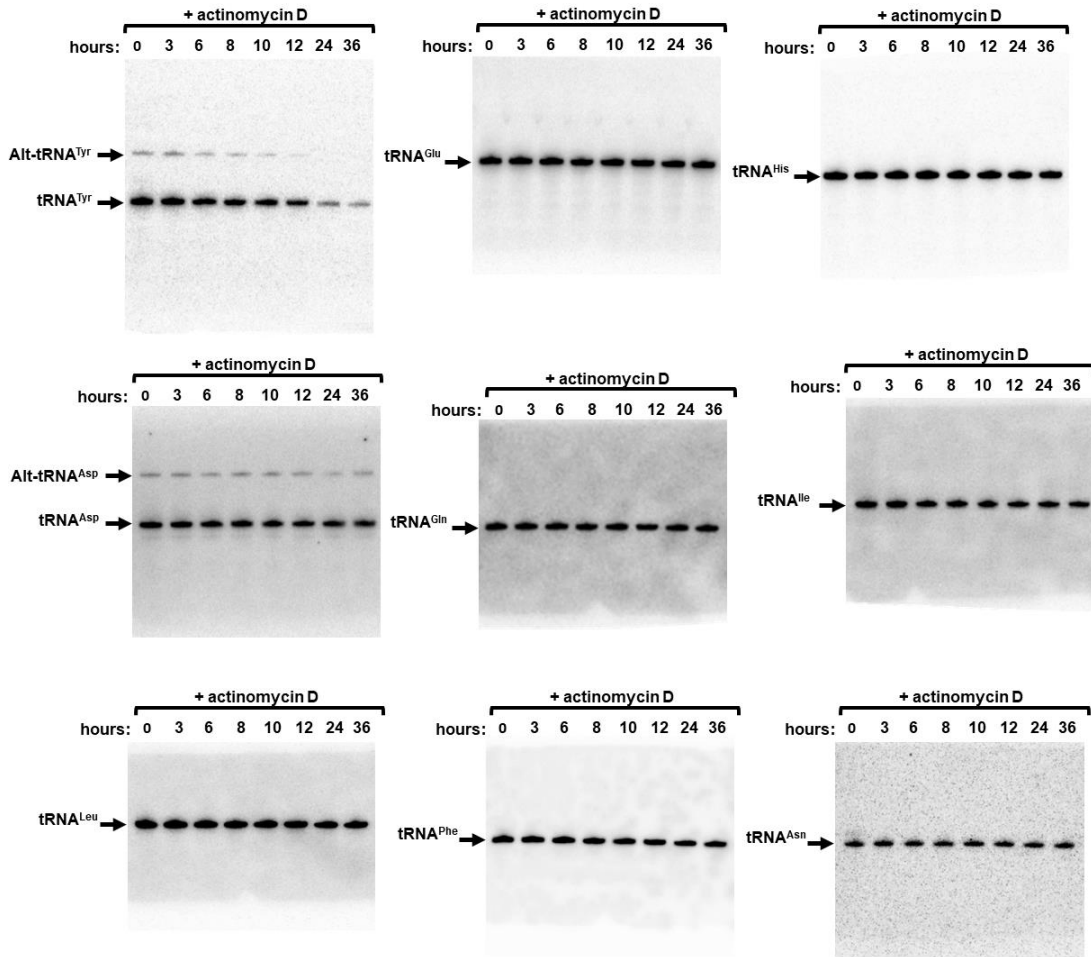


Figure D.1 Uncropped Actinomycin D northern blot membranes

Northern blot hybridization performed on the extracted total RNA samples from *T. brucei* cells subjected to Actinomycin D treatment revealing the mature and alternate conformers of tRNA^{Tyr}. The same membrane was then stripped, and probed for tRNAs: Asp, Glu, Gln, His, Ile, Leu, Phe, and Asn. The tRNA^{Glu} was used as loading control.